LOW FREQUENCY RAMAN INVESTIGATION OF WATER AND AQUEOUS SOLUTIONS

BERNARD CHARLES RICE

LOW FREQUENCY RAMAN INVESTIGATION OF WATER AND AQUEOUS SOLUTIONS

© *Bernard Charles Rice, B.Sc.*

A Thesis submitted in partial fulfillment
of the requirements for the degree of
Master of Science

Department of Chemistry
Memorial University of Newfoundland
St. John's, Newfoundland, Canada

March 1984

ABSTRACT

The Raman spectra of water and aqueous salt solutions are presented in the form of a vibrational density of states, $R(\omega)$. This $R(\omega)$ format reveals with greater definition the low frequency Raman bands due to polarizability changes in the weak bonds of intermolecular complexes. For pure water at 25°C, broad bands were observed at 66 cm^{-1} and 192 cm^{-1} due to hydrogen bond bending and stretching modes. High signal to noise ratios achieved by multiple scans permitted the construction of difference spectra which greatly assisted the measurement of peak frequencies and depolarization data. The 192 cm^{-1} band in the spectrum of water was found to be slightly polarized while the remainder of spectrum exhibited largely depolarized features. The hydrogen bond stretching mode of water shifted 6 cm^{-1} in D_2O and 17 cm^{-1} in $H_2{}^{18}O$. This mode is interpreted as arising from oxygens moving about the hydrogen involved in the hydrogen bond but with the proton remaining closer to one of the oxygens. The effects of salts on the water spectrum have also been investigated. Most salts increase the relative intensity of the water spectrum although typical structure breakers cause a decrease in the relative intensity. New bands have also been observed when salts are added to water. Reorientations of the CO_3^{2-} ion give rise to a depolarized scattering at 92 cm^{-1} in aqueous solutions. Polarized bands due to cation and anion hydrates have also been observed. The symmetric stretch of the $Mg(H_2O)_6^{2+}$ ion is observed at 359 cm^{-1} in $MgCl_2$ while a polarized band for $LiCl_{(aq)}$ occurs at 384 cm^{-1}. Polarized bands at 263 cm^{-1} for saturated $KF_{(aq)}$, 298 cm^{-1} for 10M $NaOH_{(aq)}$, 293 cm^{-1} for 11.5M $KOH_{(aq)}$, 286 cm^{-1} for 5.9M $RbOH_{(aq)}$ and in $CsOH_{(aq)}$ are assigned to stretching of the $O-H\cdots X^-$ band.

ACKNOWLEDGEMENTS .

The author wishes to thank Professor Murray H. Brooker for his continual guidance and supervision during the development of this work.

The author would also like to thank his wife Dolores whose patience and understanding assured the completion of this work.

TABLE OF CONTENTS

LIST OF TABLES

LIST OF FIGURES

INTRODUCTION

Vibrational spectroscopy allows one to develop a picture of a system of molecular units with intermolecular interactions. Peaks arising from internal modes of a molecule help to identify the molecular species present while changes in the peak maximum, ν_{max}, and full width at half height, Γ, and low frequency scattering yield information on forces acting between the species. When applied to water, a large amount of spectral activity is observed not all of which is easily translated to a simple molecular picture. In fact "H_2O" is anything but simple. The relationship between the Raman spectrum and the structure of water and aqueous solutions is not well understood. Improved definition of the bands present in the Raman spectrum is required and can be achieved through high quality multi-scan recording of the spectral data.

Most of the work on water and aqueous salt systems has been reviewed by Walrafen [1] and has been updated to about 1977 [2,3]. The original work of Walrafen [4] covered a broad base for the Raman techniques available at the time and much of the work since has confirmed his experimental findings. The low frequency intermolecular region is considered to extend from 0 → 1000 cm^{-1} for H_2O and is subdivided into two regions. The librational region extends outward from 350 cm^{-1} and this is supported by a local structure model of a C_{2V} 5 molecule unit moving in a cage of nearest neighbors [5]. This C_{2V} unit is believed to be analogous to the I_h ice structure for those waters fully hydrogen bonded. The librational region is yet to be fitted with any great certainty, but it is believed to be comprised of three peaks. The region below 350 cm^{-1}, is thought to be of a translational nature. Problems arise in the assignment of frequencies to bands in this region due to the large contribution of

scattered light from the wing of the Rayleigh peak to the Raman spectrum. Assignment of one band ranges from 170 cm^{-1} [6] to 191 cm^{-1} [7] for the O···H–O stretch. A similar band has been reported in the IR at 190 cm^{-1} and at 22 meV [8] and 8.4 $Å^{-1}$ [9] for inelastic neutron scattering and neutron diffraction studies respectively. Discrepancies are also apparent in the reported Raman frequencies for D_2O - 175 cm^{-1} [4], 191 cm^{-1} [7], and 180 cm^{-1} [10] - and for $H_2{}^{18}O$ - 181 cm^{-1} [7] and 170 cm^{-1} [10]. A weaker O···H–O bending mode has been assigned a frequency of 60 cm^{-1} for H_2O, $H_2{}^{18}O$ and D_2O [10]. The intensity of both regions drops with increasing temperature [1,4,7] while the Rayleigh scattering increases [11] faster than would be predicted by collision induced polarizability theory - phenomena which show a breakdown in the water structure.

Various effects on the Raman spectrum of water have been noticed when ionic salts are added. Addition of anions, such as bromides and chlorides, reportedly lower the intensity of the translational region while raising the intensity of the librational region [4]. Similar changes have been observed in the IR [12] and Rayleigh scattering [13] and have been interpreted as anion hydrate contribution to the librational region spectrum plus a loss of water-water interaction (structure breaking) [4,11,14,15]. Perchlorate, except for $HClO_4$, has been classified as a structure breaker in water [7,14] virtually wiping out the O···H–O 190 cm^{-1} stretch in the Raman spectrum. The presence of an isosbestic point in the infrared librational region of water has been interpreted as evidence for an equilibrium between waters of hydration and bulk water (C_{2V} molecular unit) [16] but no evidence of a water-perchlorate hydrogen bond stretch was found in the translational vibrational spectra because of the weak bond that

forms between ClO_4^- and H_2O [17,18]. Other anions such as F^- and OH^- are considered structure enhancing in water. Both IR [19] and Raman [7] studies indicate an increased intensity and ν_{max} for the O···H-O stretch band with F^- addition and recent X-ray [20] and SCF calculations with correlations for configurational interactions with single and double substitutions [21] show a symmetric $H_3O_2^-$ ion formed from an $OH^-\cdots H_2O$ interaction.

Information concerning cation effects on the low frequency water spectrum is scarce and such effects are generally considered to be small even though new peaks due to metal-oxygen vibrations of hydrated cations are often observed [2]. A Raman study of aqueous lithium halides [12] reported that in dilute solutions a tetrahedral $LI(H_2O)_4^+$ species exists with the A_1 mode at 440 cm^{-1} but that at saturation levels ion aggregates or solvent separated ion pairs form.

Refractive index studies suggest that most of the low frequency spectral changes of water in aqueous salt solutions are due to the effects of ions on H_2O - H_2O interactions [19], although recent Raman studies show that intense scattering also arises from reorientations of anisotropic ions [7]. Newer Rayleigh scattering studies [22] also showed the contribution from anisotropic ions. Poor correlation between solution entropies for polyatomic ions and shifts for the first moment of the IR librational bands for their aqueous solutions were interpreted to indicate that anion reorientation is contributing to the solution entropy [14]. These reorientational bands of anisotropic molecules and ions are easily seen in the Raman spectrum when the spectrum is recast in a density of states format $R(\omega)$.

This study begins with a look at the Raman spectrum of water and its isotopic analogues D_2O and $H_2{}^{18}O$ in an $R(\omega)$ format in the hope that a

more precise assignment of the low frequency bands may be obtained. Isotope shifts observed for the O···H-O stretch show that hydrogen-oxygen stretching is different for the two oxygens involved. Raman spectral evidence for cation effects on the low frequency spectrum of aqueous solutions is reported for LiCl, $MgCl_2$ and $CaCl_2$. A polarized band is observed in aqueous LiCl at 384 cm^{-1} and is similar to the symmetric stretch for the hexahydrated magnesium ion which appears at 359 cm^{-1}. No evidence of such a band is seen for $CaCl_2$. Strong anion-water interactions are reported for F^- and OH^- and a polarized band appearing in the Raman spectra of their aqueous solutions is assigned to an O-H···X^- symmetric stretch. The presence of the structure breaking ClO_4^- ion is shown to disrupt both water-water interactions and hydroxide-water interactions. The polarizability anisotropy of the CO_3^{2-} ion gives rise to a reorientational band in the depolarized spectra of its aqueous solutions. The frequency of this band is very close to that for NO_3^- [7].

The spectra for all of the solutions studied were cast in an $R(\omega)$ format to obtain more detail from the low frequency Raman spectra. No attempt is made to test the relationship of $R(\omega)$ to $\alpha(\omega)$ from the IR but a comparison of $R(\omega)$ for the depolarized spectrum of water and $\alpha(\omega)$ for water show similarities between the two spectra.

THEORY

The primary problem in the study of low frequency Raman scattering is correcting for the contribution from Rayleigh scattering. Molecular processes giving rise to bands in this region are generally of a weak nature and arise from such actions as reorientational motions of molecules with permanent anisotropy or collision induced anisotropy, intermolecular vibrations of hydrogen bonded species and, vibrations of molecules with

weak bonds or containing heavy atoms. Difference bands may also be present in this region. The difference in intensity between the Rayleigh scattered light and the low frequency Raman scattered light may be so great that the Raman band only appears as a deformation of the Rayleigh wing. Determination of band shapes and positions of the low frequency modes requires removal of (or accounting for) the contribution of the Rayleigh wing to the spectrum.

Some understanding of the functional form of the scattering in this region has been found in the study of temperature effects on the scattering of some glasses. Stolen [23] and Hass [24] have reported a spectral dependence for glasses in the low frequency Raman of $|1+n(\omega)|$ where

$$n(\omega) = \left[e^{-h\omega/2\pi kT} - 1\right]^{-1}$$

That is to say, much of the shape of the $\omega=0$ peak is due to a thermal population factor. When the spectra are corrected for the thermal factor, the spectra appear in the form of a vibrational density of states. Hass has shown that, when a density of states spectrum is recast in an $I(\omega)$ form at different temperatures, the experimental spectra match the calculated spectra very closely. Shuker and Gammon [25] have shown the dependence of viscous liquids on the population factor and a common frequency factor. Under the assumption that the scattering is due to vibrations and the modes have short lived correlation functions, the scattering is first order, disorder allowed [26]. The result is

$$I(\omega) = \sum_b C_b (1/\omega)[1+n(\omega)]g_b(\omega)$$

where C_b is the coupling constant over the vibration at band b and $g_b(\omega)$ is the density of states of vibration b. Hence to cast the $I(\omega)$ spectrum in a form of $g_b(\omega)$ the spectrum can be multiplied by the factor

$\omega/[1+n(\omega)]$. Recently it has been shown that the coupling constant may vary across the band [27] in which case the application of this function may not be a true representation of the density of states.

Lund et al. [10, 28] have arrived at the same function from another approach. These workers derive a function, $R(\omega)$, which is proportional to the energy absorbed in a scattering process.

$$R(\omega)=\omega\left[S^{>}(\omega)-S^{<}(\omega)\right].$$

Here $S^{>}(\omega)$ and $S^{<}(\omega)$ refer respectively to the Stokes and anti-Stokes scattered light intensities. The mean scattered light intensity $S(\omega)$ is given by $S(\omega)=1/2\left[S^{>}(\omega)+S^{<}(\omega)\right]$ and is a function of the molecular polarizabilities

$$S(\omega)=\int_{-\infty}^{\infty} e^{-i\omega t}\langle\alpha(0)\,\alpha(t)\rangle dt$$

where $I_{if}=(I_0 k_f^4/16\pi^2 R^2 \epsilon_0^2)(1/2\pi)S(\omega)$ is the intensity of scattered light of frequency $\omega=\omega_i-\omega_f$ and subscripts i and f refer to the initial and final states of the transition. From the principle of balanced states,

$$\left[\frac{S^{<}(\omega)}{S^{>}(\omega)}\right]=e^{\frac{-h\omega}{2\pi kT}}$$

and

$$R(\omega)=S^{>}(\omega)\,\omega\left[1-e^{-h\omega/2\pi kT}\right].$$

It can be easily shown that $\left[1-e^{-h\omega/2\pi kT}\right]=[1+n(\omega)]$. Lund goes a step further in showing the relationship of $R(\omega)$ to $\alpha(\omega)$, the IR absorption coefficient. In the process he has assumed that in the far IR for most liquids $\alpha(\omega)$ is proportional to $\omega\epsilon''$. This approximation results in:

$$\alpha(\omega)=\omega\tanh\left[\frac{h\omega}{4\pi kT}\right]\int_{-\infty}^{\infty} e^{-i\omega t}\langle\vec{u}(0)\cdot\vec{u}(t)\rangle dt$$

where $\langle\vec{u}(0)\cdot\vec{u}(t)\rangle$ is the dipole moment correlation function. Since $S(\omega)=1/2\left[S^{>}(\omega)+S^{<}(\omega)\right]$ then

$$S^{>}(\omega)=\frac{2S(\omega)}{\left[1+e^{-h\omega/2\pi kT}\right]}$$

and

$$R(\omega)=2S(\omega)\omega\left[\frac{1-e^{\frac{-h\omega}{2\pi kT}}}{1+e^{\frac{-h\omega}{2\pi kT}}}\right]$$

which is easily shown to be:

$$R(\omega)=2\omega\tanh\left[\frac{h\omega}{4\pi kT}\right]\int_{-\infty}^{\infty}e^{-i\omega t}\langle\alpha(0)\,\alpha(t)\rangle dt.$$

This is strikingly similar to the formula for the infrared absorption coefficient except for the dependence of the two processes on different selection rules. In the high temperature low frequency limit the $R(\omega)$ function approaches the classical second moment M_2. The second moment has its roots in the 'Method of Moments' approach to creating a Heisenberg picture from the energy domain (ie. the Fourier transform of the energy spectrum). The second moment is the Fourier transform of the second time derivative of the rotational correlation function.

$$G_r(t)=\langle 1/2\left[3\left[\vec{u}(0)\cdot\vec{u}(t)\right]^2-1\right]\rangle$$

[29].

$$M_2=\frac{\int_{-\infty}^{\infty}I(\omega)\omega^2 d\omega}{\int_{-\infty}^{\infty}I(\omega)\,d\omega}=-FT\left[\frac{d^2G_r(t)}{dt^2}\right]$$

Although the second moment has been used to approximate the $R(\omega)$ spectrum [30], it has a different meaning in its derivation and should not be equated rigidly in its interpretation.

Discrepancies exist in the literature [10, 30, 28] as to which function (tanh or exponential) should be applied. Since most Raman experiments only measure the Stokes shifts, the function to be applied should be the

exponential form as this will relate $S^{>}(\omega)$ to $R(\omega)$ directly. In order to use the hyperbolic tan function both Stokes and anti-Stokes shifts must be collected and one added to the other.

The function one applies depends on the ultimate goal. If comparison with the IR absorption coefficients is to be performed, the density of states function or $R(\omega)$ must be used provided of course there is a possibility of comparison with the IR (ie. $\epsilon'=\epsilon'(\omega)/n(\omega)c$ where $n(\omega)$ is the index of refraction or $K_e=1$). In the case where no comparison is necessary, either of the functions (hyperbolic tan, exponential, or classical second moment) will enable easier viewing of the low frequency Raman as they virtually remove the effect of the Rayleigh line. In the present study, the exponential form of the $R(\omega)$ was used.

One practical problem with any of these approaches to data treatment is the apparent increase of the noise with increasing frequency. This can be minimized through repetitive scans and signal averaging. The relative increase in noise is not unexpected as the functions are designed to study the $\omega=0$ band and this increase represents the deterioration of the S/N ratio of the $\omega=0$ band with increasing ω.

EXPERIMENTAL

In order to study the effects of ions on the low frequency region of water in the Raman spectrum, it is necessary to maintain high purity and homogeneity in the solutions used. Reagent grade salts were purified with activated charcoal in distilled water to remove any fluorescing materials. The charcoal was removed by filtration through fine frits and the salts recrystallized. The solutions were then prepared by dissolving the required amounts of the salts in doubly distilled water. For the saturated solutions, the salts were added in excess and equilibrated for one week. Solutions

were filtered through fine frits to remove any particles which might give rise to Tyndall scattering. The sample tubes were protected from solvent evaporation with Parafilm. In the case of the isotopic waters, treatment was excused on the grounds that the solutions were already of relatively high purity - D_2O, 99.8% D and $H_2{}^{18}O$, 99% ^{18}O - and on the high cost due to loss of solution that may occur during treatment. The aqueous solutions appear in Table 1. In addition to these solutions, spectrograde methanol and methanol 5.1M in NaOH were prepared. NaOH and 1:1 NaOH:KOH melts were also prepared for comparison.

The spectra were recorded at 298 K on a CODERG PH0 Raman spectrometer using the 488 nm line of a CONTROL model 553A argon ion laser. The laser power varied between 150 mW and 600 mW c.w. depending on the scattering ability of the sample. The incident light was vertically polarized and the scattered light, collected at right angles to the incident beam, was analyzed through a vertically or horizontally aligned polaroid film to give I_{VV} or I_{VH} polarizations. A quarter waveplate was employed to overcome the instrument polarization preference. The sample tubes were masked at the entry and exit points of the laser beam to minimize scattering from the glass. The slit widths for the double monochrometer were set at 2 cm^{-1}. The PMT was cooled to -20°C and signals collected via photon counting. The scan rate was 50 cm^{-1}/min. and the counts were one point per wavenumber for scans to 1000 cm^{-1} and two points per wavenumber for scans to 400 cm^{-1}. The spectra were wavenumber calibrated with the 351.64 cm^{-1} plasma line. Spectra were collected ten times in both I_{VV} and I_{VH} orientations and the digital output recorded on disk at the M.U.N. Computer Services VAX - 11/780. Data processing involved signal averaging to produce intensity and density of

Table 1

Aqueous solutions studied

Solution	Concentration
LiCl (Sat.)	15.03m
$MgCl_2$ (Sat.)	5.70m
$CaCl_2$ (Sat.)	6.71m
KF (Sat.)	15.89m
KCl (Sat.)	4.65m
NaCl (Sat.)	6.11m
K_2CO_3 (Sat.)	8.10m
K_2CO_3	1M
LiOH	2.5M (0.010M in carbonate)
KOH	11.5M (0.031M in carbonate)
NaOH	10M (0.074M in carbonate)
RbOH	5.9M (0.26M in carbonate)
CsOH	8.6M (2.56M in carbonate)
NaOH + $NaClO_4$	5M in each
NaOD in D_2O	10M

states spectra for both orientations of the scattered light. The resulting spectra were then plotted on a TEKTRONIX 4662 digital interactive plotter with the aid of a TEKTRONIX 4051 graphics terminal. Further data treatment was applied to the pure water and to the saturated lithium, calcium,

and magnesium chloride solutions to provide a relative intensity comparison. Intensity spectra were first calibrated to the integrated absorption of the ν_2 H-O-H bending region of the water. Since the bending region of the water is not constant with concentration [31,32], a second set of solutions was prepared and the ν_2 water region was further calibrated with the symmetric stretch region of the nitrate ion (linearly concentration dependent) by the addition of 0.5M Potassium Nitrate as an internal standard. The result was a set of scaled intensity spectra for the low frequency region without the introduction of a material which could itself contribute to the low frequency scattering. Finally the $R(\omega)$ spectra were scaled to have the same ratio of integrations as was apparent in the intensity spectra over a region where the spectra changed little with frequency. Subtraction files were created for some spectra by subtracting the I_{VH} data from the corresponding I_{VV} data to give the isotropic Raman spectrum $I_{ISO} = I_{VV} - 4/3\ I_{VH}$.

DISCUSSION

Water

The earlier work [4] on the intermolecular vibration region of water has not been improved much even in recent years. This is due to attempts to fit this low intensity region in the $I(\omega)$ format. The intermolecular Raman spectrum of water is shown in Fig. 1. In the range above 300 cm^{-1} there is a broad weak envelope, the number of components of which are not visibly evident. Below 300 cm^{-1} there is a broad peak at about 190 cm^{-1} and evidence of some intensity at about 70 cm^{-1}. Below this frequency, information becomes lost as the intensity of the Rayleigh scatter becomes more intense. The same features are present in both the polar-

Fig. 1. I_{VV} (a) and I_{VH} (b) spectra of H_2O. Weak features due to translations and librations of water are observed from 100 cm^{-1} to 1000 cm^{-1}. A mostly depolarized nature is exhibited in the spectra.

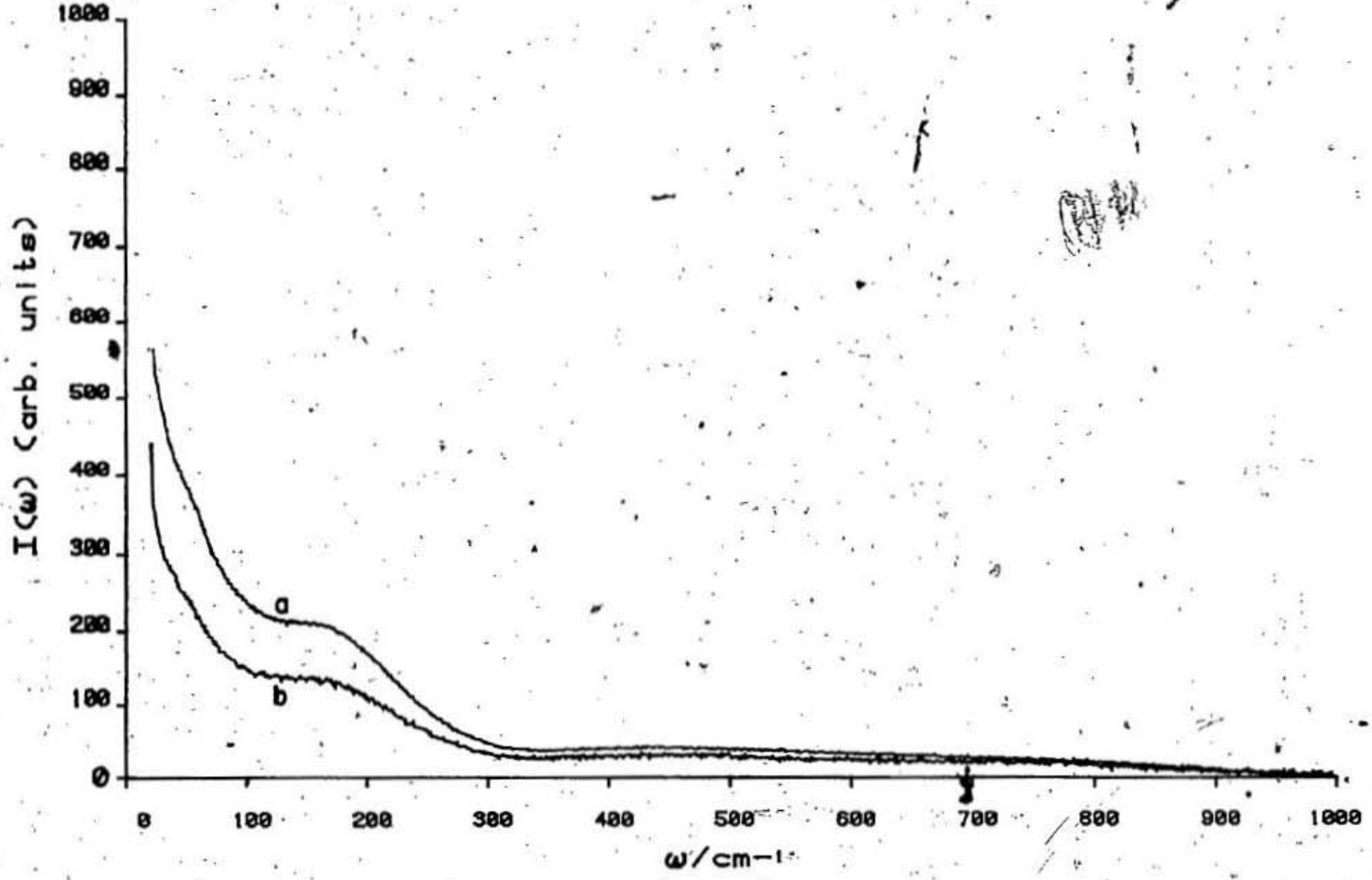
I(ω) (arb. units)
1000
900
800
700
600
500
400
300
200
100
0
a
b
0
100
200
300
400
500
600
700
800
900
1000
ω/cm⁻¹

ized and depolarized spectra. It is unclear as to whether any polarized Raman components are present since the drop in the Rayleigh scatter is so large when the polaroid analyzer is reoriented.

The spectrum of water in an $R(\omega)$ format appears in Fig. 2 and the data for H_2O, $H_2{}^{18}O$ and D_2O is given in Table 2.

Table 2

Low frequency spectral data for water

cm^{-1}

		$\nu_{O\cdots H-O}$ bend	$\nu_{O\cdots H-O}$ str	ν_{lib}
H_2O	I_{VV}	66 (68)	192 (252)	250 → 1000 (220) at 550
	I_{VH}	66 (40)	196 (162)	250 → 1000 (156) at 550
$H_2{}^{18}O$	I_{VV}	55 (215)	175 (482)	250 → 1000 (392) at 550
	I_{VH}	55 (170)	178 (408)	250 → 1000 (358) at 550
D_2O	I_{VV}	55 (187)	186 (466)	→ 800
	I_{VH}	55 (143)	186 (376)	→ 800

Brackets contain relative intensities.

A multi-component region exists between 300 cm^{-1} and 1000 cm^{-1}. No attempt has been made in this work to analyze the number of components in this region, but the presence of two or more bands is a necessity and due to the relatively steep slope on the high frequency wing it is probable that three peaks would be required. A fit of this region [33] from the

Fig. 2. $R(\omega)$ spectra for H_2O. Transformed I_{VV} data (a) and I_{VH} data (b) show the same band features as in Fig. 1 but with greater definition. The hydrogen bond stretch is seen at 192 cm^{-1} in the polarized spectrum and a weaker depolarized O···H–O bending mode is observed at 66 cm^{-1}. The band at 192 cm^{-1} is slightly polarized as demonstrated by the isotropic spectrum (c).

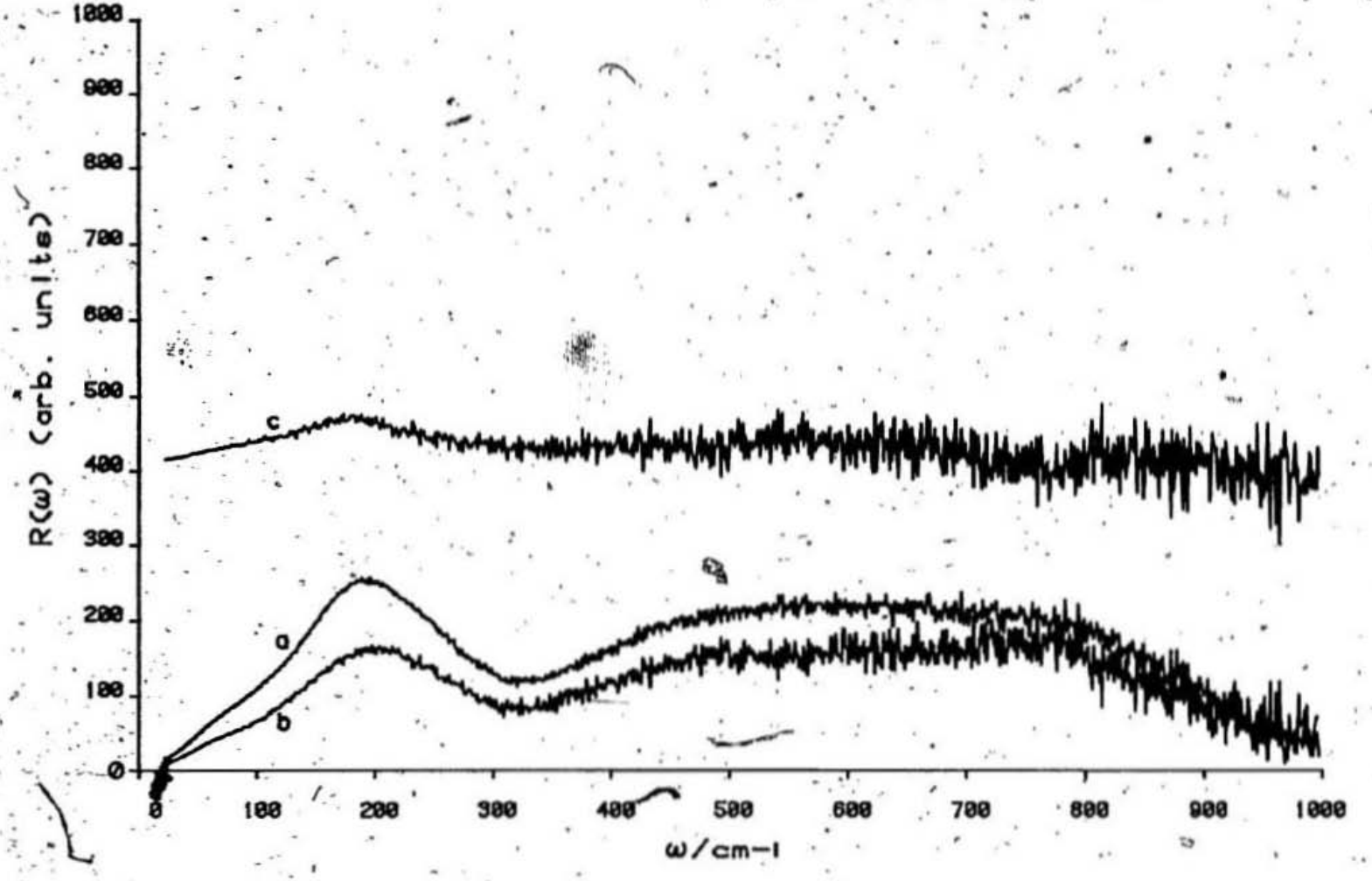
R(ω) (arb. units)
1000
900
800
700
600
500
400
300
200
100
0
c
a
b
0
100
200
300
400
500
600
700
800
900
1000
ω/cm-1

$I(\omega)$ format has incorporated three bands at 425, 550, and 740 cm^{-1} with half-widths ranging between 200 and 250 cm^{-1}. Below 300 cm^{-1} the bands in the $R(\omega)$ (Fig. 2) stand out more so than in the $I(\omega)$ format. The band assigned to the hydrogen bond stretching mode [4,6,7,10] appears at 192 cm^{-1} and the O···H-O bending mode occurs at about 66 cm^{-1}. No peaks are visible below 50 cm^{-1}. The subtraction spectrum shows a slight polarization characteristic for the 192 cm^{-1} band, but the maximum occurs at about 178 cm^{-1}. The depolarized spectrum shows the maximum at a slightly higher frequency than does the polarized spectrum. The reason for this difference is unclear but it might be due to the influence of stray Rayleigh scattered light.

The $I(\omega)$ and $R(\omega)$ spectra for $H_2{}^{18}O$ and D_2O are shown in Figs. 3 to 6. Comparison of the frequency range between 300 cm^{-1} and 1000 cm^{-1} for H_2O and $H_2{}^{18}O$ reveals little difference while the envelope for D_2O is shifted to lower frequencies. This independence of mass for the central atom and large dependence on mass for the attached atoms leads to the conclusion that the modes are librational in nature and confirms the earlier assignment of this region to librations of the water species [4]. The assignment of the 192 cm^{-1} band of water to O···H-O stretching is supported by the frequency shift to 175 cm^{-1} for $H_2{}^{18}O$ and 186 cm^{-1} for D_2O. The 66 cm^{-1} band drops in frequency to 55 cm^{-1} for both $H_2{}^{18}O$ and D_2O. Pure translational modes should exhibit frequency shifts of the ratio $(18/20)^{1/2} = 0.9487$ for both D_2O and $H_2{}^{18}O$. The shifts for the stretching modes of $H_2{}^{18}O$ and D_2O are 0.9211 and 0.9474 respectively. An independence of the O···H-O stretching mode with deuteration was reported in previous studies [4,7,10]. The present work reveals only a slight shift in this mode for D_2O. There is however a greater uncertainty

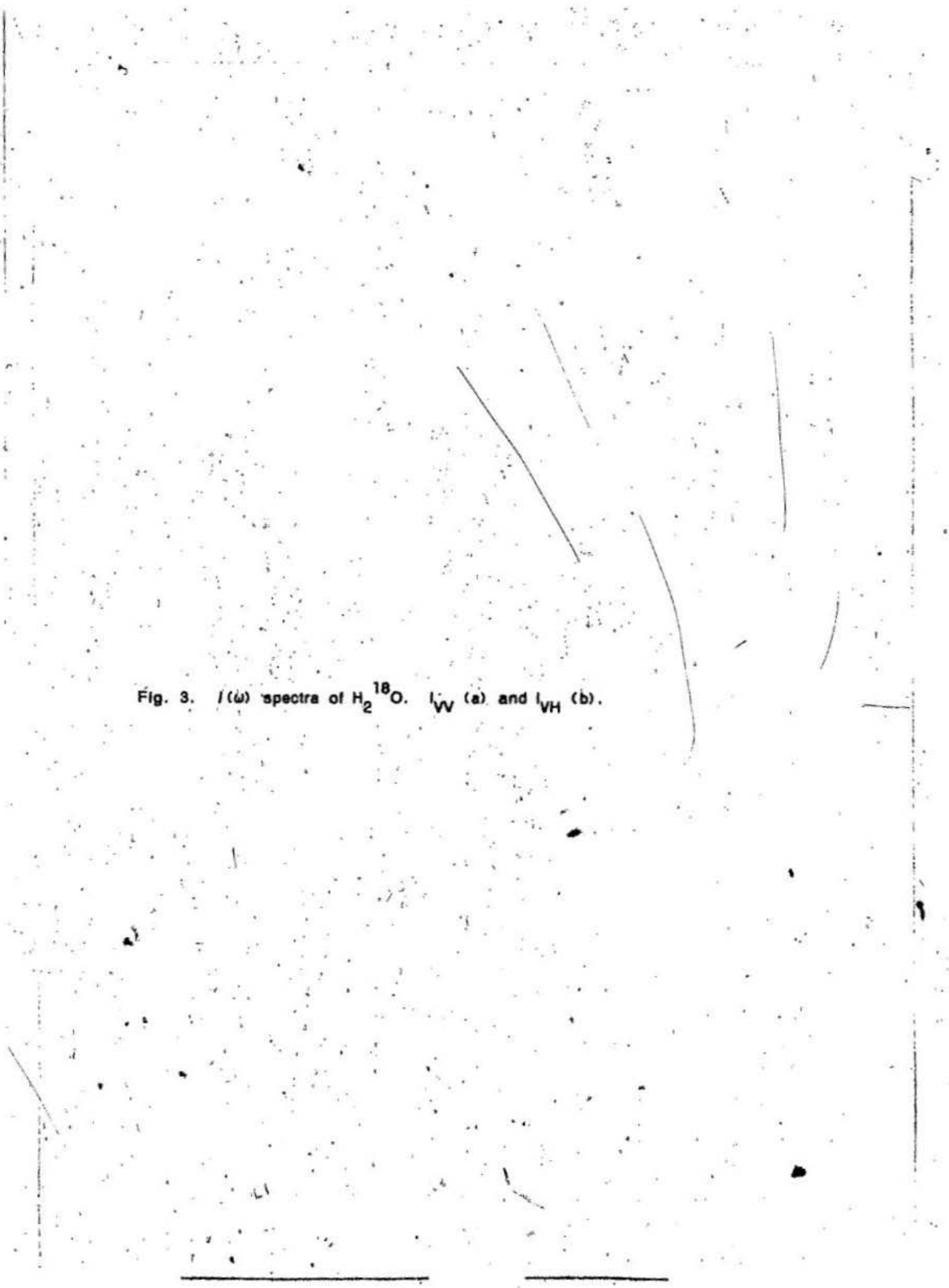

Fig. 3. $I(\omega)$ spectra of $H_2{}^{18}O$. I_{VV} (a) and I_{VH} (b).

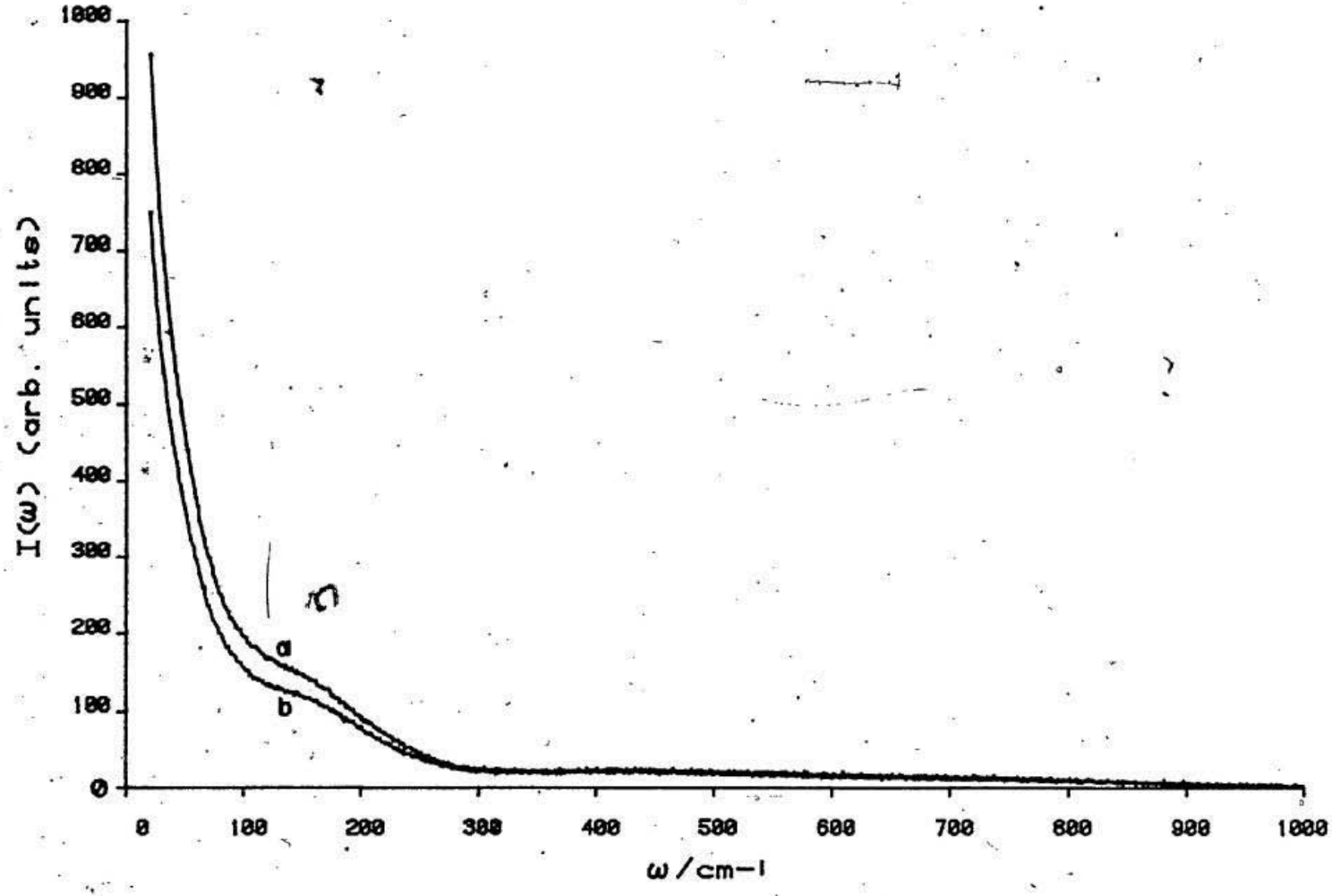
I(ω) (arb. units)
1000
900
800
700
600
500
400
300
200
100
0
a
b
0
100
200
300
400
500
600
700
800
900
1000
ω / cm-1

Fig. 4. $R(\omega)$ spectra for $H_2{}^{18}O$. Transformed I_{VV} (a) and I_{VH} (b) spectra show that the O···H–O stretch is slightly polarized and shifts 17 cm^{-1} from that of H_2O to 175 cm^{-1} confirming the assignment of this band to oxygen moving about the hydrogen [7]. The hydrogen bond bending mode is seen at 55 cm^{-1}.

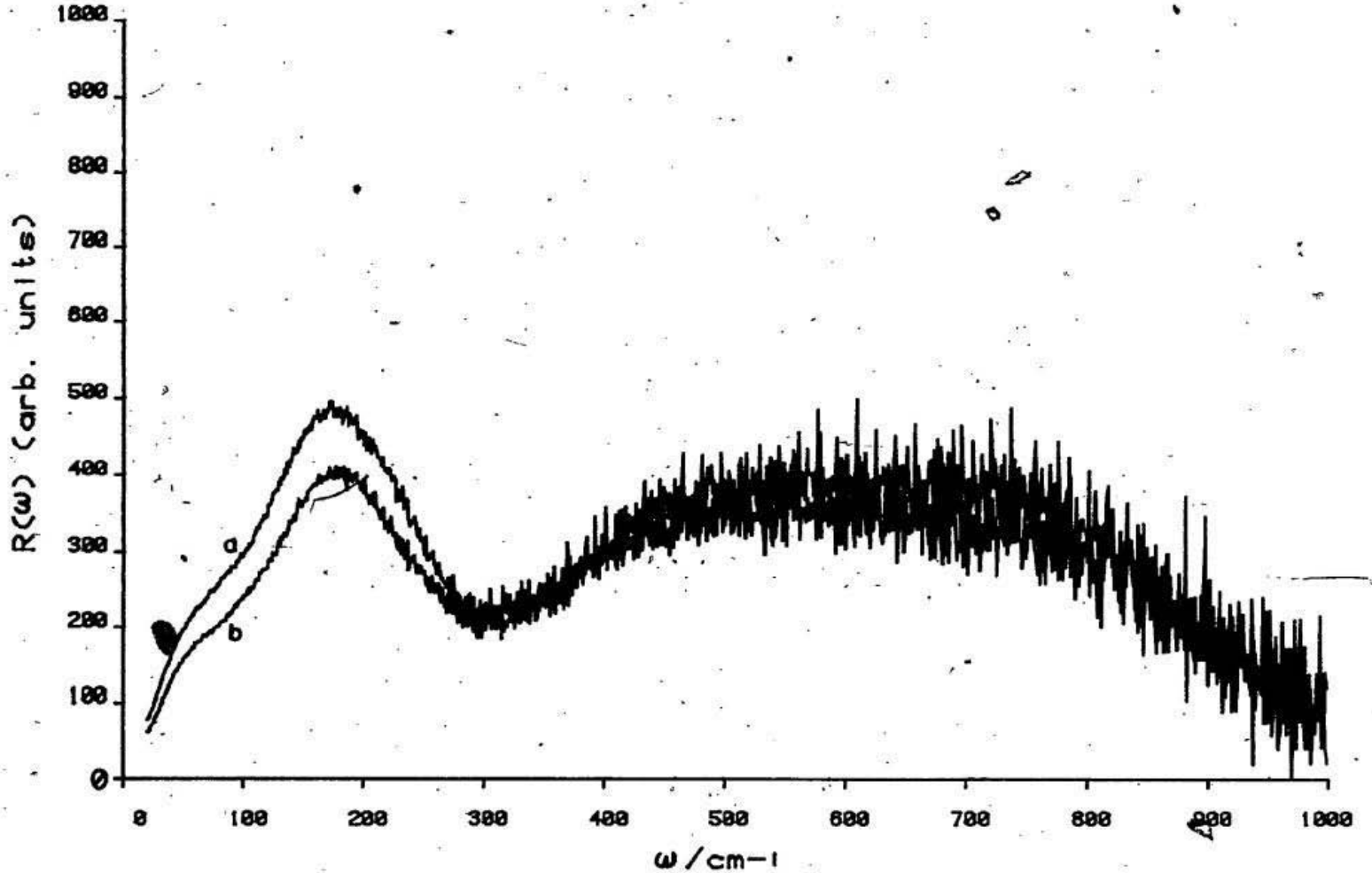
R(ω) (arb. units)
1000
900
800
700
600
500
400
300
200
100
0
a
b
0
100
200
300
400
500
600
700
800
900
1000
ω / cm-1

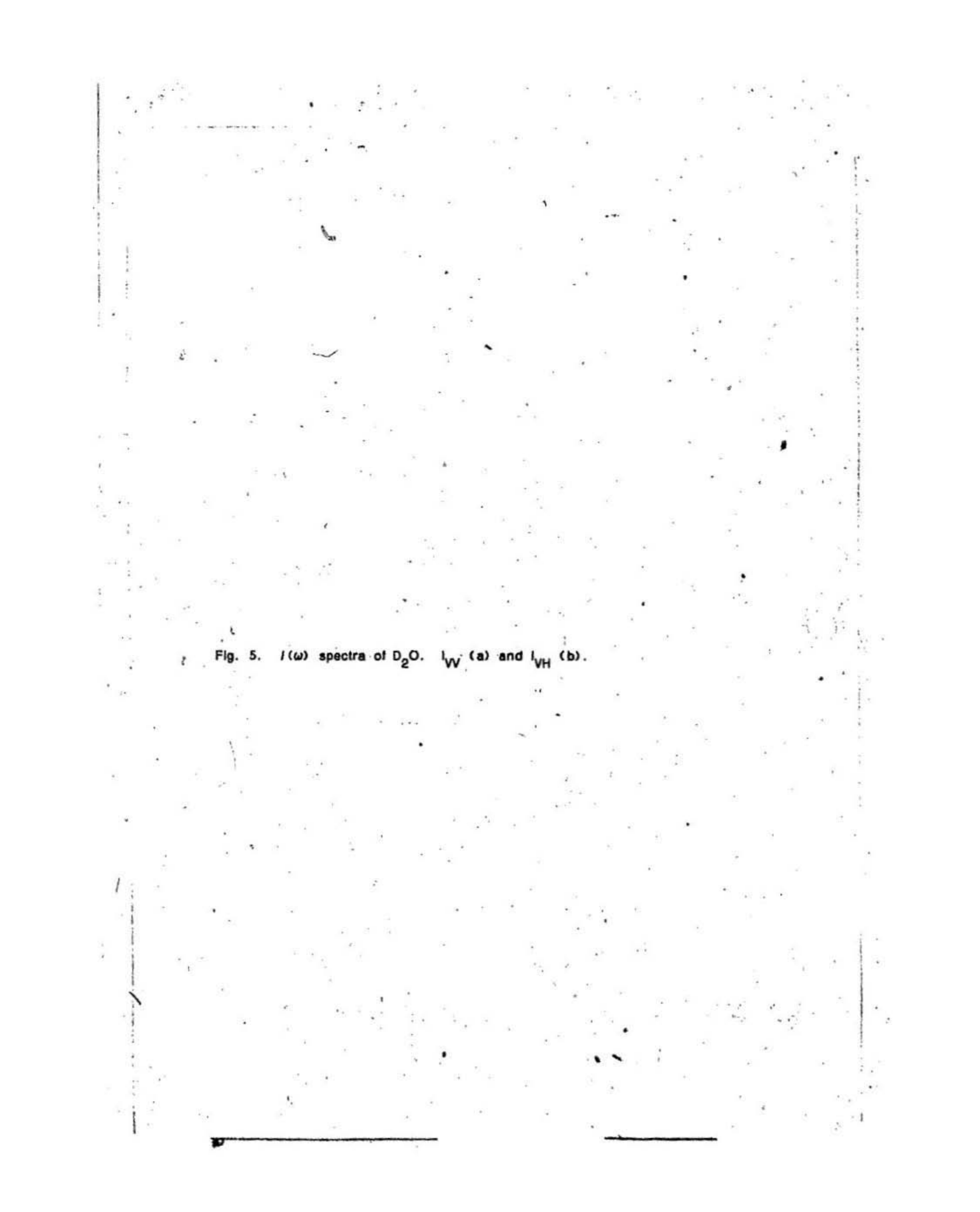

Fig. 5. $I(\omega)$ spectra of D_2O. I_{VV} (a) and I_{VH} (b).

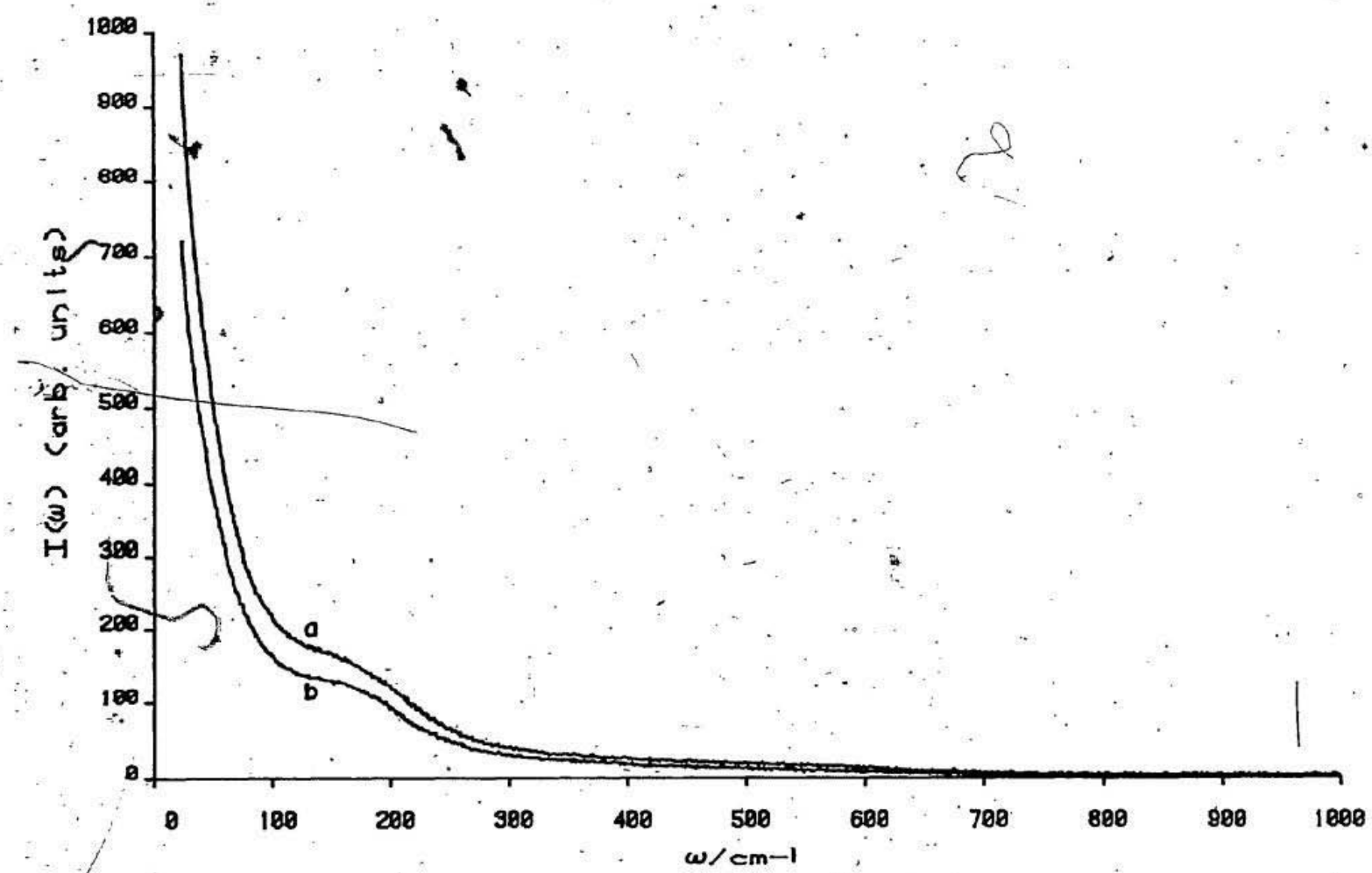
I(ω) (arb. units)
1000
900
800
700
600
500
400
300
200
100
0
a
b
0
100
200
300
400
500
600
700
800
900
1000
ω/cm⁻¹

Fig. 6. $R(\omega)$ spectra for D_2O. I_{VV} based data (a) and that of I_{VH} (b) show the librational region ending at about 800 cm^{-1}. The shift of the O···H–O stretching mode to 186 cm^{-1} suggests that the oxygens are moving about a non-stationary hydrogen.

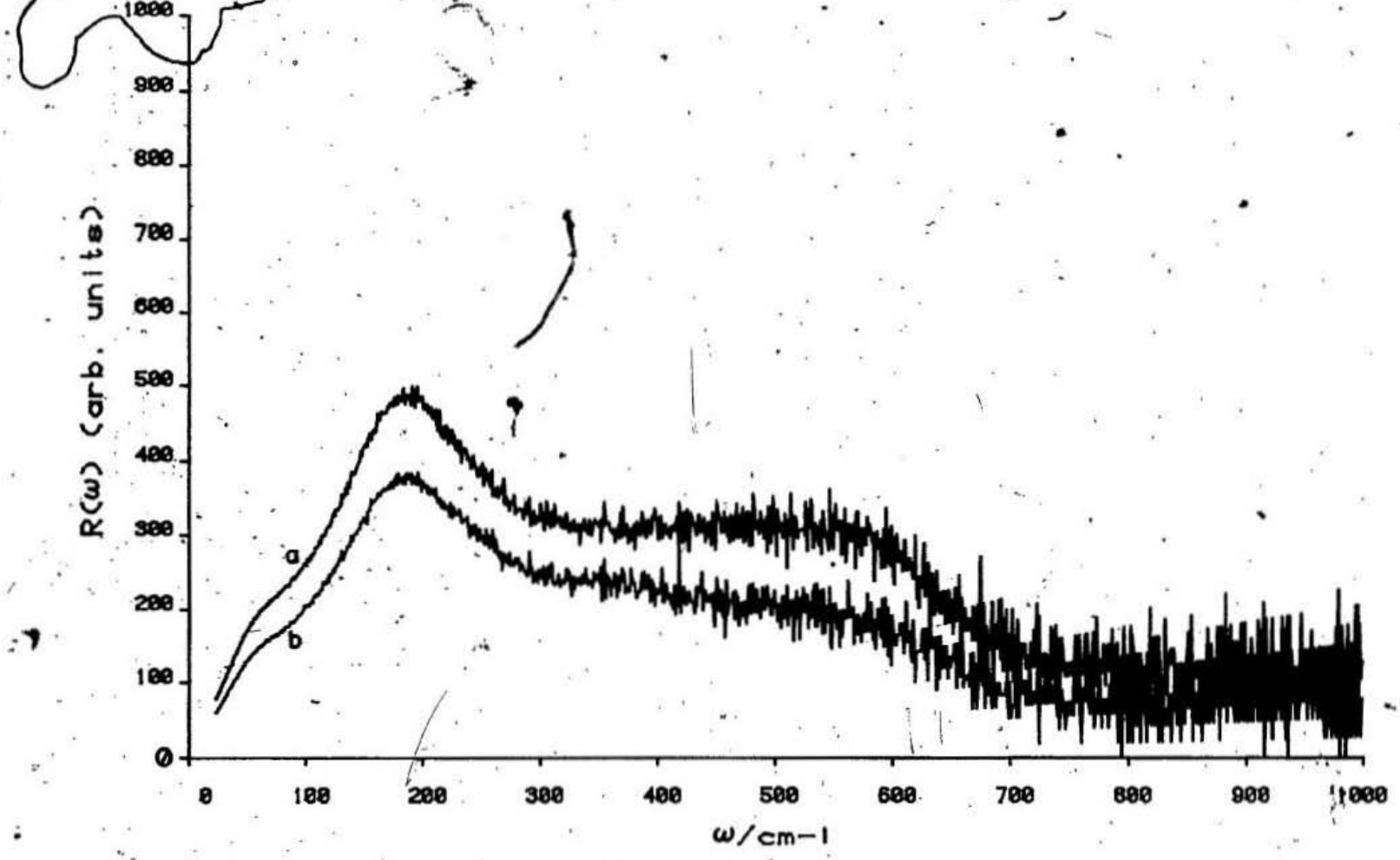
R(ω) (arb. units)
1000
900
800
700
600
500
400
300
200
100
0
a
b
0
100
200
300
400
500
600
700
800
900
1000
ω/cm−1

in the quote frequency (186 cm^{-1}) for the stretching mode because of overlap from the librational band. If the shift for the hydrogen bond stretching mode is real then the picture of two oxygens moving about the hydrogen as suggested by Brooker and Perrot [7] should be adjusted to show oxygen movement about a non-stationary hydrogen, i.e. the hydrogen remains closer to one of the oxygens, the oxygen to which it is hydrogen bonded. This would be further support for the assignment of the 192 cm^{-1} band in the Raman spectrum of water to a restricted translation of a water molecule from an intermolecular hydrogen-oxygen bond.

Moskovits and Michaelian [6] have reported a band at 170 cm^{-1} in the $I(\omega)$ spectrum for H_2O with a shift to 160 cm^{-1} for D_2O as a restricted translation mode. They also reported this band to be depolarized, the bands of the librational region to be weakly polarized, and the presence of a weak slightly polarized band at 290 cm^{-1}. No support for these findings were observed in the present study.

The comparison of the $R(\omega)$ depolarized spectrum of water and IR absorption coefficients for water, taken from [34], is presented in Fig. 7. It is apparent that the two have some similar features. Librations cover the same region and the contour of the wings of the envelopes are roughly the same. Deviation in the contours occur between 500 and 700 cm^{-1} and is to be expected as the different selection rules will cause certain modes to be inactive or active to different extents. In the translation region, the peak maxima positions almost coincide. The 66 cm^{-1} band is not evident from the IR data shown. The overlay of the wing intensities in the libration region is purely accidental as no scale matching was performed. Still, the plot does show some support for Lund's definition of $R(\omega)$ [10, 28].

Fig. 7. Comparison of (a) the $R(\omega)$ spectra for H_2O from I_{VH} data with (b) $\alpha(\omega)$ for H_2O from refractive index infrared studies [34].

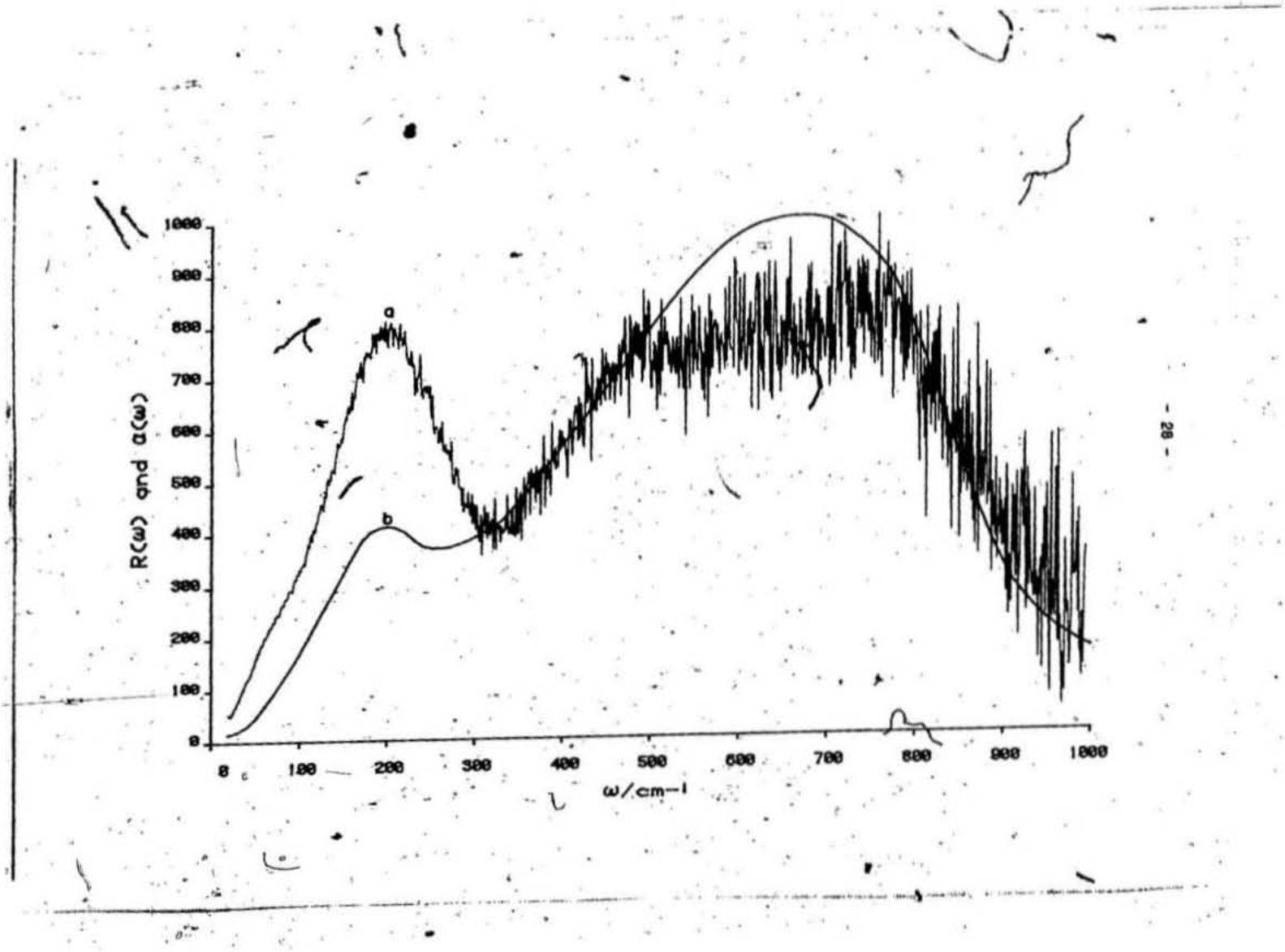
R(ω) and α(ω)
1000
900
800
700
600
500
400
300
200
100
0
a
b
0
100
200
300
400
500
600
700
800
900
1000
ω/cm-1

Addition of cations

It has been previously shown that additions of ions to water causes changes in the infrared contour of the 20 → 1000 cm^{-1} region [14, 16, 19]. Various ions are able to enhance or reduce the intensity in certain regions. Others still, show contributions from the ions themselves. In the Raman it has been reported that anionic species cause measurable enhancement of the intensity of the librational region [4]. However, in this study, it will be shown that the addition of anions to water can also alter the spectra of the region below 300 cm^{-1} and in some cases contribute bands which are due to the reorientations of the anion itself. The effects on the spectrum of water from the addition of cations are reported as being very weak and to date are unavailable. The $I(\omega)$ Raman spectra for water and saturated aqueous solutions of $CaCl_2$, $MgCl_2$ and LiCl appear in Figs. 8 and 9. These spectra were scaled with an internal reference and show the true ratio of the intensities of the scattered light. The effects of the different cations are clearly visible both with respect to the intensity and the band shape.

The $R(\omega)$ spectra for these same solutions are presented in Figs. 10 and 11 and are summarized in Table 3. Difference spectra were constructed to reveal the I_{ISO} spectrum from $I_{VV} - 4/3\ I_{VH}$ and are included. The true meaning of the changes observed is not completely clear. What can be said to be true is that with the addition of these salts there is an increase in structure of the solution, the degree of which is not as independent of cationic species as once thought [1]. The band shape of the water libration region undergoes many changes with the various cations used, and the 192 cm^{-1} band of water is shifted to higher frequencies (196 cm^{-1} for $CaCl_2$, 204 cm^{-1} for $MgCl_2$ and 193 cm^{-1} for LiCl) and

Fig. 8. I_{VV} Raman spectral data for saturated solutions of (a) $CaCl_2$, (b) $MgCl_2$, (c) LiCl, and that of water (d). The spectra were intensity scaled by the use of a 0.5M KNO_3 internal standard.

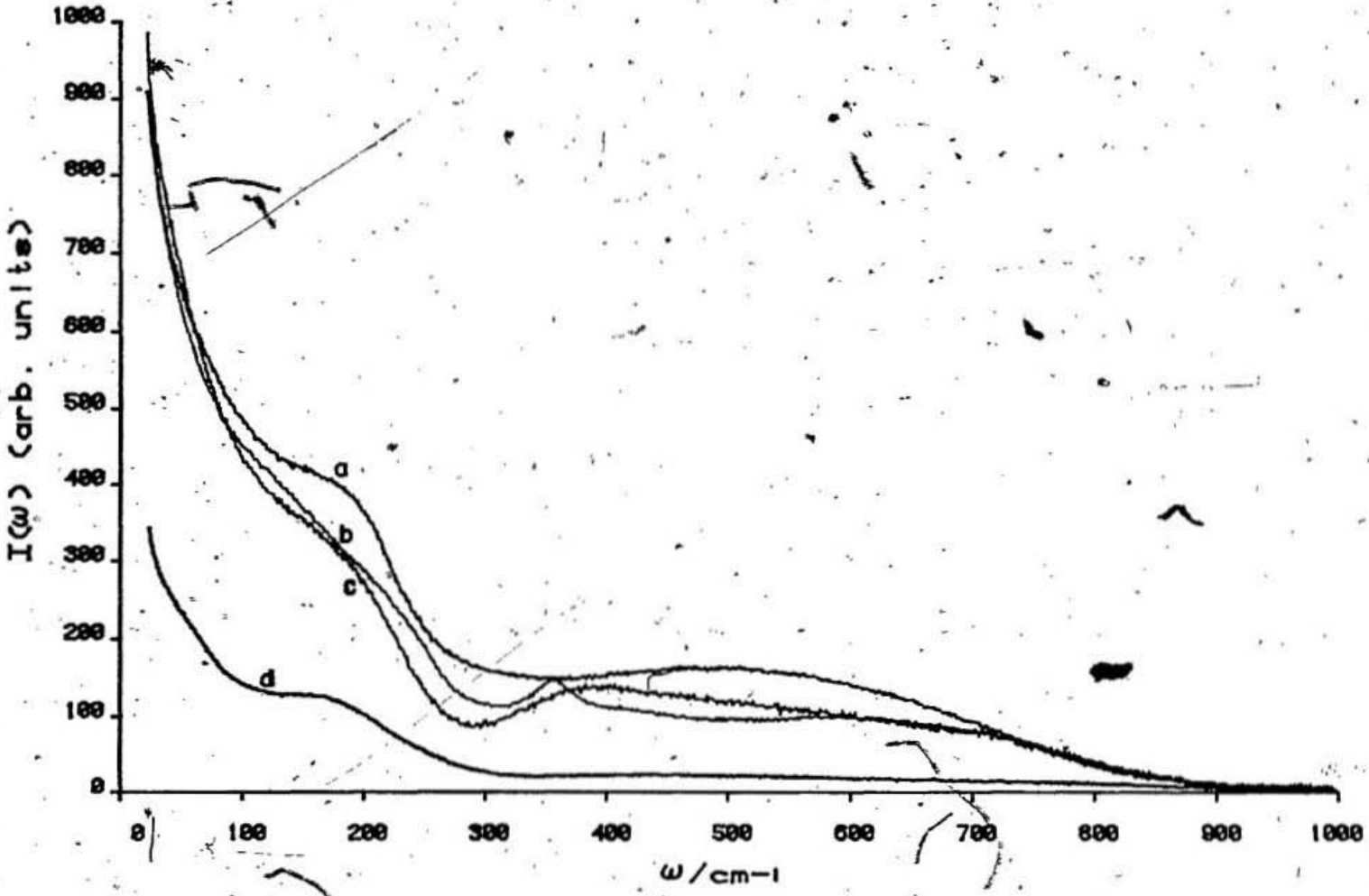
I(ω) (arb. units)
1000
900
800
700
600
500
400
300
200
100
0
a
b
c
d
0
100
200
300
400
500
600
700
800
900
1000
ω / cm-1

Fig. 9. I_{VH} Raman spectral data for saturated solutions of (a) $CaCl_2$, (b) $MgCl_2$, (c) LiCl, and for water (d) intensity scaled with a 0.5M KNO_3 internal standard.

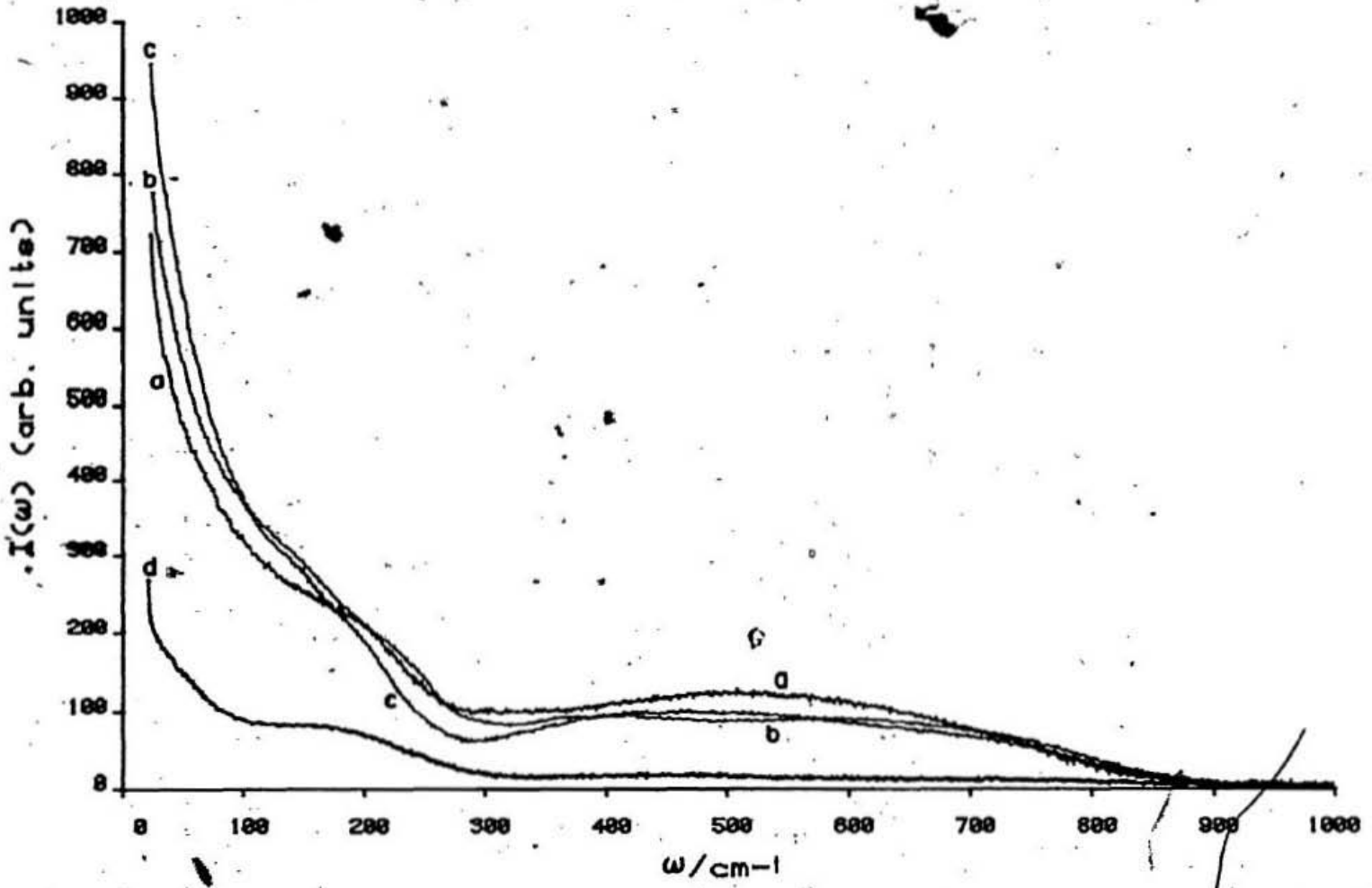
I(ω) (arb. units)
ω/cm-1
a
b
c
d
1000
900
800
700
600
500
400
300
200
100
0
0
100
200
300
400
500
600
700
800
900
1000

Fig. 10. $R(\omega)$ spectra from transformed I_{VV} spectral data for saturated aqueous chloride solutions. The 192 cm^{-1} band of water (d) shifts to 196 cm^{-1} for $CaCl_2$ (a), 204 cm^{-1} for $MgCl_2$ (b) and 193 cm^{-1} for LiCl (c). Various changes in the contour of this region show that cation effects on the spectrum of water are real.

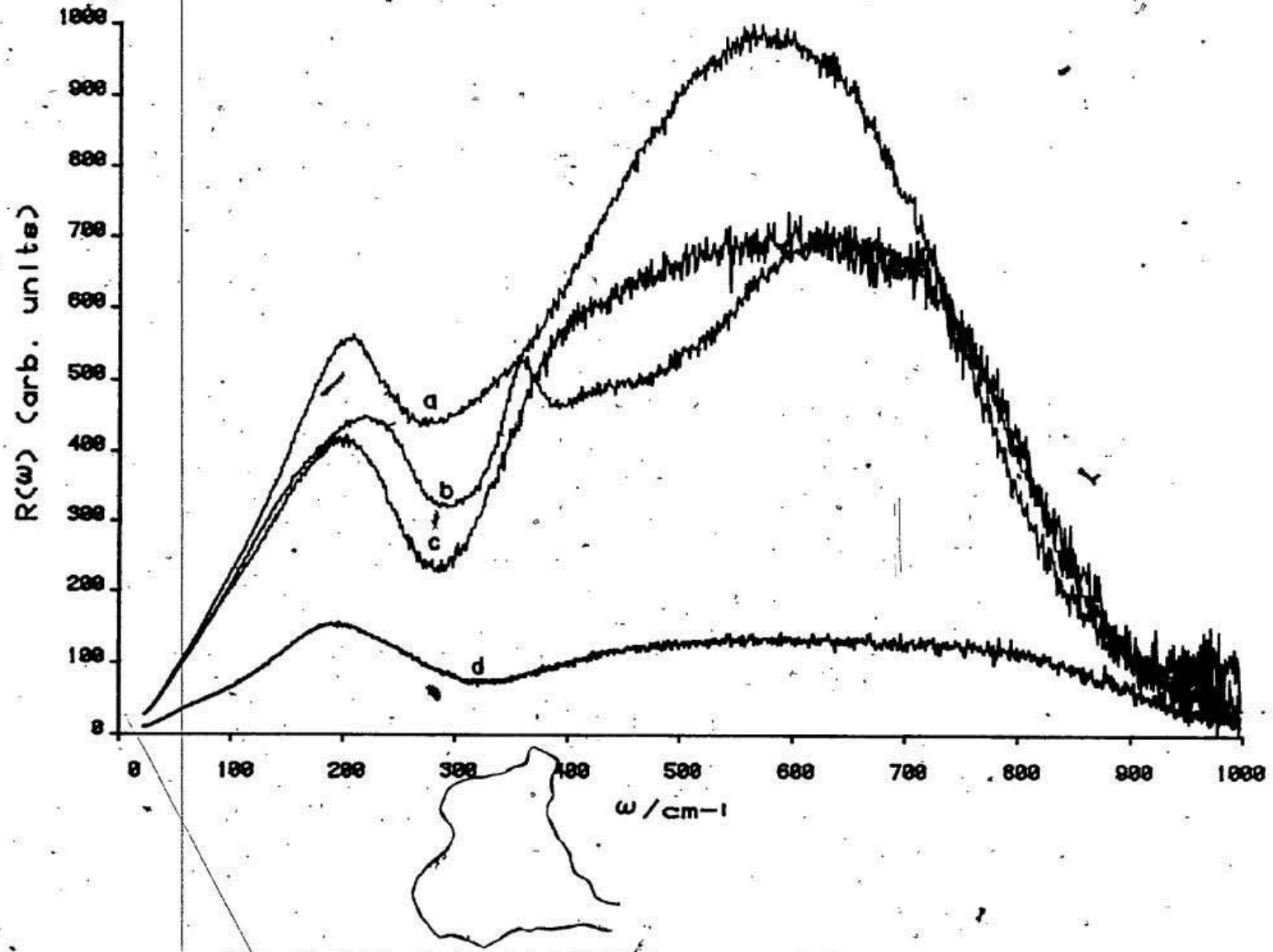
R(ω) (arb. units)
1000
900
800
700
600
500
400
300
200
100
0
a
b
c
d
0
100
200
300
400
500
600
700
800
900
1000
ω / cm-1

Fig. 11. $R(\omega)$ spectra from transformed I_{VH} spectral data for saturated aqueous chloride solutions. $CaCl_2$ (a), $MgCl_2$ (b), LiCl (c), and H_2O (d).

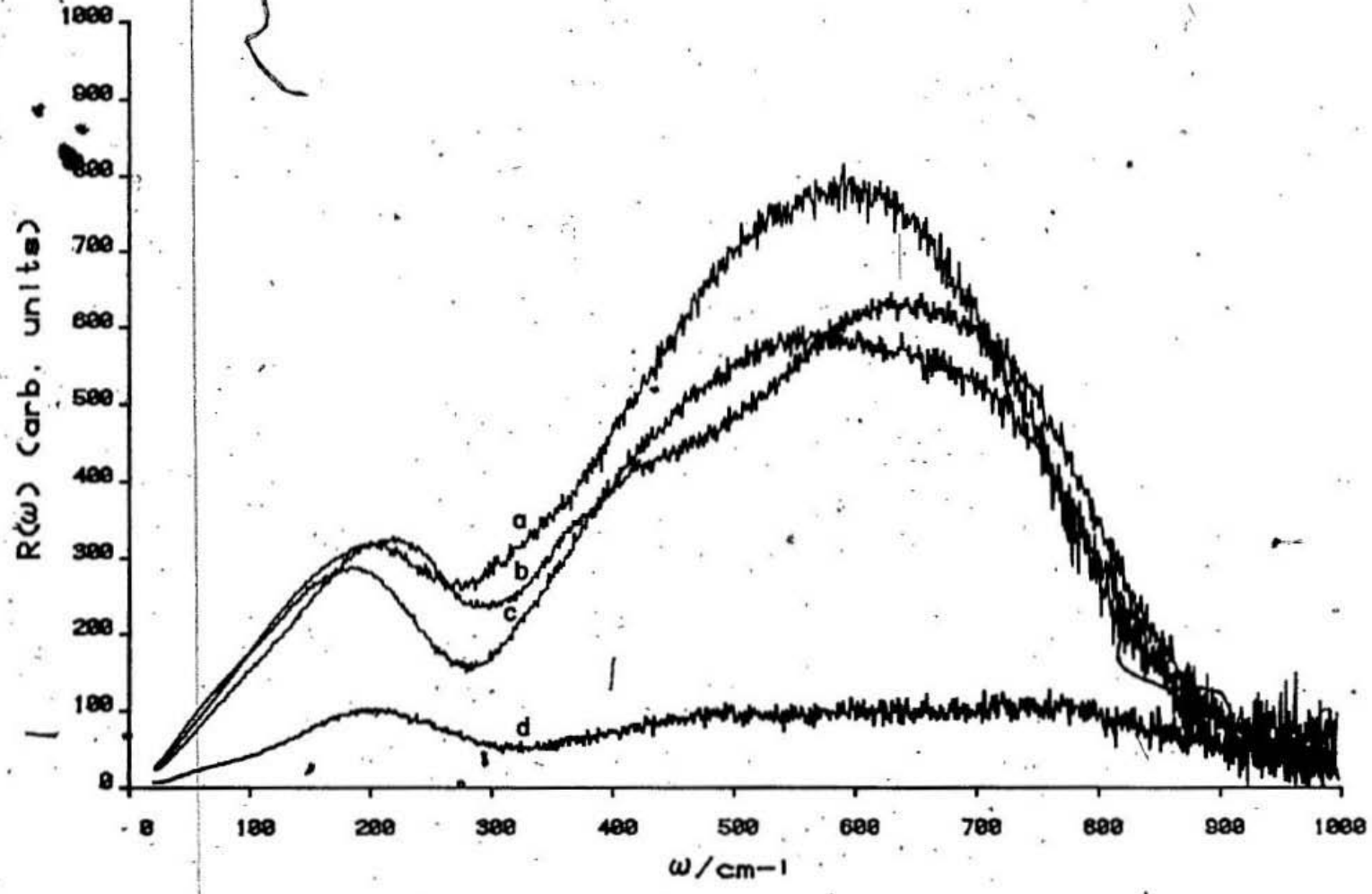
R(ω) Carb. units
1000
900
800
700
600
500
400
300
200
100
0
0
100
200
300
400
500
600
700
800
900
1000
ω / cm-1
a
b
c
d

Table 3

Spectral data for saturated alkali and alkaline earth chloride solutions

		$\nu_{O\cdots H-O\ str}$ / cm^{-1}	$\nu_{M\cdots O\ str}$ / cm^{-1}	ν_{IIb} / cm^{-1}
$CaCl_2$	I_{VV}	196 (275)		574 (1000)
	I_{VH}	195 (136)		593 (778)
$MgCl_2$	I_{VV}	204 (230)	361 (158)	648 (694)
	I_{VH}	195 (160)	361 (88)	643 (628)
LiCl	I_{VV}	193 (406)	396	597 (694)
	I_{VH}	186 (289)		569 (586)
H_2O	I_{VV}	192 (154)		550 (135)
	I_{VH}	195 (100)		550 (94)

Brackets contain relative intensities.

increases in intensity. This is contrary to that reported in [4] and implies some cation enhancement of the O···H–O stretch. The band at 66 cm^{-1} in water is absent from the aqueous solution spectra. Although the ions present were chosen so as not to contribute scattering due to their own anisotropy, changes in band maxima and shape cannot be interpretated as solely due to enhanced water modes. The presence of weakly hydrated species could give rise to such changes.

Clement and Fourche have recorded total Rayleigh scattering intensity at zero frequency for these chloride solutions to 1M concentrations [15]. The ratio of intensities for their work and the present study are given in Table 4. The difference in magnitude between the two sets of data are probably due to concentration differences. The two studies show the

Table 4

Ratio of scattering intensities for aqueous chloride solutions

	$R(\nu)$ at 293 cm^{-1}	ref. [15]
H_2O	1.00	1.00
LiCl	3.03	1.16
$MgCl_2$	4.02	1.33
$CaCl_2$	4.69	>>> 1.51

scatter for $CaCl_2$ > $MgCl_2$ > LiCl > H_2O and suggest a stronger ability for solutions to scatter light with increasing size of the cation present. In fact these workers reported that the intensity from hydrated chloride is very weak and that most of the intensity of the Rayleigh scatter is a result of hydrated cations and water.

Thermodynamic calculations [35] indicate that the presence of hydrated cationic species is more probable than anionic hydrates for the same charge/mass ratio. Vibrational modes due to metal oxygen vibrations of discrete $M(H_2O)_6^{2+}$ species are well documented [2]. For $Mg(H_2O)_6^{2+}$, the A_{1g} symmetric stretch is assigned to a polarized band at 362 cm^{-1} [36]. The presence of this band and its polarized character are shown in Fig. 12 and Table 5. The difference spectrum shows the partially polarized character of the 204 cm^{-1} peak and the symmetric stretch at 359 cm^{-1}. Above this band, the difference spectrum is flat indicating the pure depolarized nature of this region. From examination of the depolarized spectrum for the $MgCl_2$ solution, it is apparent that there exists some underly-

Fig. 12. $R(\omega)$ spectra for saturated $MgCl_2$ (aq). The isotropic component (c) is created from I_{VV} (a) − 4/3 I_{VH} (b). Polarized peaks at 222 cm^{-1} and 359 cm^{-1} represent the O···H–O stretching and M···O stretching modes respectively in the solution. The flat portion of the difference spectrum from 500 → 1000 cm^{-1} indicates the pure depolarized nature of this region.

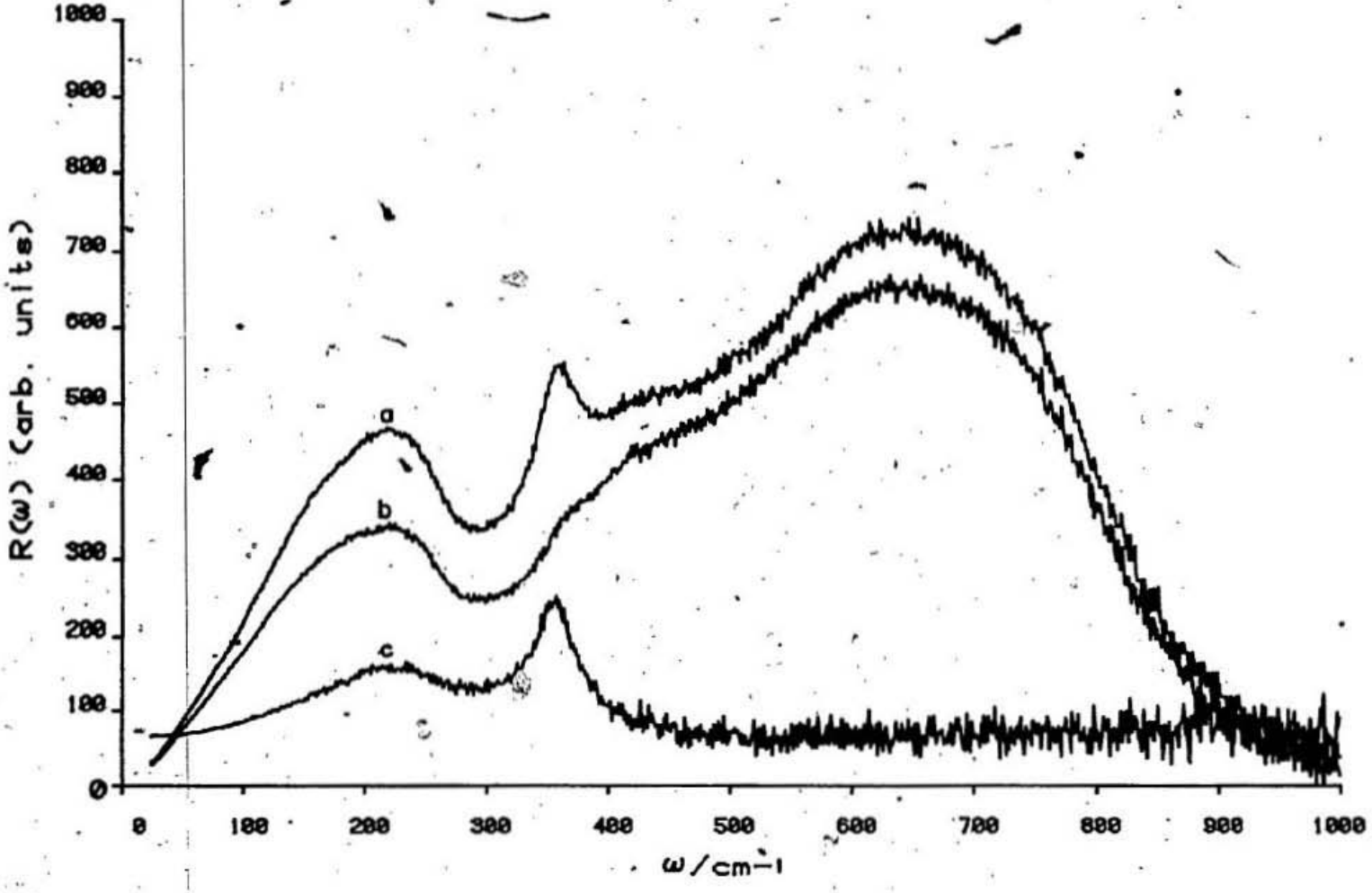
R(ω) (arb. units)
1000
900
800
700
600
500
400
300
200
100
0
a
b
c
0
100
200
300
400
500
600
700
800
900
1000
ω/cm⁻¹

Table 5

I_{ISO} for saturated aqueous alkali and alkaline earth chloride solutions

cm^{-1}

	$\nu_{O\cdots H-O}$ str	$\nu_{M\cdots O}$ str
$MgCl_2$	222 (93)	359 (165)
LiCl	220 (74)	384 (98)
$CaCl_2$	195 (151)	

Brackets contain relative intensities.

ing intensity in the 350 → 450 cm^{-1} region. Additional bands may arise from the E_g and F_{2g} Raman active internal modes of the octahedral complex. These modes are the ν_2 and ν_5 respectively and usually occur lower in frequency than the symmetric stretch. In the case of $Al(H_2O)_6^{3+}$, ν_1 appears at 542 cm^{-1}, ν_2 at 473 cm^{-1} and ν_5 at 347 cm^{-1} [37]. The bands present in the depolarized spectrum of $MgCl_2$ occur at the same frequency as the symmetric stretch and higher. The band at 361 cm^{-1} may be the residual of the symmetric stretch or ν_5 with a frequency quite close to ν_1 as ν_2 is rarely seen. The presence of depolarized intensity at 420 cm^{-1} does not fit the pattern for octahedral species and may just be due to intensity enhancement of one of the water librational components.

The Li^+ ion is reported to be hydrated in aqueous solutions with a tetrahedral arrangement of water molecules for dilute solutions with an A_1 mode at 440 cm^{-1}. Ion aggregates or solvent separated ion pairs in saturated solutions have been reported to give a polarized band at 360

cm^{-1} [12]. In the present study a single polarized band was observed at 384 cm^{-1} for saturated LiCl through the use of a difference spectrum (Fig. 13). The existence of a depolarized band at 400 cm^{-1} as claimed by Michaelian and Moskovits [38] was not observed. The authors report resulted from a difference spectrum between a pure water spectrum and the aqueous solution spectrum and it was assumed that the new bands arising were due solely to the interactions of the ions with water. This, of course, neglects the fact that the water spectrum itself may be different in the salt solution than it is in the pure state. Whether or not the band at 384 cm^{-1} is due to the A_1 mode of the tetrahedral hydrate of the lithium ion or an ion aggregate symmetric stretch of the type:

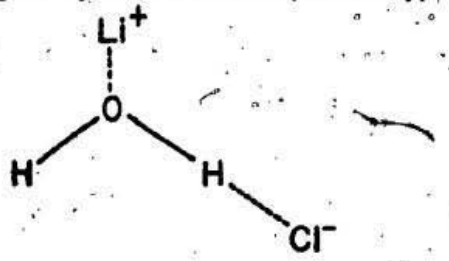

cannot be concluded without further isotope studies using the $R(\omega)$ format for analysis. The shift of a polarized band at 360 cm^{-1} for $^6Li^+$ to 335 cm^{-1} for $^7Li^+$ in saturated chloride solutions reported by Nash [12] was assigned to solvent separated ion aggregates. The polarized bands were extracted from curve resolving of $I(\omega)$ spectra. This technique can be unreliable in the low frequency region where background intensity from Rayleigh scattering is high. The original unresolved spectra reported by Nash are similar to those presented in this study.

The $R(\omega)$ spectra in Fig. 14 show the results for $CaCl_2$. A hexahydrate species has been assigned a $Ca^{2+}\cdots OH_2$ stretch at about 390 cm^{-1} [39] but it is generally believed to be too weak to be seen. Unfor-

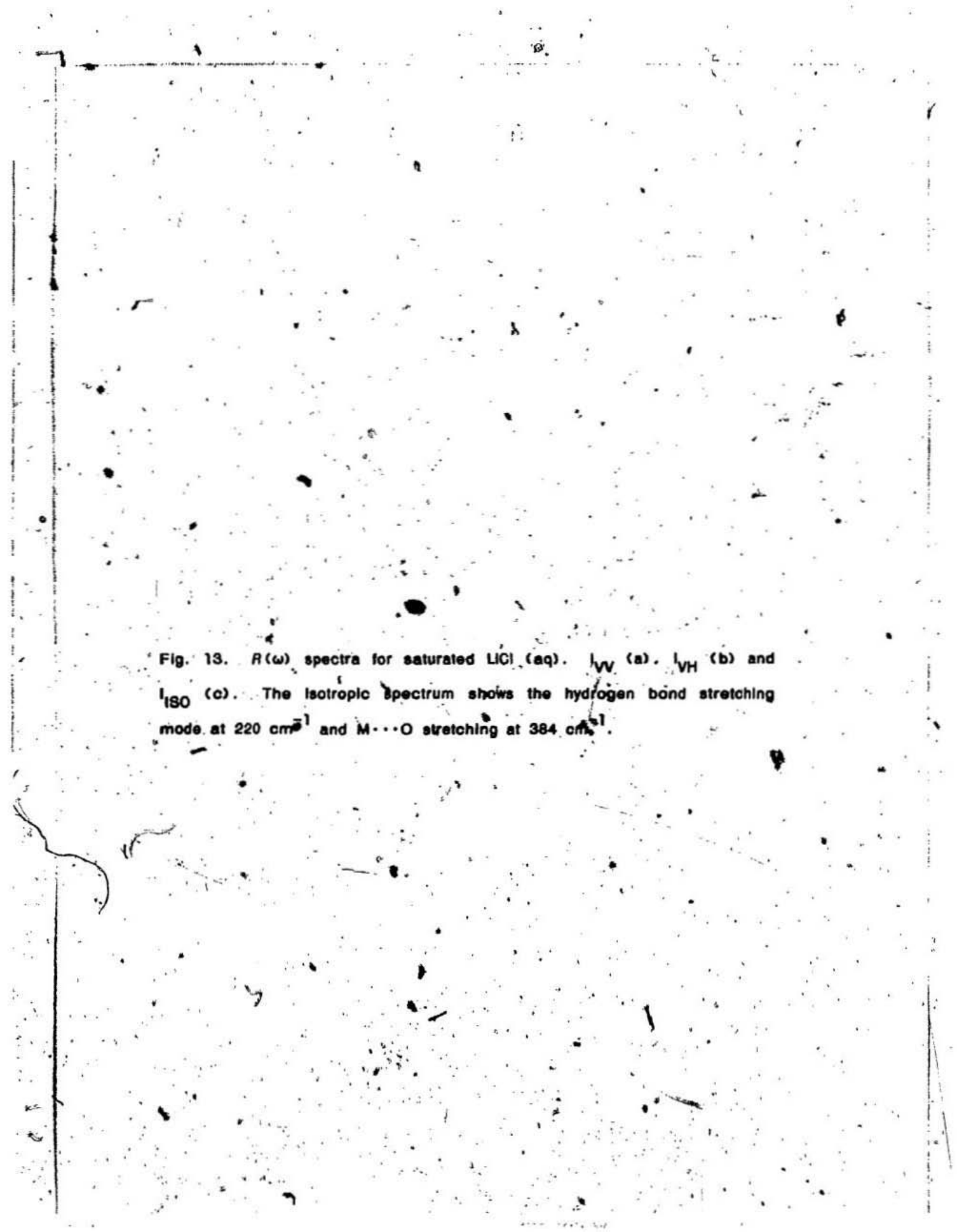

Fig. 13. $R(\omega)$ spectra for saturated LiCl (aq). I_{VV} (a). I_{VH} (b) and I_{ISO} (c). The isotropic spectrum shows the hydrogen bond stretching mode at 220 cm^{-1} and M···O stretching at 384 cm^{-1}.

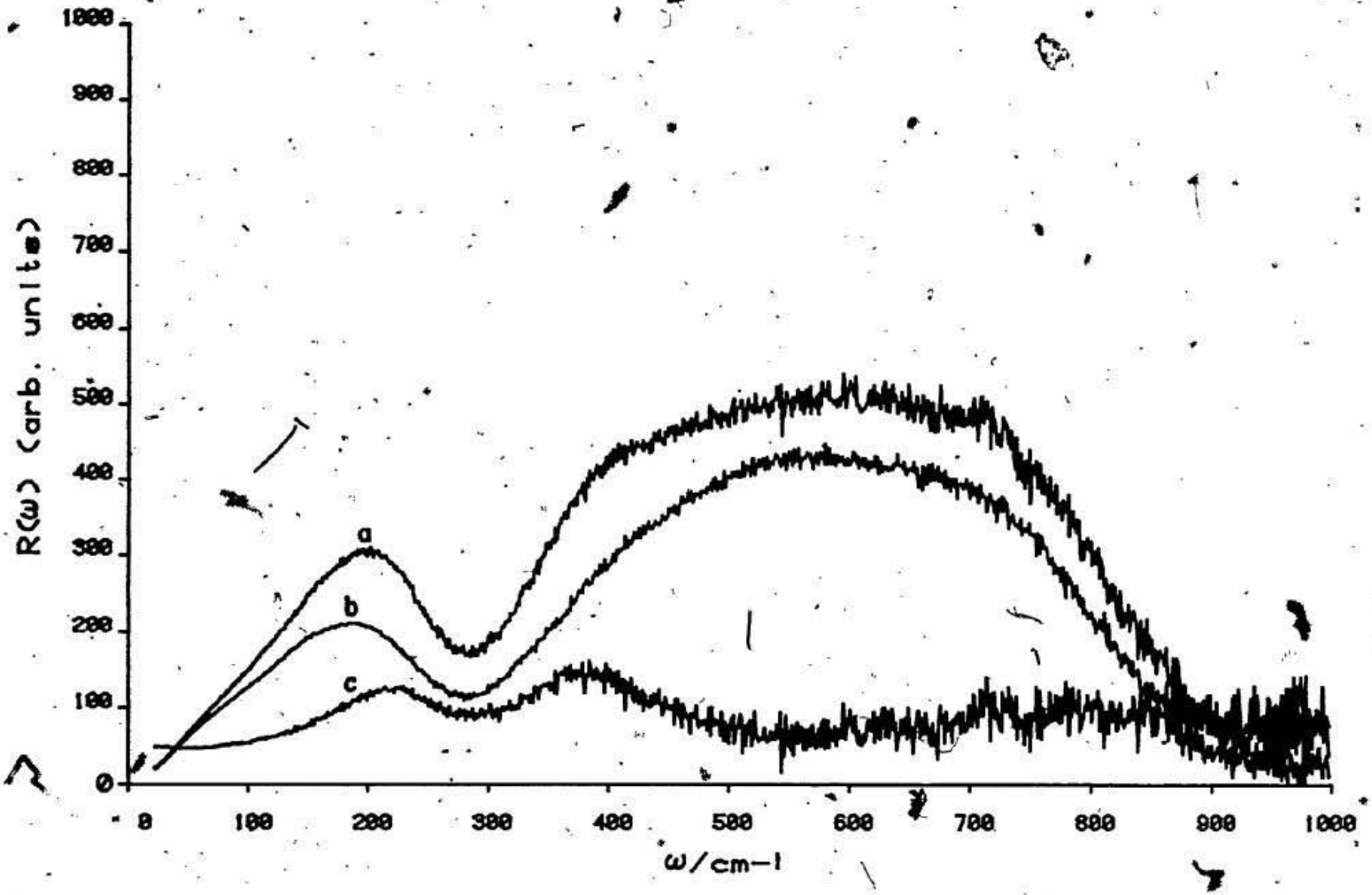
R(ω) (arb. units)
1000
900
800
700
600
500
400
300
200
100
0
a
b
c
0
100
200
300
400
500
600
700
800
900
1000
ω/cm-1

Fig. 14. $R(\omega)$ spectra for saturated $CaCl_2$ (aq). I_{VV} (a). I_{VH} (b) and I_{ISO} (c). The O···H–O stretching band appears at 195 cm^{-1} but no evidence of a discrete band arising from the stretching of the hydrated Ca^{2+} ion is observed.

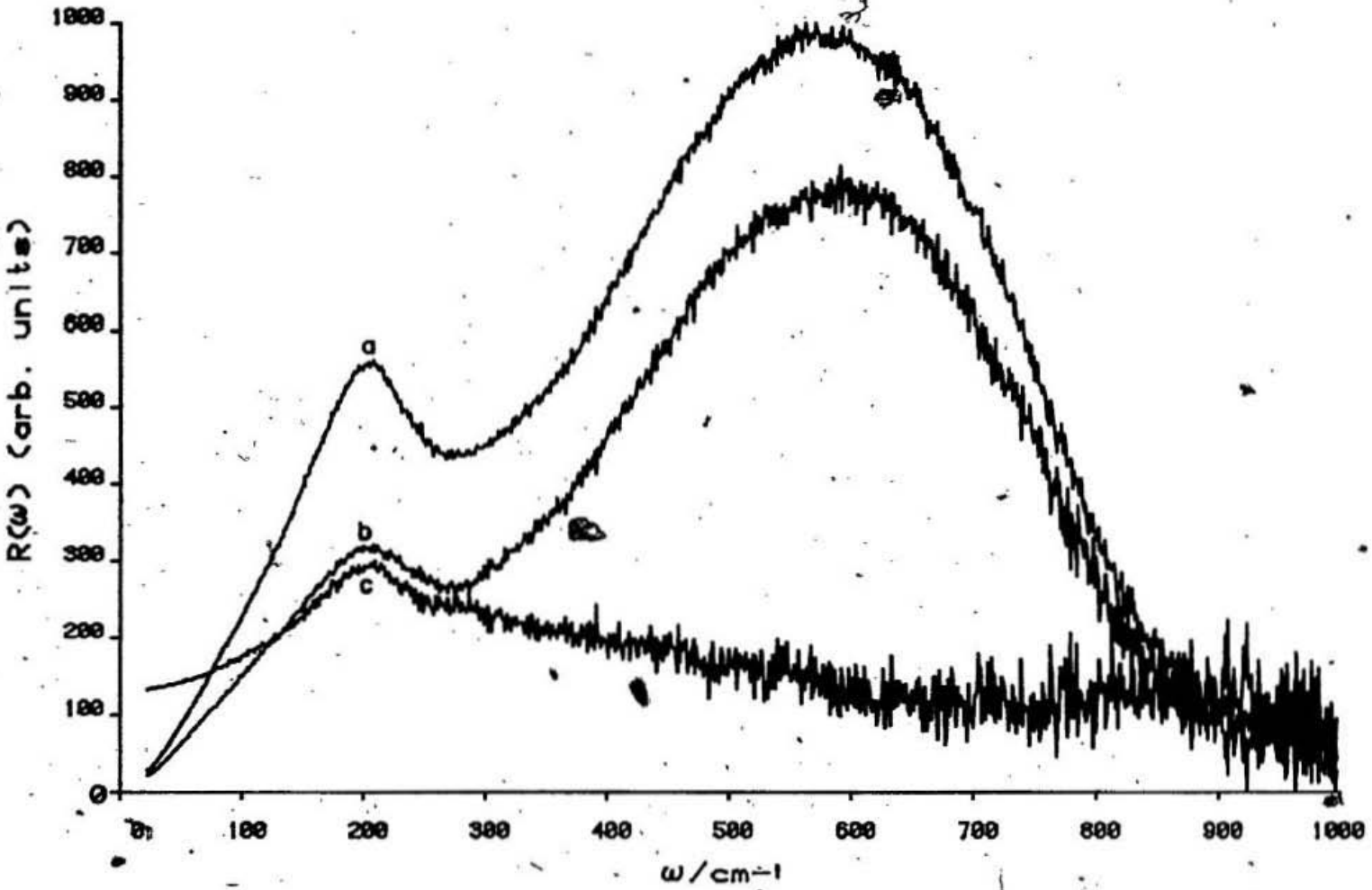
R(ω) (arb. units)
1000
900
800
700
600
500
400
300
200
100
0
a
b
c
0
100
200
300
400
500
600
700
800
900
1000
ω / cm⁻¹

tunately, no support is found from the $R(\omega)$ spectrum for either viewpoint. Aside from the slightly polarized 195 cm^{-1} band, the difference spectrum shows only a broad slowly decreasing polarized signal continuing out to about 700 cm^{-1}.

Addition of anions

Anisotropic anions added to water can themselves give rise to low frequency Raman bands as well as affect the bands due to the water itself. NO_3^- has been shown to have a hindered rotational band at 93 cm^{-1} and CN^- a band at 133 cm^{-1} [7]. The depolarized spectra of saturated (8.10 m) aqueous K_2CO_3 and 1 M aqueous K_2CO_3 scaled as a function of concentration using the CO_3^{2-} band at 1063 cm^{-1} as an internal reference are shown in Fig. 15. Below 350 cm^{-1} two bands are observed and their frequencies are listed in Table 6.

Table 6

I_{VH} data for K_2CO_3

cm^{-1}

	$\nu_{CO_3^{2-}}$ hin. rot.	$\nu_{O\cdots H-O}$ str	ν_1
K_2CO_3 (sat.)	92 (22.3)	196 (236)	1063 (1000)
K_2CO_3 (1 M)	70 (6.4)	186 (61)	1063 (128)

Brackets contain relative intensities.

The shift in of the O···H–O stretch for water at 186 cm^{-1} to 196 cm^{-1} and the growth in intensity of this band with $[K_2CO_3]$ are both results of increased hydrogen bonding in solution from a larger presence of CO_3^{2-}. With the spectra redrawn and intensities normalized to the O···H-O stretch band (Fig. 16), there is clear evidence for growth of the

Fig. 15. $R(\omega)$ spectra of 1 mol L^{-1} and saturated aqueous K_2CO_3 solutions from 0 → 1000 cm^{-1}. The saturated solution (8.10 m) (a) and the 1 mol L^{-1} solution (b) were intensity scaled as a function of concentration at the CO_3^{2-} ν_1 (1063 cm^{-1}). The increased intensity below 300 cm^{-1} for the saturated solution shows additional structuring of water to be dependent on the carbonate concentration.

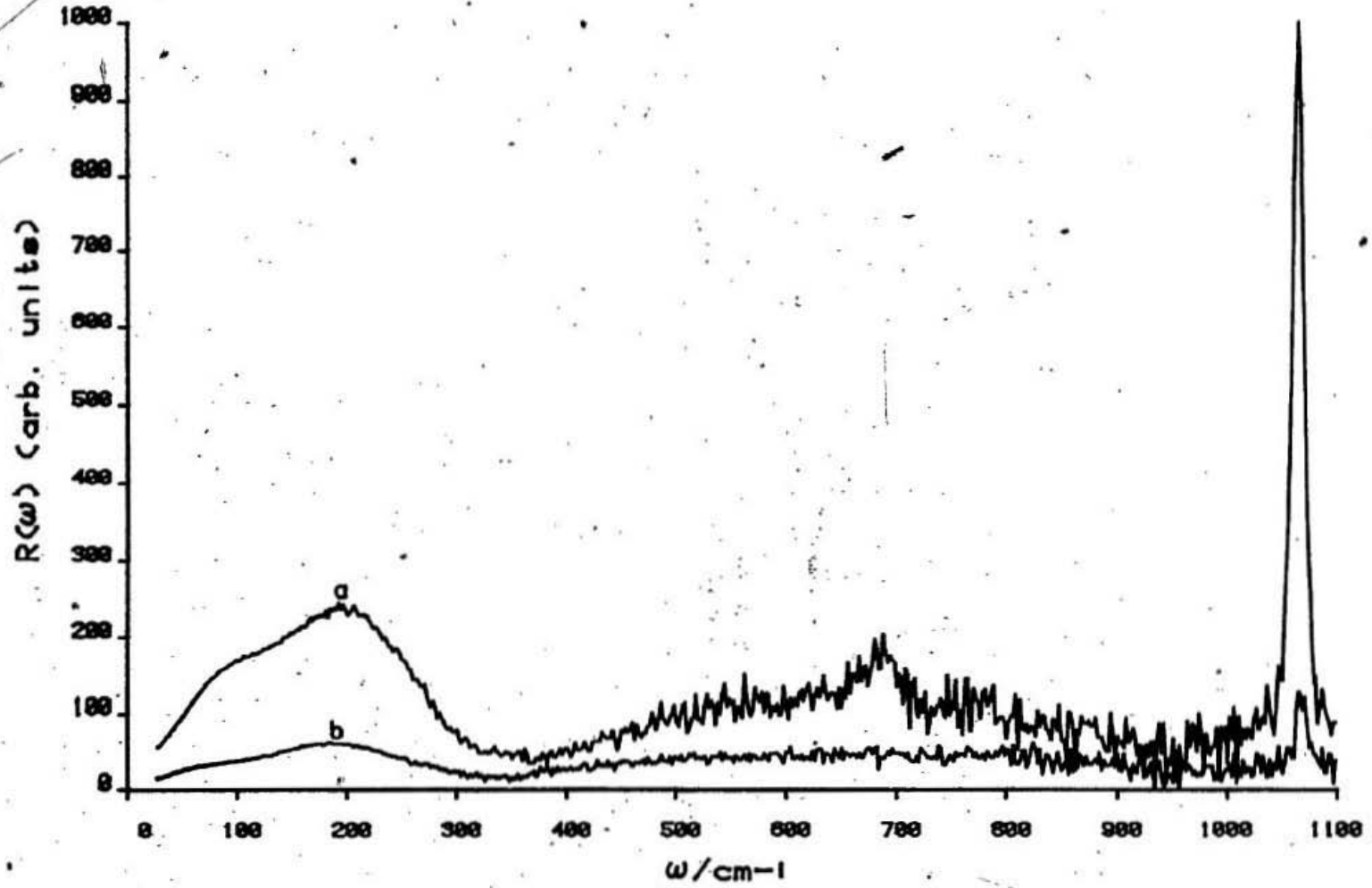
R(ω) (arb. units)
1000
900
800
700
600
500
400
300
200
100
0
a
b
0
100
200
300
400
500
600
700
800
900
1000
1100
ω/cm-1

Fig. 16. $R(\omega)$ spectra of 1 mol L^{-1} and saturated aqueous K_2CO_3 solutions normalized to the O···H–O stretching mode of water. The spectra for saturated K_2CO_3 (aq) (a) marks a growth in intensity at 92 cm^{-1} over that of the 1 mol L^{-1} solution (b) from the larger presence of hindered rotating CO_3^{2-} ions.

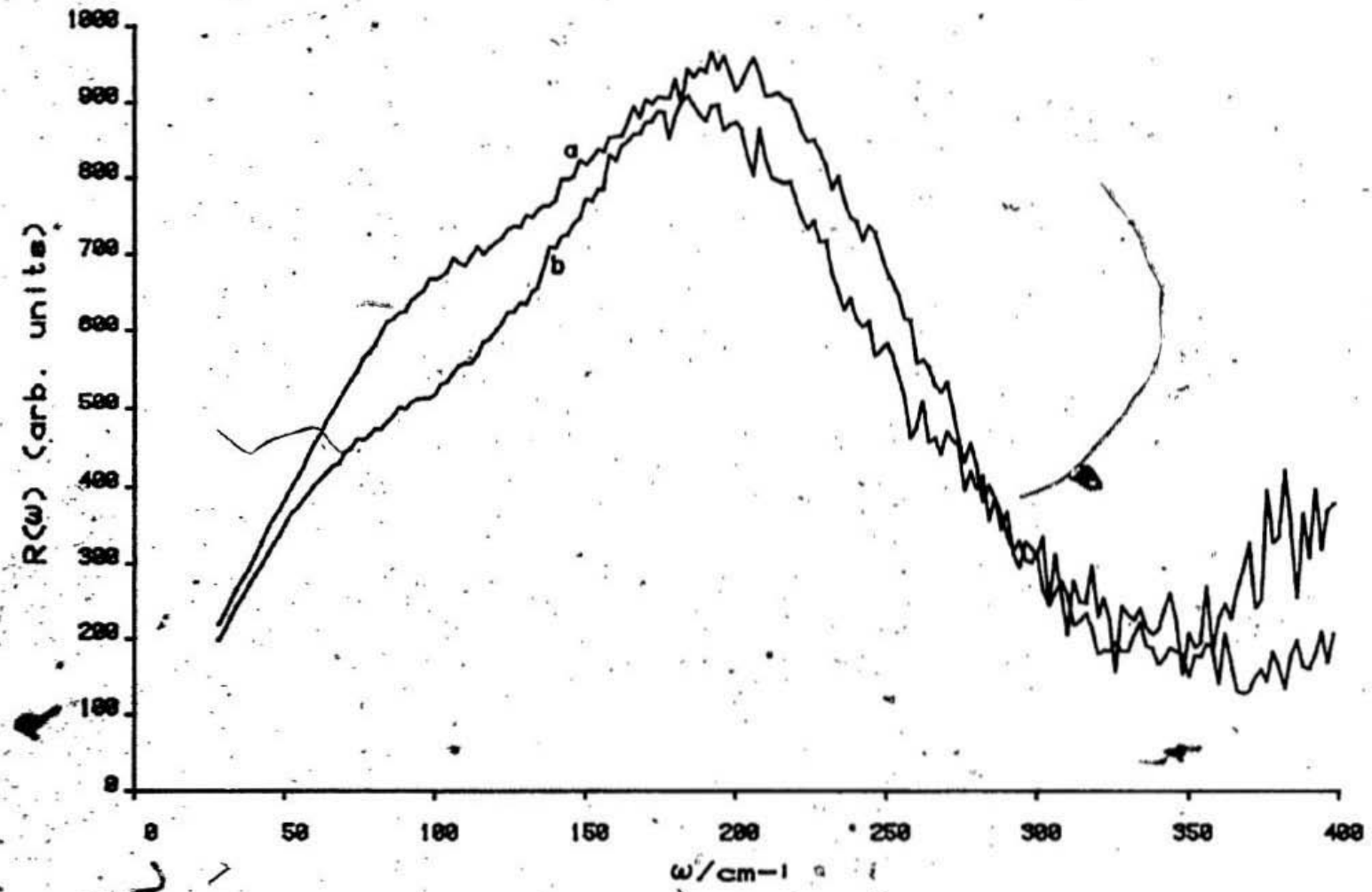
1000
900
800
700
600
500
400
300
200
100
0
R(ω) (arb. units)
a
b
0
50
100
150
200
250
300
350
400
ω/cm-1

reorientational CO_3^{2-} band on the low frequency wing. In the 1M K_2CO_3 solution the weak CO_3^{2-} band gives intensity at about 70 cm^{-1} compared to the O···H-O bending mode of water at 66 cm^{-1}. The band increased in intensity and gave a clear feature at 92 cm^{-1} in the saturated solution. This reported result for the librations of CO_3^{2-} is in close agreement with that reported for NO_3^-. The intensity of the reorientational peak due to CO_3^{2-} at 92 cm^{-1} is not as intense relative to the O···H-O peak at 196 cm^{-1} as was observed for the NO_3^- peak at 92 cm^{-1}. This could be due to the small polarizability of CO_3^{2-} compared to NO_3^- or it could be due to an increase in the O···H-O stretch intensity as a result of stronger hydrogen bonding with carbonate.

The presence of halides in solution does not give rise to any noticeable hindered anionic reorientational intensity as the anions are spherically symmetric and collision induced anisotropy is expected to be small. However, spherically symmetric anions can still affect the shape of the low frequency region of water as is shown in Figs. 17 and 18 and in Table 7.

Table 7

Spectral data for aqueous halides

cm^{-1}

	$\nu_{diff\ O\cdots H_2O\ str}$	$\nu_{O-H\cdots X^-}$	$\nu_{O\cdots H-O\ str}$	
			I_{VV}	I_{VH}
NaCl	187	-	183	178
KCl	181	-	176	171
KF	-	263		192

Aside from the higher intensity of the O···H-O stretching band in KCl

Fig. 17. $R(\omega)$ spectra for saturated aqueous NaCl. I_{VV} (a). I_{VH} (b). The isotropic component (c) shows only the slightly polarized character of the O···H–O stretch.

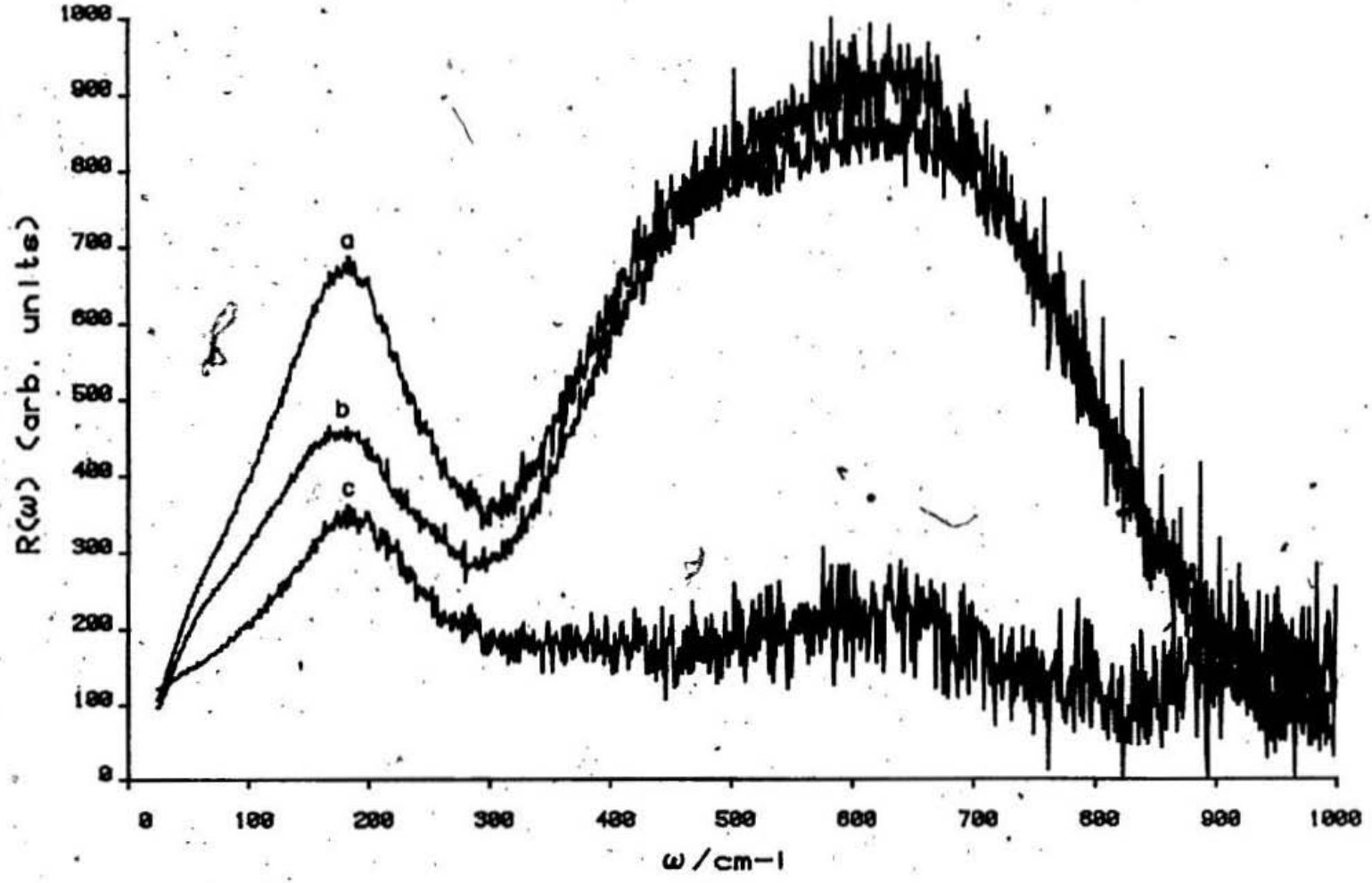
R(ω) (arb. units)
ω / cm−1
a
b
c
0
100
200
300
400
500
600
700
800
900
1000

Fig. 18. $R(\omega)$ spectra of saturated aqueous KCl. I_{VV} (a), I_{VH} (b). As in the case of the previous figure only the O···H–O stretch is observed in the isotropic spectrum (c). The shift of the O···H–O stretch to 176 cm^{-1} in the I_{VV} spectrum from 183 cm^{-1} for NaCl (Fig. 17) is not enough evidence to suggest that this band arises from stretching of hydrated cations although there may be some secondary cation effects.

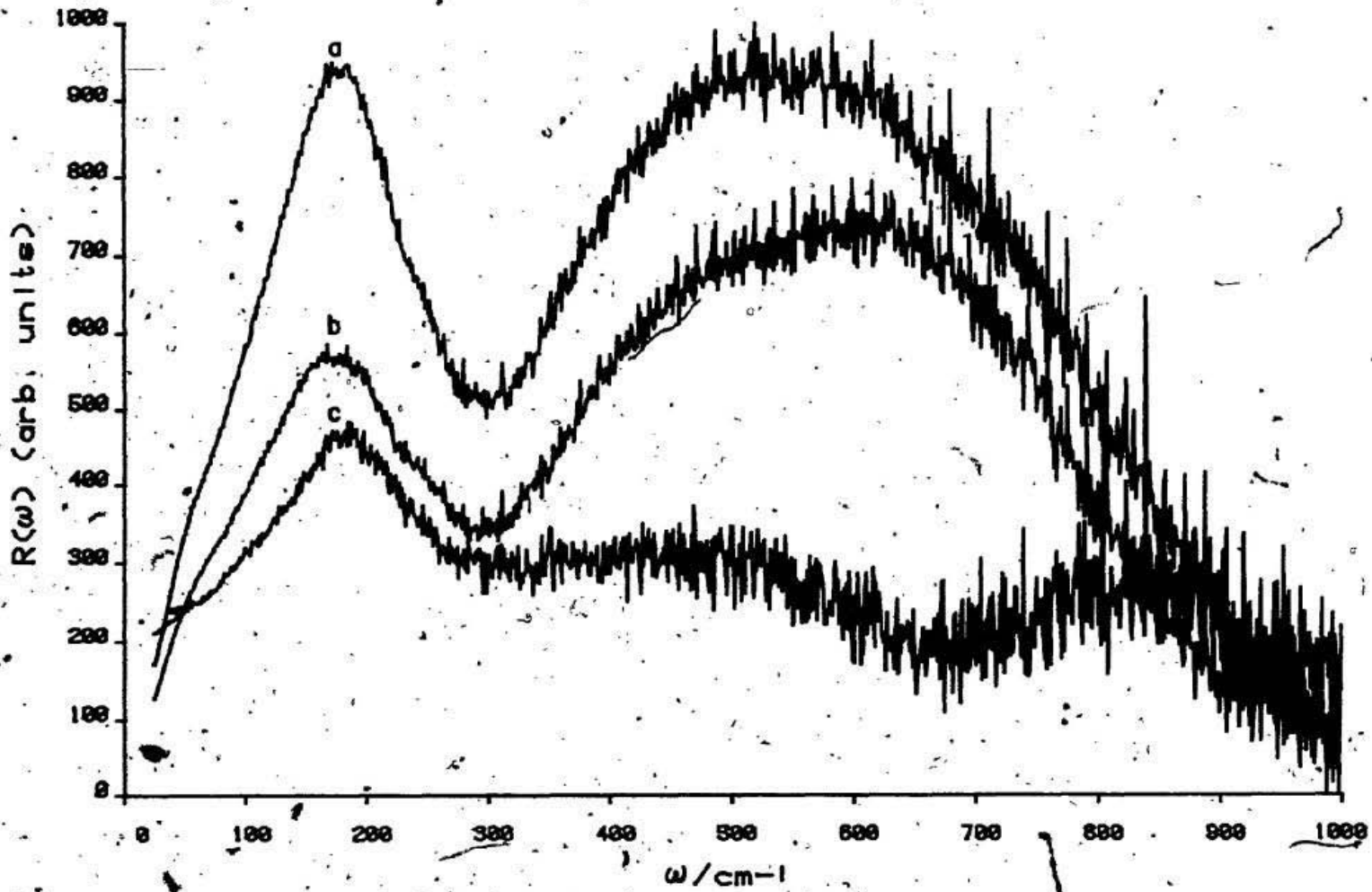
R(ω) (arb. units)
ω/cm⁻¹
a
b
c
0
100
200
300
400
500
600
700
800
900
1000

(such intensity differences are also noted in the I.R. [19]), no other differences are observed when compared to NaCl. The shift in frequency of this band is not enough evidence for cation-water interaction. Such interactions have been reported for these ions but at the same time Rayleigh scatter from chloride-water interaction was taken to be approximately zero [15]. This is contrary to Raman studies which suggest mostly anion-water contribution to the low frequency region. The present work suggests that the differences between the spectra for NaCl and KCl and the spectrum of water on page 16 are primarily due to anion-water interactions. Cation-water effects for Na^+ and K^+ may be present but they are very weak compared to those of Li^+, Mg^{2+} and Ca^{2+} and are negligible compared to $Cl^- \cdots H_2O$ interactions.

The spectrum of saturated aqueous KF is given in Fig. 19. Comparison of KCl and KF spectra shows changes in the contour of the H_2O librational region and a shift of the O···H-O stretching band to 278 cm^{-1} for KF. Careful examination of the KF spectra reveals that the polarized and depolarized maxima in the 200 → 300 cm^{-1} region do not coincide suggesting the presence of a new polarized band for $KF_{(aq)}$. The subtraction spectrum shows the presence of this new band at 263 cm^{-1}. The presence of this peak is further supported by the fact that the subtraction spectrum for $KCl_{(aq)}$ showed only the partly polarized O···H-O peak at 178 cm^{-1}. The 263 cm^{-1} band of $KF_{(aq)}$ is not due to a collision induced restricted rotation of the F^- ion as such a band would also be present in the depolarized spectrum. Fluoride is spherically symmetric and is not expected to experience any torque from the surrounding media. The polarized band is assigned to a hydrogen bond stretching mode between F^- and H_2O. The 192 cm^{-1} band in the depolarized KF spec-

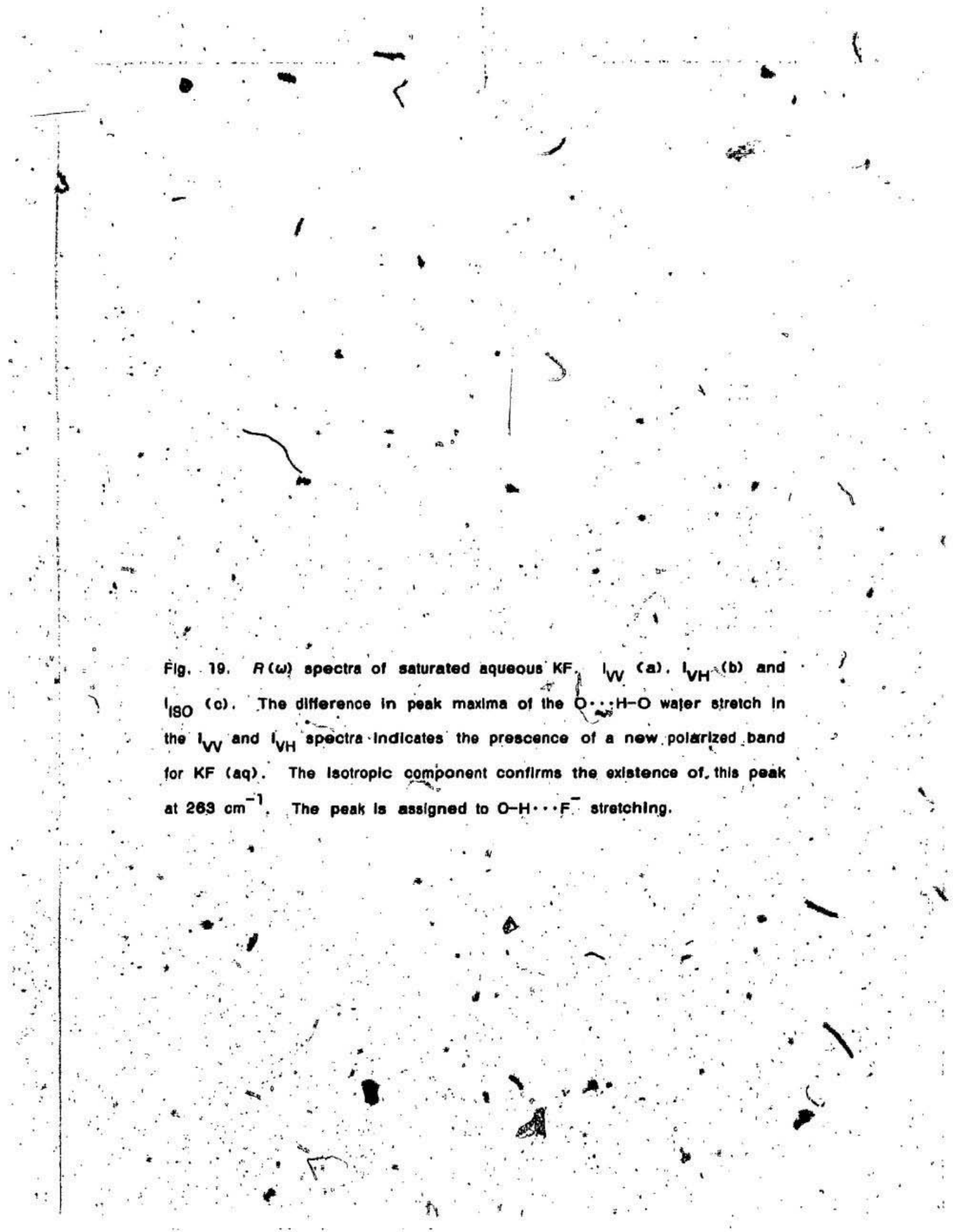

Fig. 19. $R(\omega)$ spectra of saturated aqueous KF. I_{VV} (a), I_{VH} (b) and I_{ISO} (c). The difference in peak maxima of the O···H–O water stretch in the I_{VV} and I_{VH} spectra indicates the prescence of a new polarized band for KF (aq). The isotropic component confirms the existence of this peak at 263 cm^{-1}. The peak is assigned to O–H···F^- stretching.

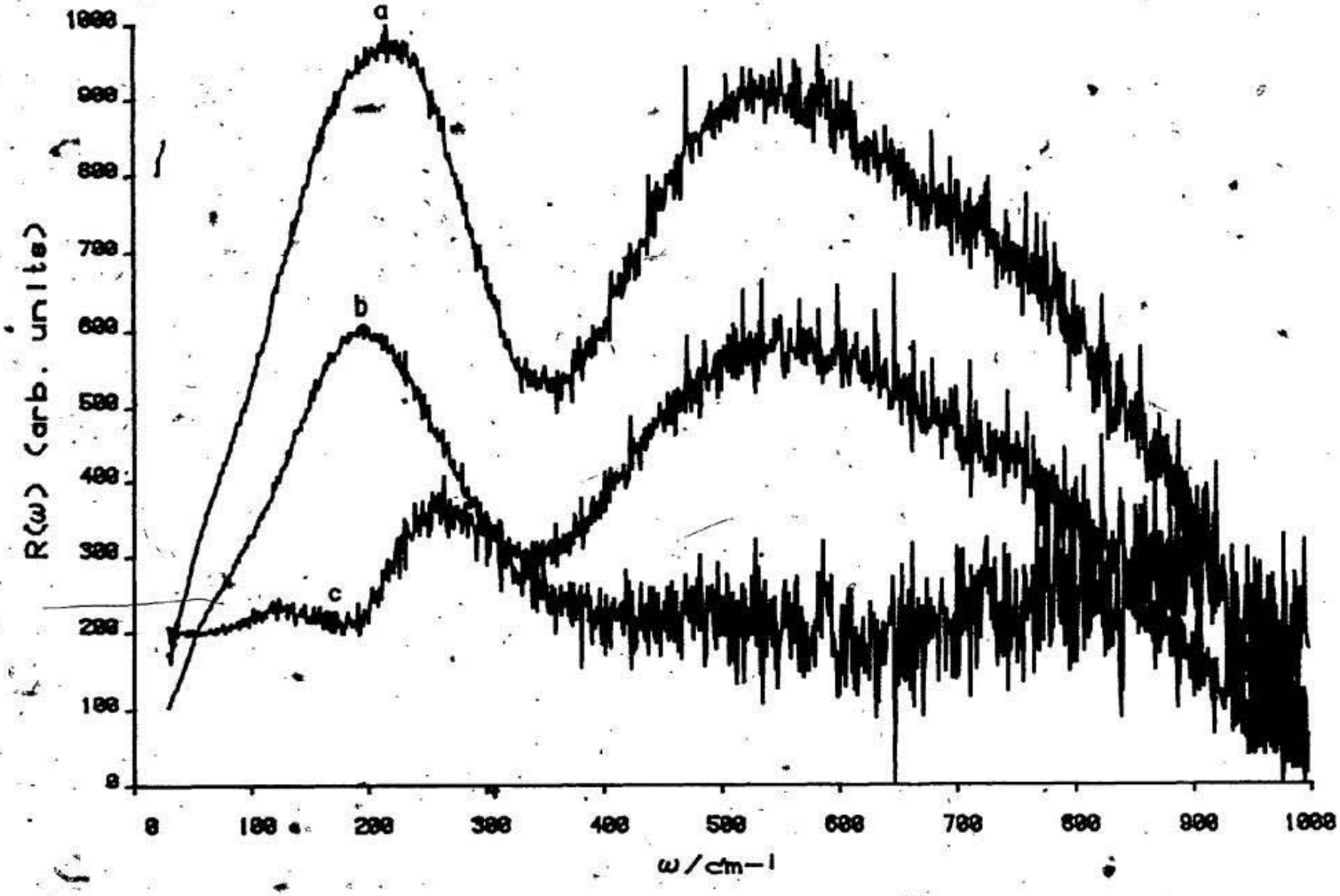
a
b
c
R(ω) (arb. units)
ω / cm−1
0
100
200
300
400
500
600
700
800
900
1000

trum is the anisotropic component of the partially polarized O···H–O stretching mode. F^- is more strongly attracted to H than is the O of a water molecule and hence the tighter hydrogen bond with the fluoride ion gives rise to a higher stretch frequency. In terms of translation, this higher energy hydrogen bond means a more restricted movement of H_2O.

Hydroxide ion like the fluoride ion does not itself give rise to anisotropy in the low frequency region. Although not spherically symmetric, the size and polarizability and polarizability anisotropy of hydrogen is very small and additionally it is unlikely that the anion would experience any measurable torque from the surrounding molecules. The relevant data taken from the spectra of the aqueous alkali metal hydroxides is given in Table 8 and the $I(\omega)$ spectra for these solutions appear in Figs. 20 → 26.

Table 8

I_{VV} data for aqueous hydroxides

cm^{-1}

	$\nu_{O\cdots H-O\ str}$	$\nu_{O-H\cdots OH^-\ str}$
LiOH(3.8SM)	181	316
NaOH (10M)	172	298
KOH (11.5)	169	293
RbOH (5.8S)	168	286
CsOH	?	277?
NaOH (5M)	194	287
NaOH / $NaClO_4$ (5M in each)	194	–
NaOD	174	271

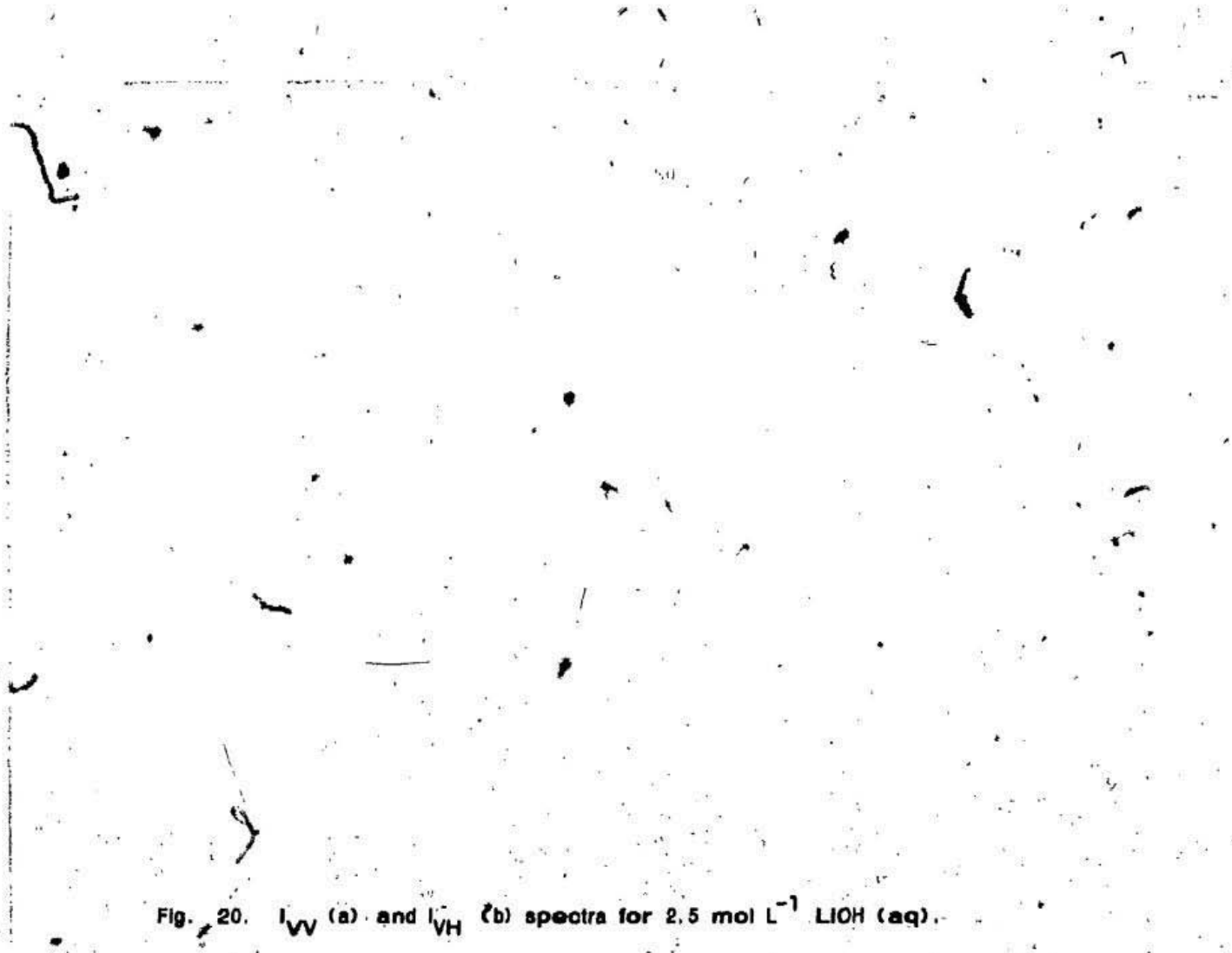

Fig. 20. I_{VV} (a) and I_{VH} (b) spectra for 2.5 mol L^{-1} LiOH (aq).

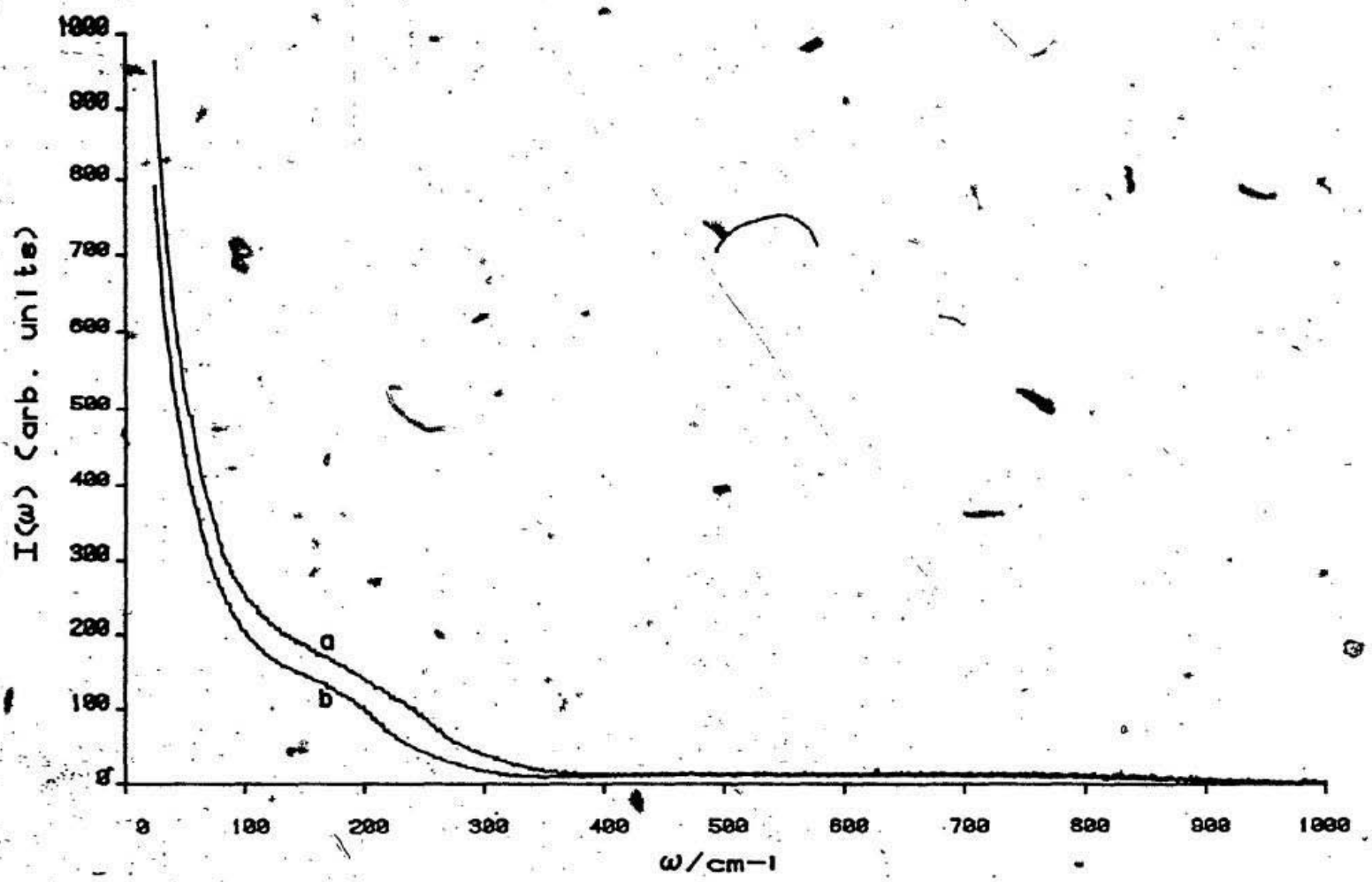
I(ω) (arb. units)
1000
900
800
700
600
500
400
300
200
100
0
a
b
0
100
200
300
400
500
600
700
800
900
1000
ω/cm-1

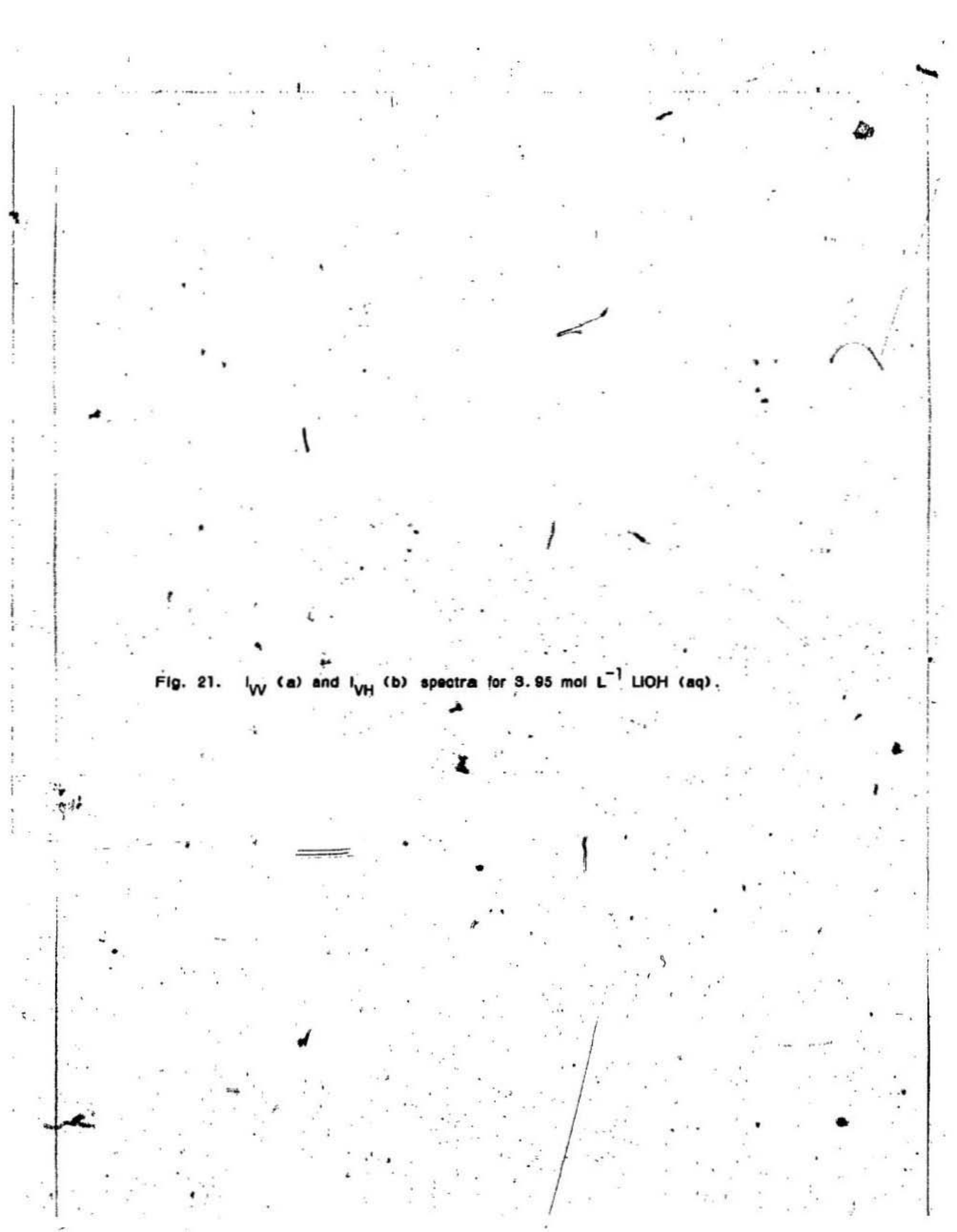

Fig. 21. I_{VV} (a) and I_{VH} (b) spectra for 3.95 mol L^{-1} LiOH (aq).

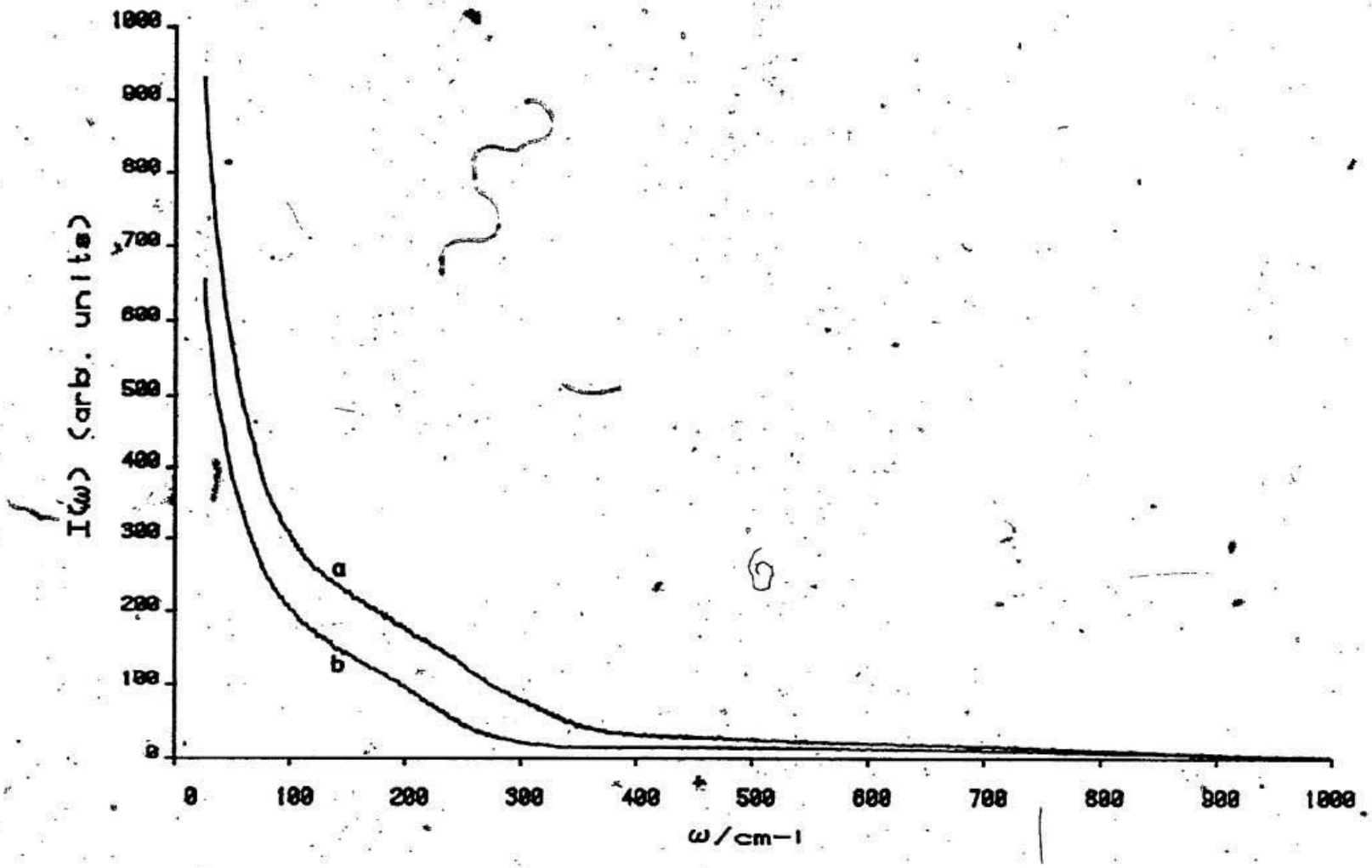
I(ω) (arb. units)
1000
900
800
700
600
500
400
300
200
100
0
a
b
0
100
200
300
400
500
600
700
800
900
1000
ω/cm-1

Fig. 22. I_{VV} (a) and I_{VH} (b) spectra for 10 mol L^{-1} NaOH (aq).

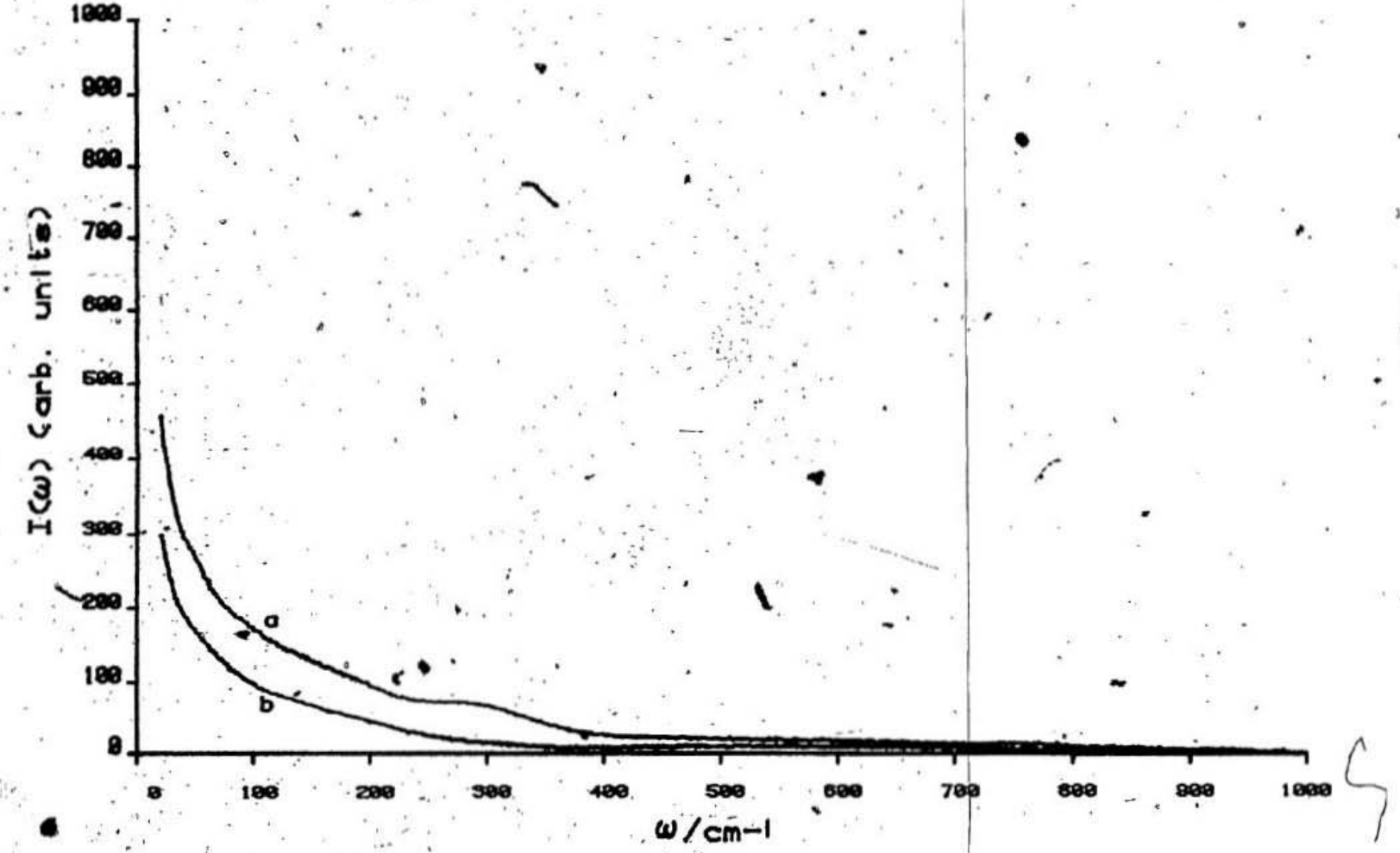
I(ω) (arb. units)
1000
900
800
700
600
500
400
300
200
100
0
a
b
0
100
200
300
400
500
600
700
800
900
1000
ω / cm⁻¹

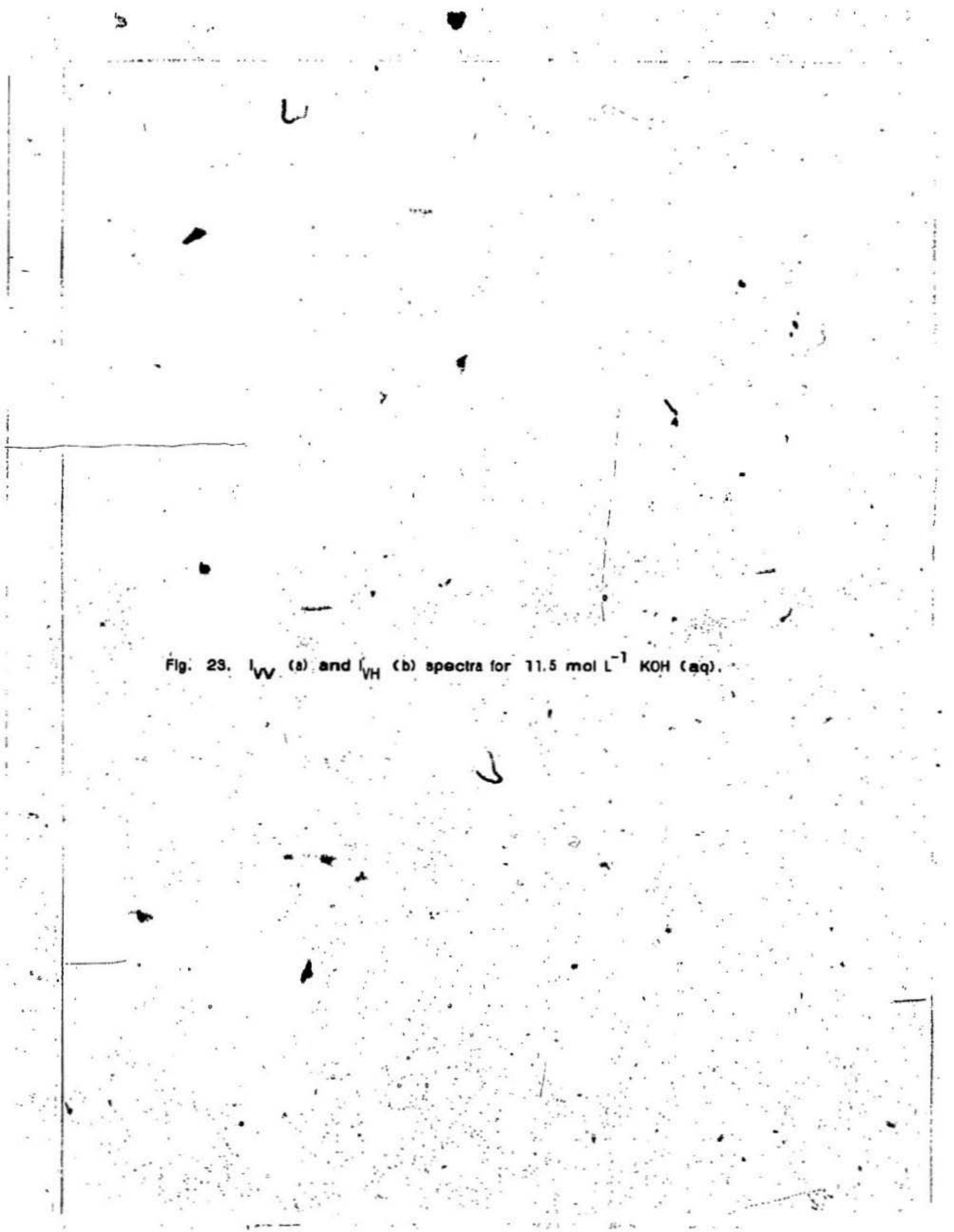

Fig. 23. I_{VV} (a) and I_{VH} (b) spectra for 11.5 mol L^{-1} KOH (aq).

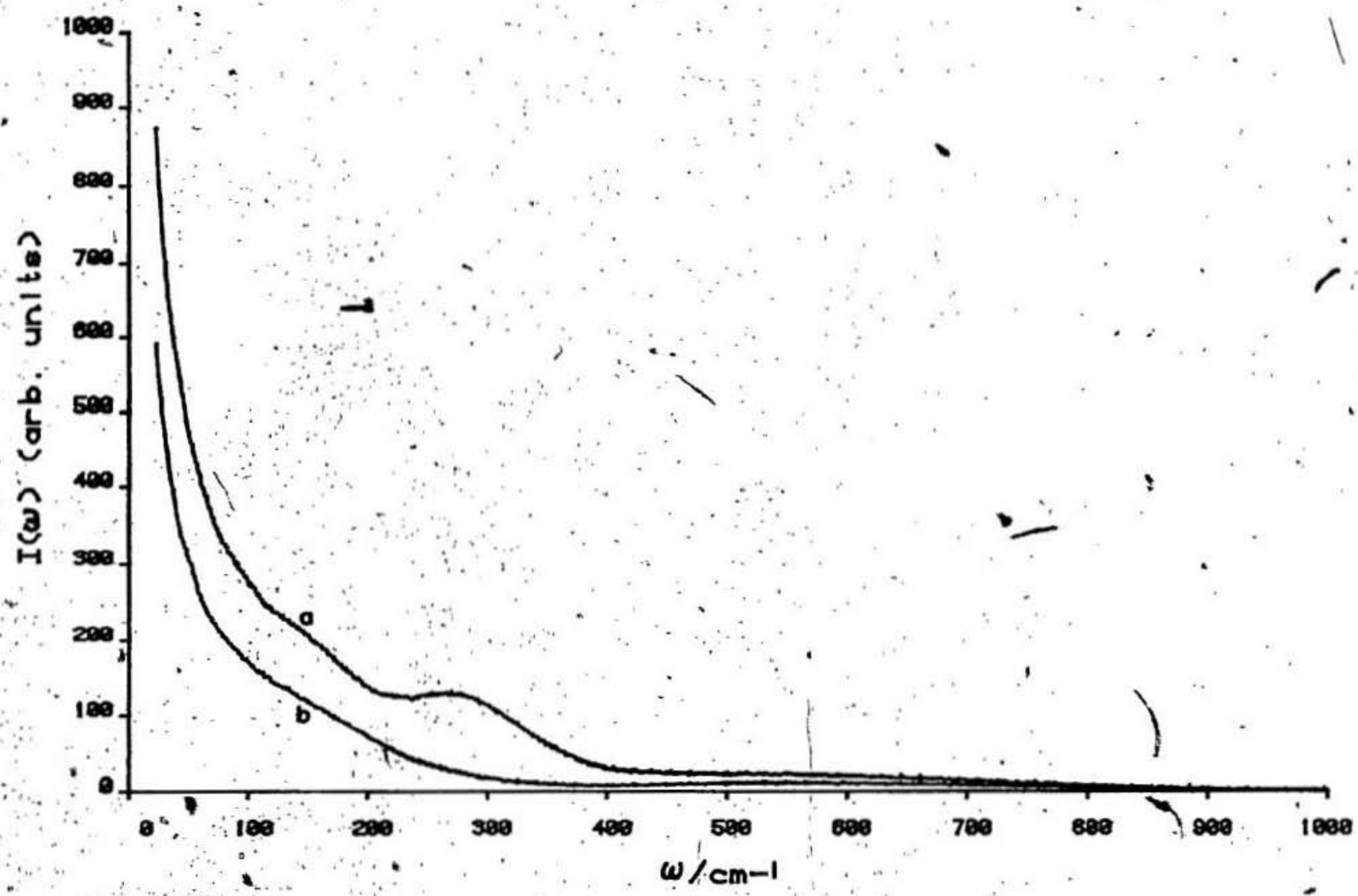
I(ω) (arb. units)
1000
900
800
700
600
500
400
300
200
100
0
a
b
0
100
200
300
400
500
600
700
800
900
1000
ω/cm-1

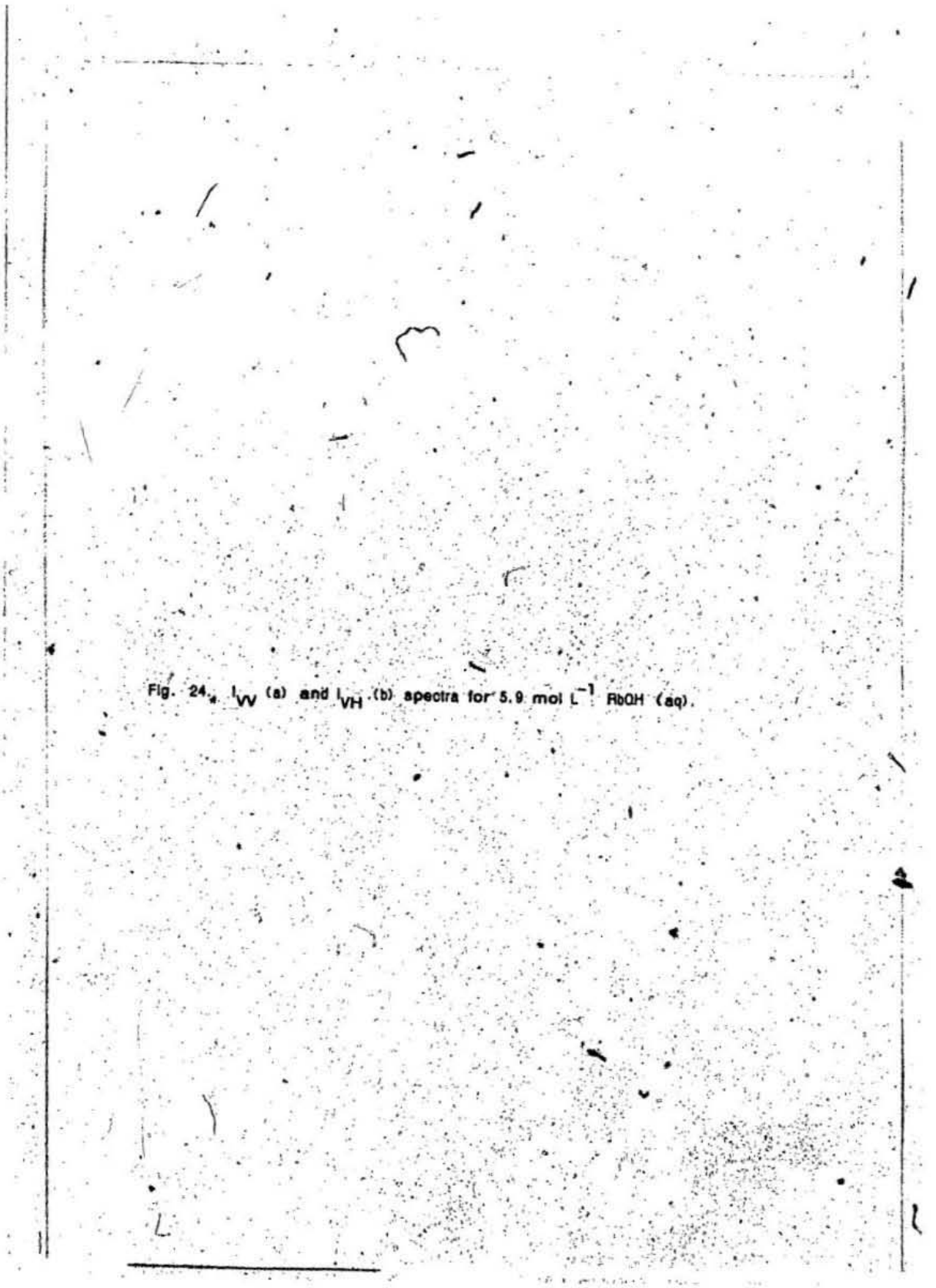

Fig. 24. I_{VV} (a) and I_{VH} (b) spectra for 5.9 mol L^{-1} RbOH (aq).

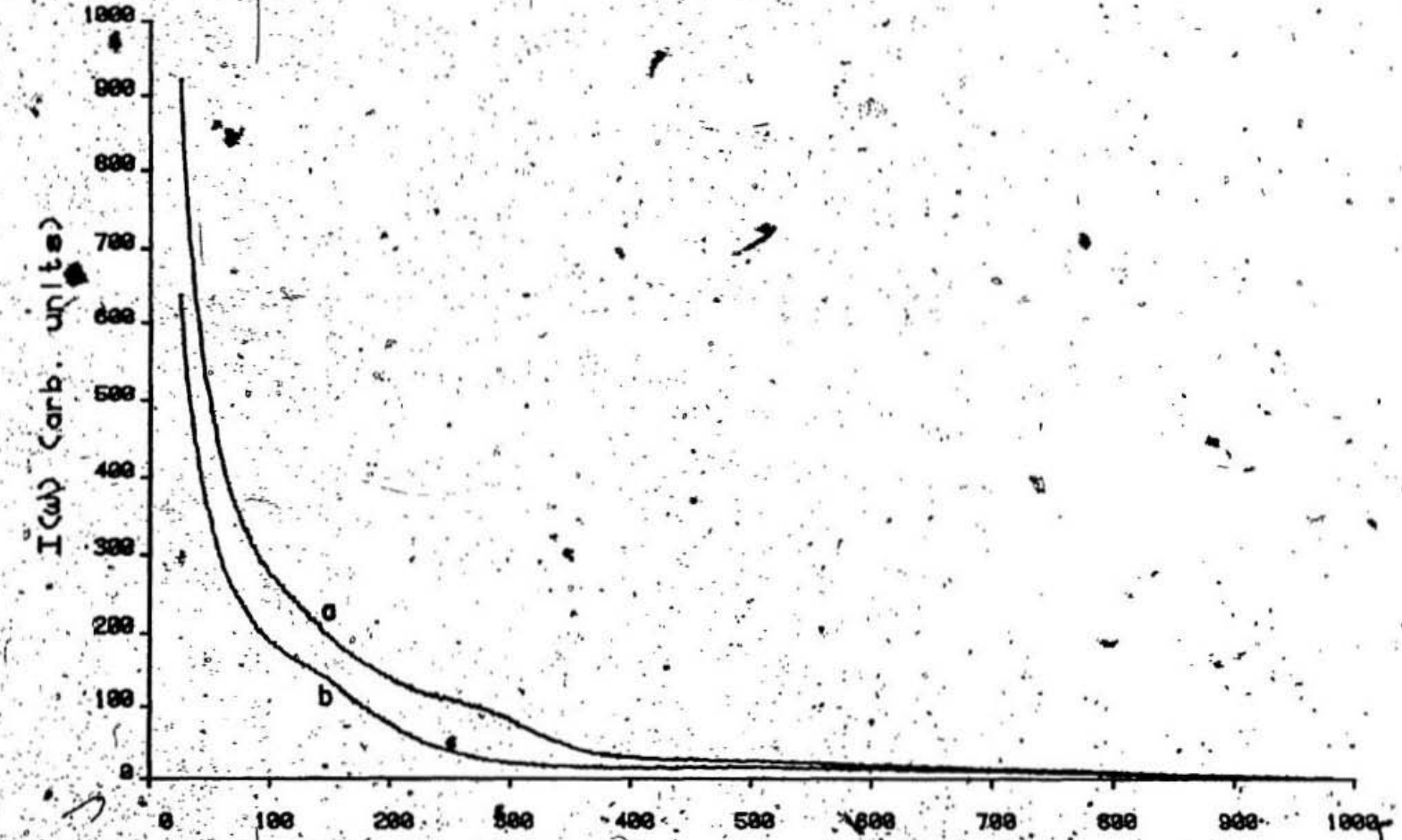
I(ω) Carb. units
1000
900
800
700
600
500
400
300
200
100
0
a
b
0
100
200
300
400
500
600
700
800
900
1000
ω/cm-1

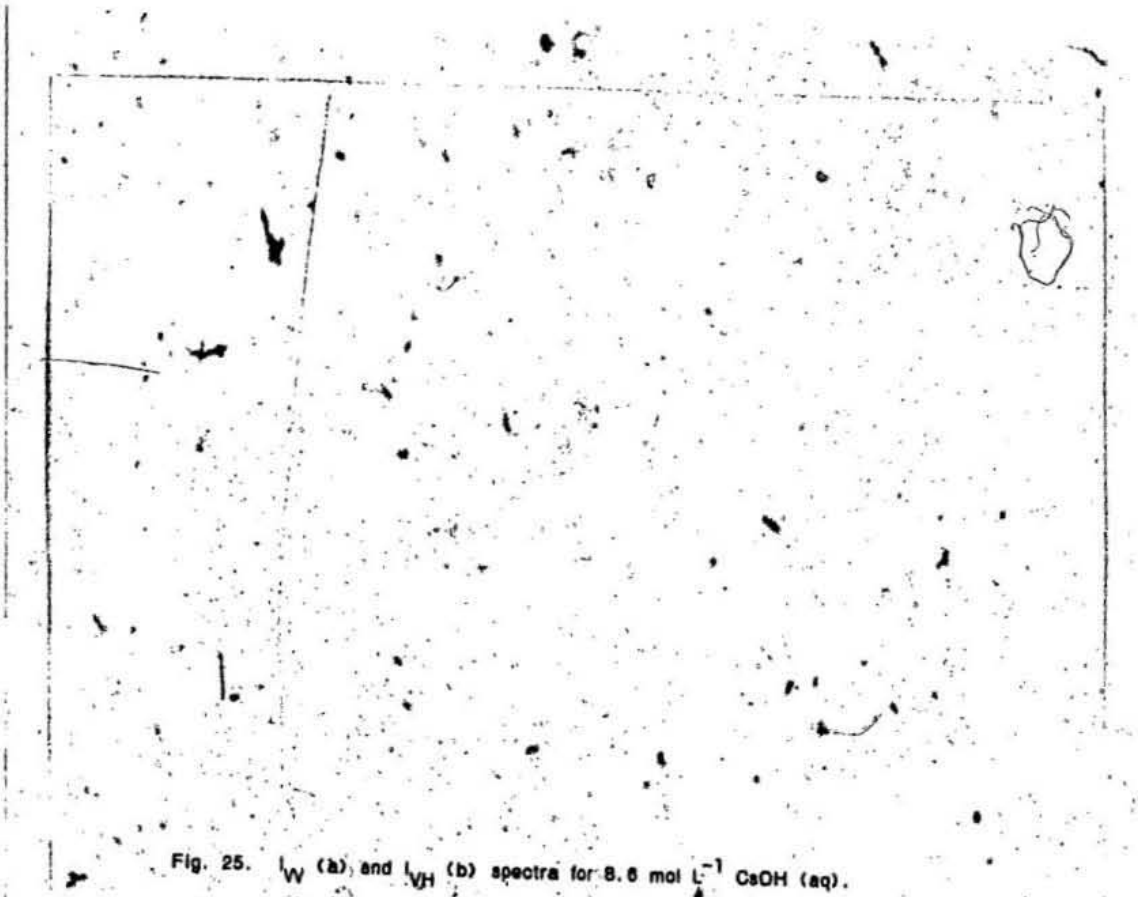

Fig. 25. I_{VV} (a) and I_{VH} (b) spectra for 8.6 mol L^{-1} CsOH (aq).

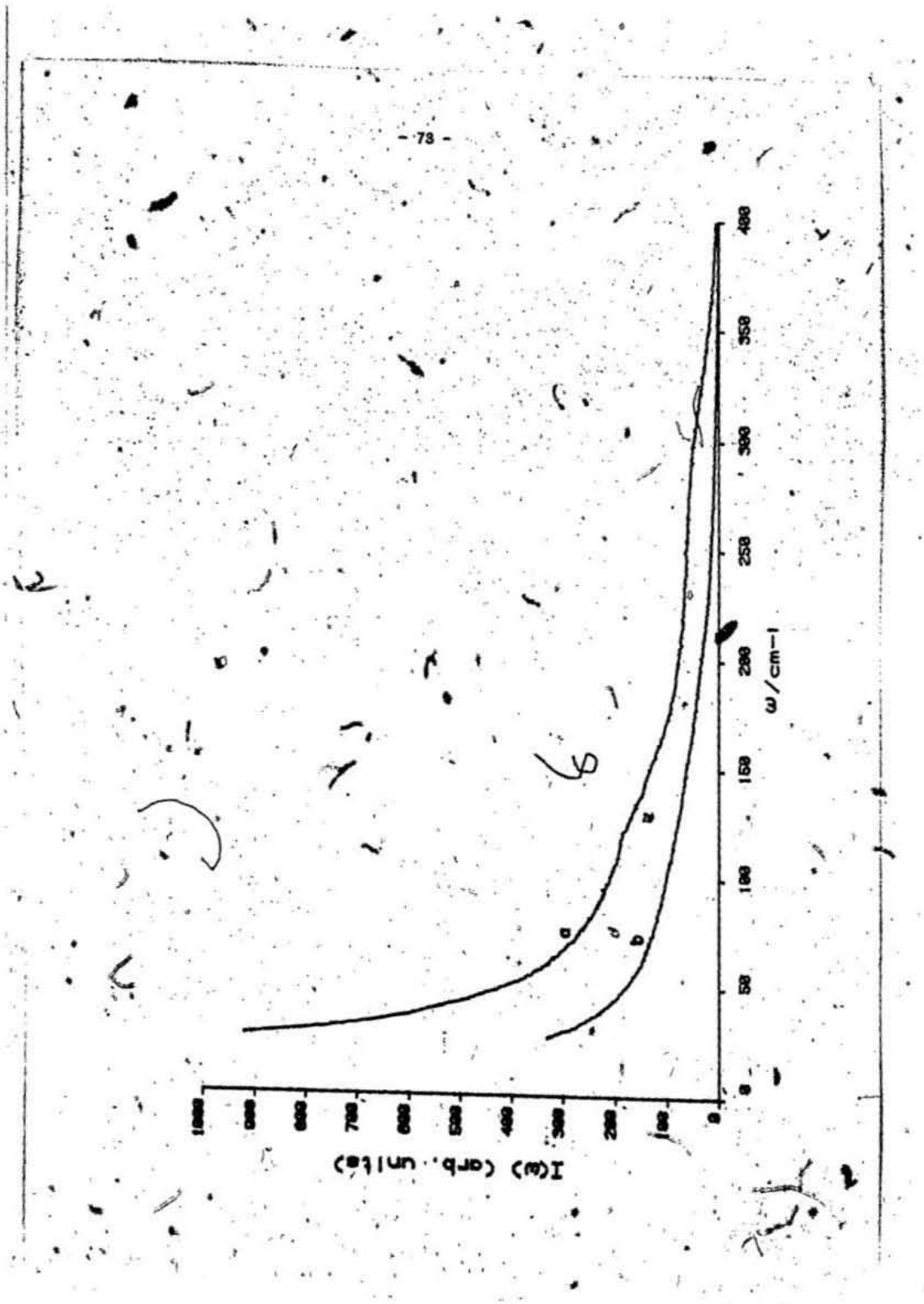
I(ω) (arb. units)
ω/cm-1
a
b

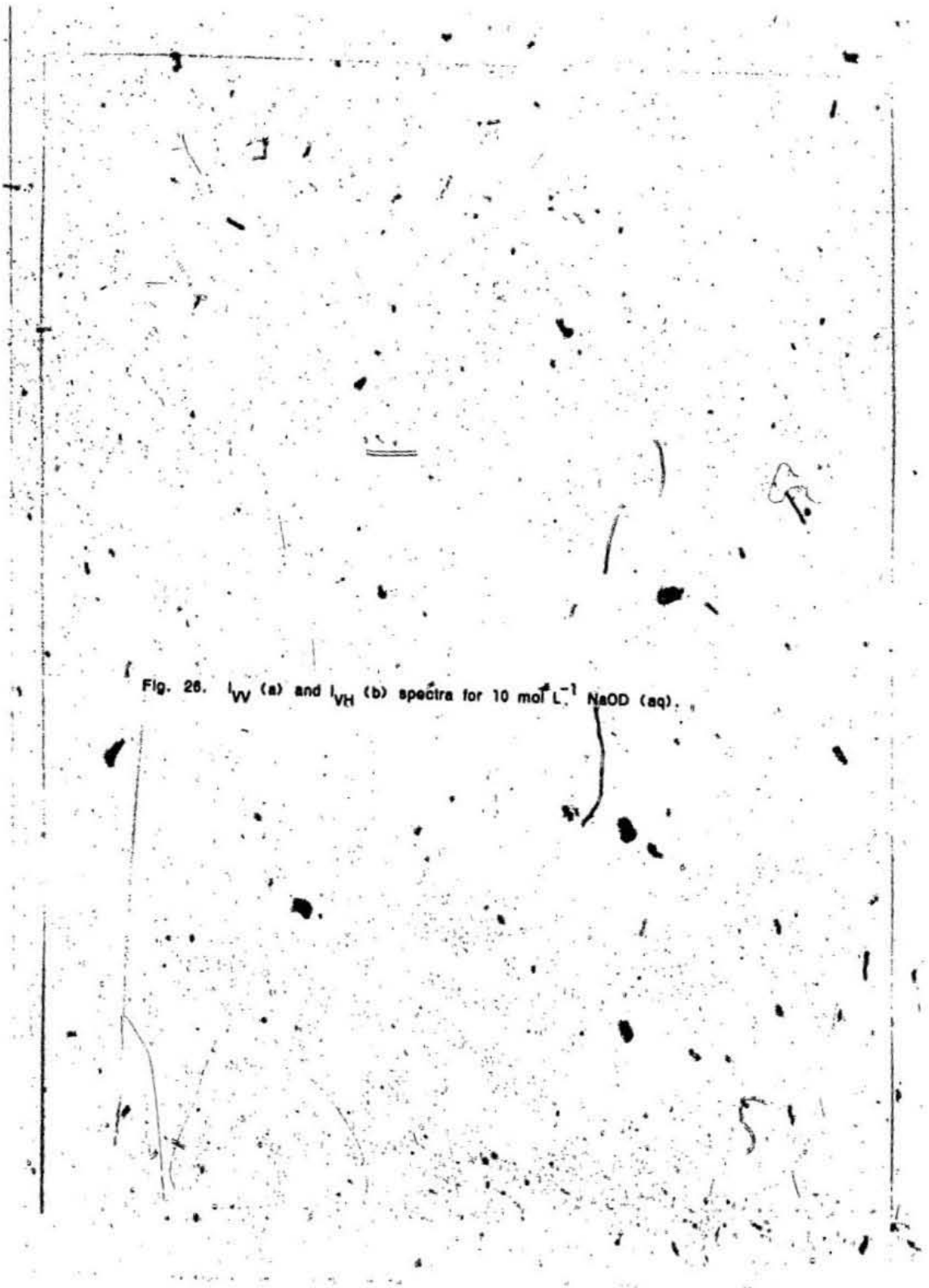

Fig. 26. I_{VV} (a) and I_{VH} (b) spectra for 10 mol L^{-1} NaOD (aq).

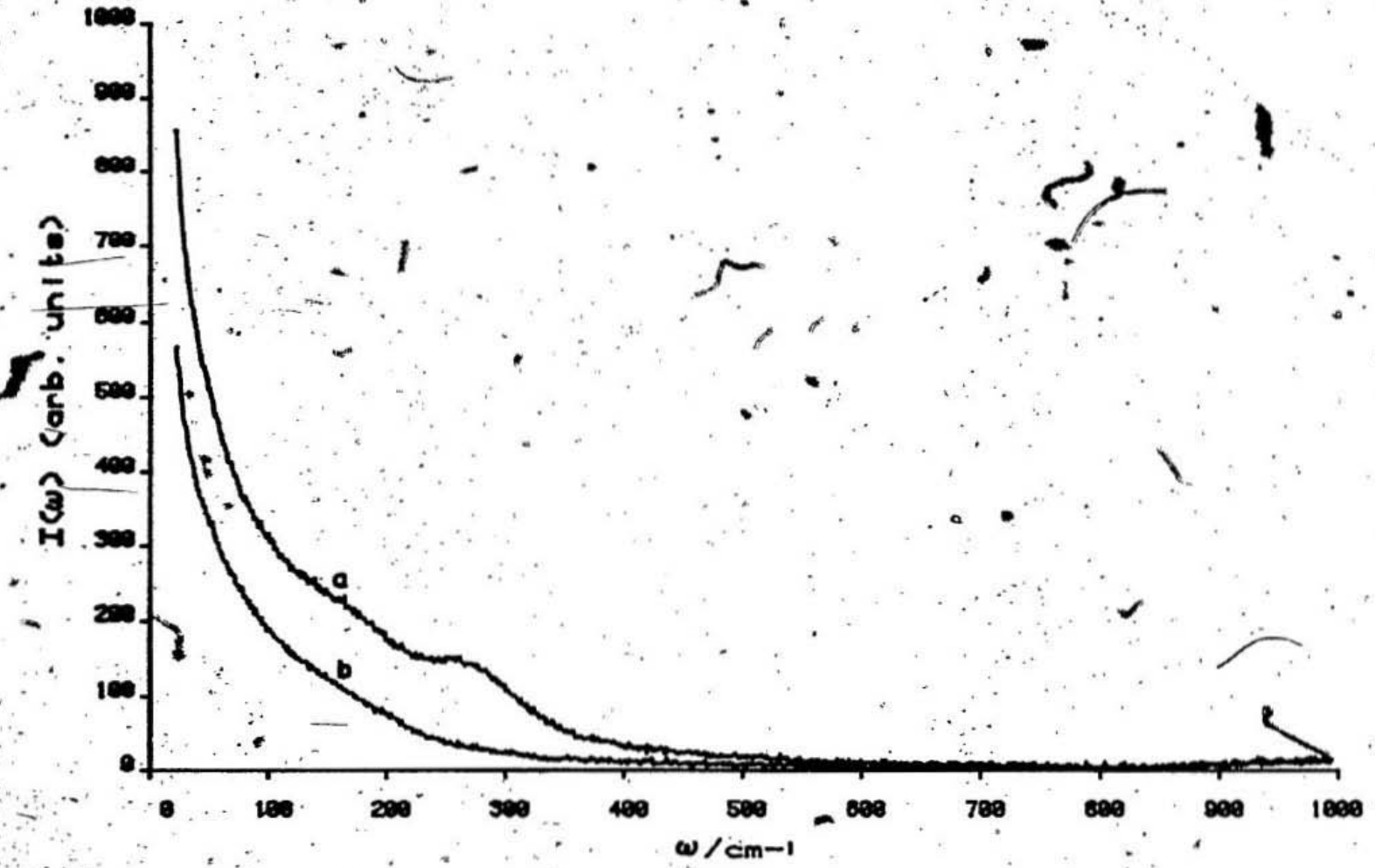
I(ω) (arb. units)
1000
900
800
700
600
500
400
300
200
100
0
a
b
0
100
200
300
400
500
600
700
800
900
1000
ω / cm⁻¹

For the hydroxides of Na, K, Rb and Cs the spectra show polarized bands in the region of 250 → 300 cm^{-1}. Because the band in each case is polarized, it cannot be due to a libration of OH^-. These peaks are assigned to hydrogen bond stretches of the $H-O-H\cdots OH^-$ complex and occur at 298 cm^{-1} for NaOH, 293 cm^{-1} for KOH and 286 cm^{-1} for RbOH (Figs. 27, 28, 29, 30). The small differences in frequencies can be attributed to concentration effects and secondary effects of the cation on the water structure. Ion pairs of the type M^+OH^- would show a greater cation dependence than is observed and a tetrahedral species of the type $M(OH)_4^{3-}$ would be expected to have a force constant (and hence frequency) which was also very cation dependent. The relative intensities of the band would also be expected to be very cation dependent whereas the observed intensities are proportional only to the OH^- concentration. The $H-O-H\cdots OH^-$ band for CsOH is present in Fig. 31, but the frequency reported (271 cm^{-1}) is low due to small $[OH^-]$. The amount of hydroxide present is not known for certain as a high degree of carbonate impurity was found (page 10). The low OH^- concentration compounded with a baseline subtraction at 400 cm^{-1} (not at a true zero) prevents an accurate frequency assignment.

In addition to $OH^-\cdots H_2O$ interactions there is $H_2O\cdots H_2O$ stretching present as indicated by the peaks at 172, 169, and 168 cm^{-1} for NaOH, KOH and RbOH respectively. The slight shift in this band may be due to secondary cation effects or to a weakening of the $H_2O\cdots H_2O$ interaction due to the strength of the $OH^-\cdots H_2O$ interaction. There may also be a small intensity contribution from the 92 cm^{-1} band of CO_3^{2-} impurity (see page 10). This is similar to the case of aqueous KF where two types of hydrogen bonding were observed. The $OH^-\cdots H_2O$ stretches are of

Fig. 27. $R(\omega)$ spectra for 10 mol L^{-1} NaOH (aq). Data from the I_{VV} spectrum (a) show the presence of a polarized band at 298 cm^{-1} completely absent from the I_{VH} transformed data (b). The polarized band is assigned to the H-O-H···OH^- symmetric stretching mode. The O···H-O stretching mode of water shifts to a lower frequency of 172 cm^{-1} in the depolarized spectrum which may be a result of weakened water-water interactions or from secondary cation effects.

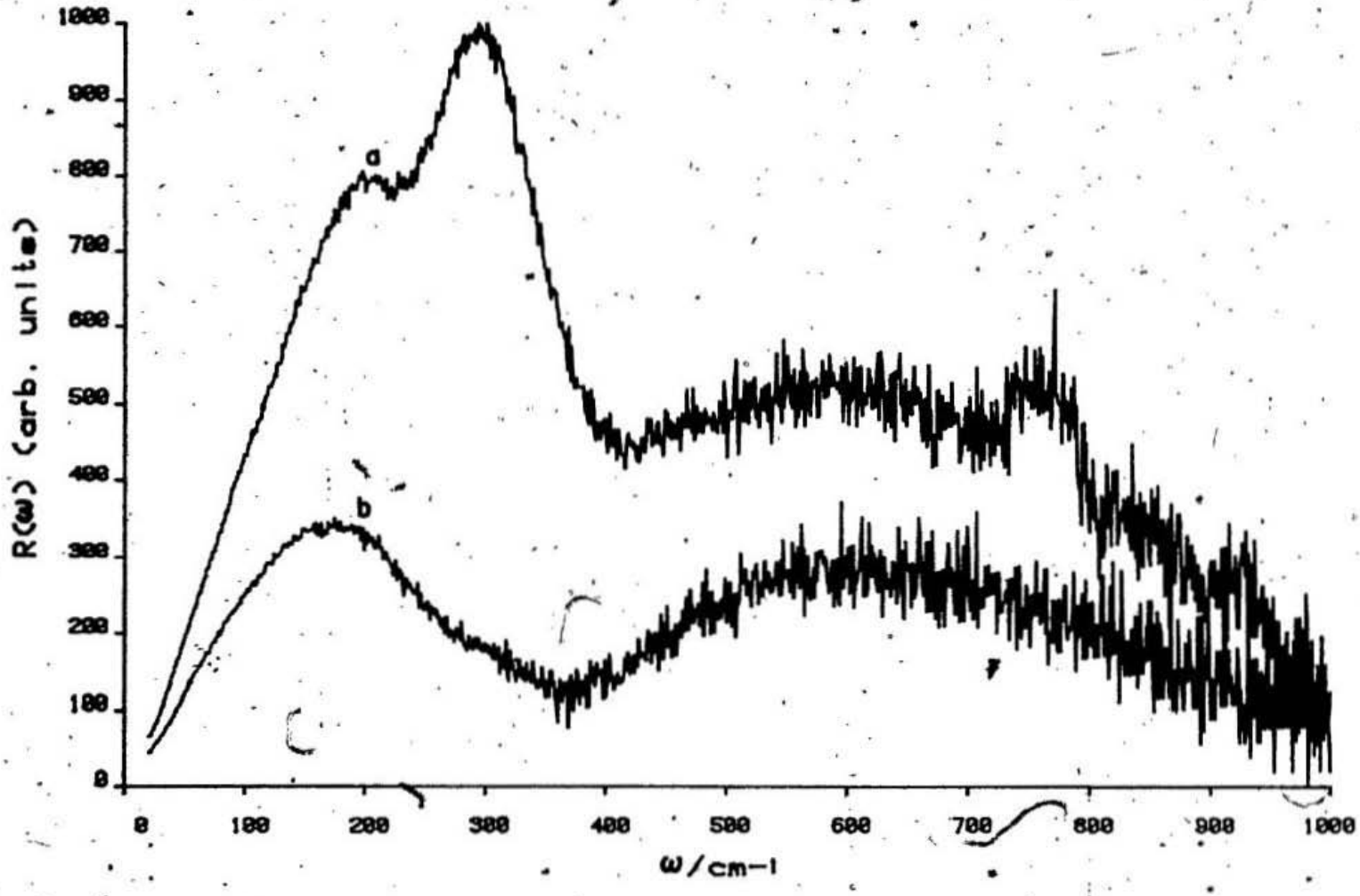
R(ω) (arb. units)
1000
900
800
700
600
500
400
300
200
100
0
a
b
0
100
200
300
400
500
600
700
800
900
1000
ω / cm-1

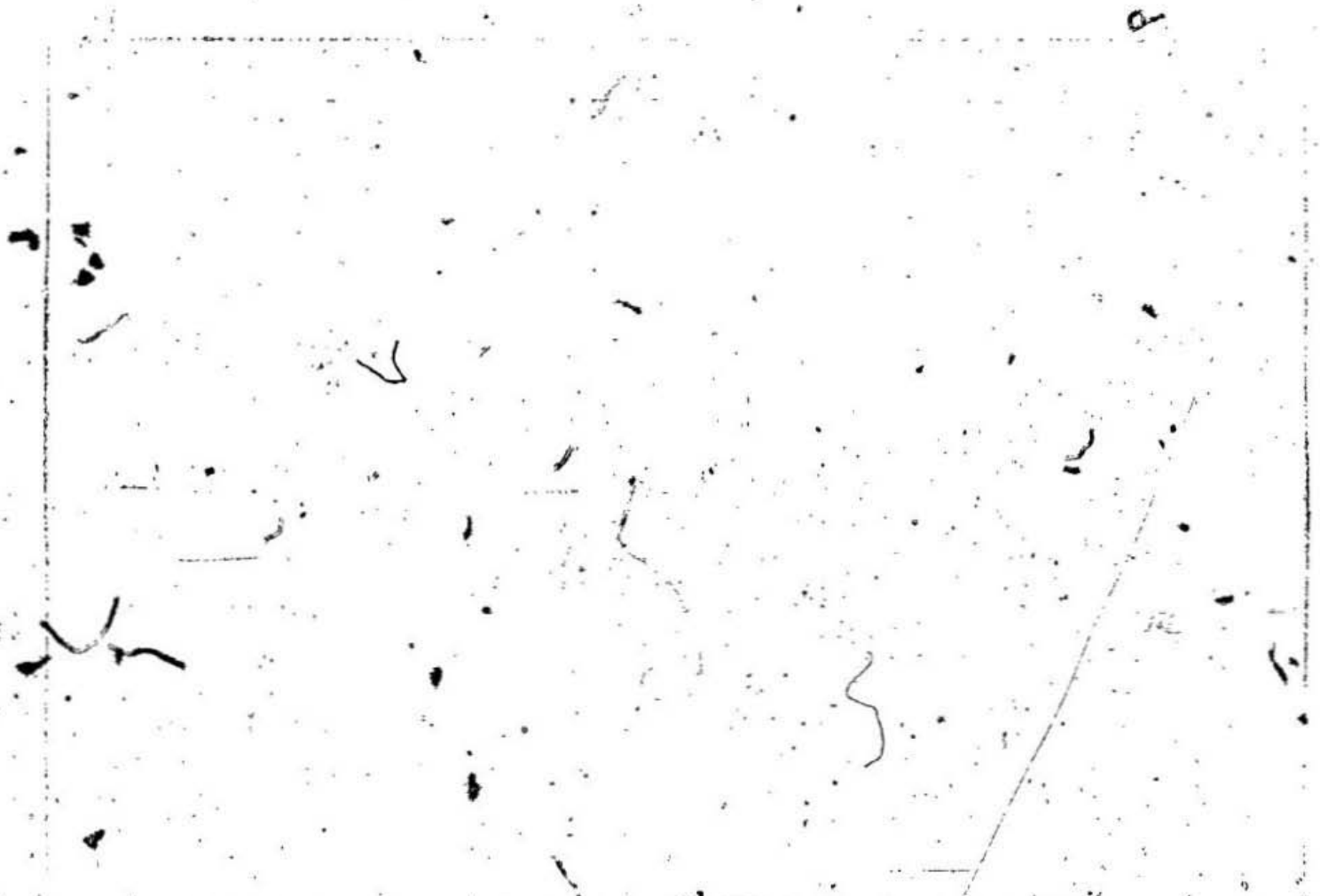

Fig. 28. $R(\omega)$ spectra for 11.5 mol L^{-1} KOH (aq). The band at 293 cm^{-1} in the transformed I_{VV} spectrum (a) does not appear in the data obtained from the I_{VH} spectrum (b). This polarized band is assigned to symmetric stretching of the $H\text{-}O\text{-}H\cdots OH^-$ unit. The $O\cdots H\text{-}O$ stretching mode of water shifts to 169 cm^{-1} in the depolarized spectrum.

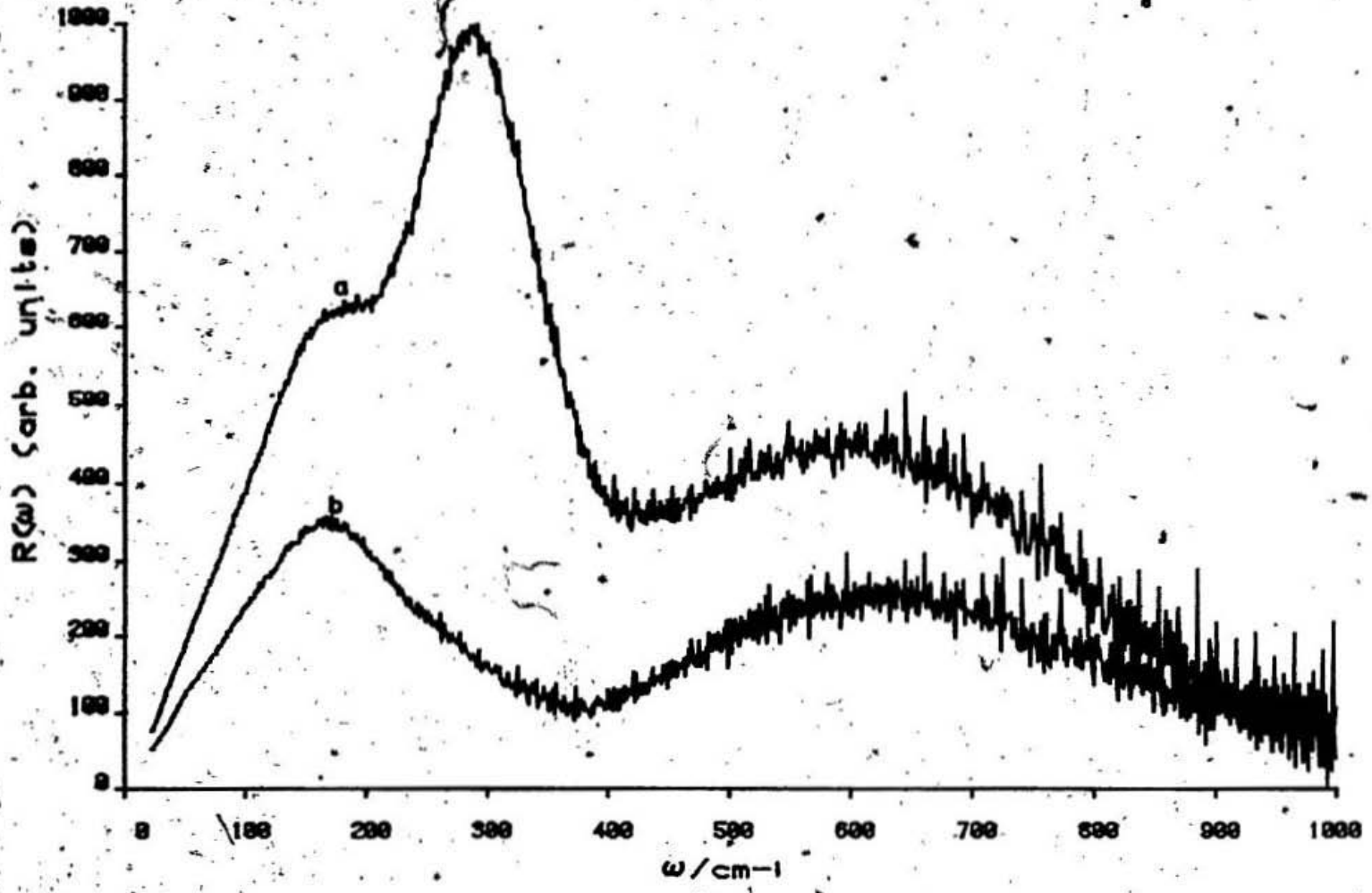
R(ω) (arb. units)
1000
900
800
700
600
500
400
300
200
100
0
a
b
0
100
200
300
400
500
600
700
800
900
1000
ω / cm⁻¹

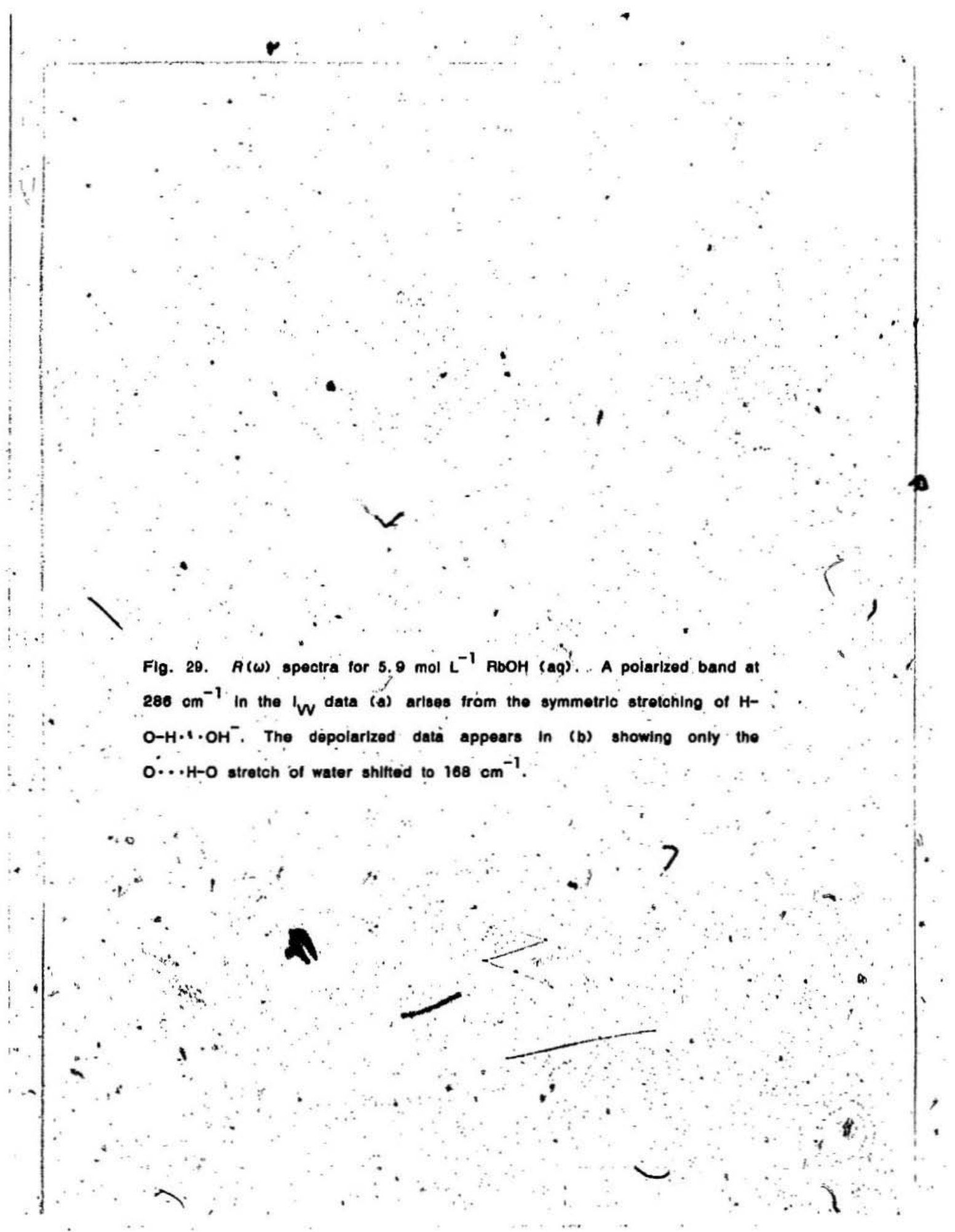

Fig. 29. $R(\omega)$ spectra for 5.9 mol L^{-1} RbOH (aq). A polarized band at 286 cm^{-1} in the I_{VV} data (a) arises from the symmetric stretching of H-O-H···OH^-. The depolarized data appears in (b) showing only the O···H-O stretch of water shifted to 168 cm^{-1}.

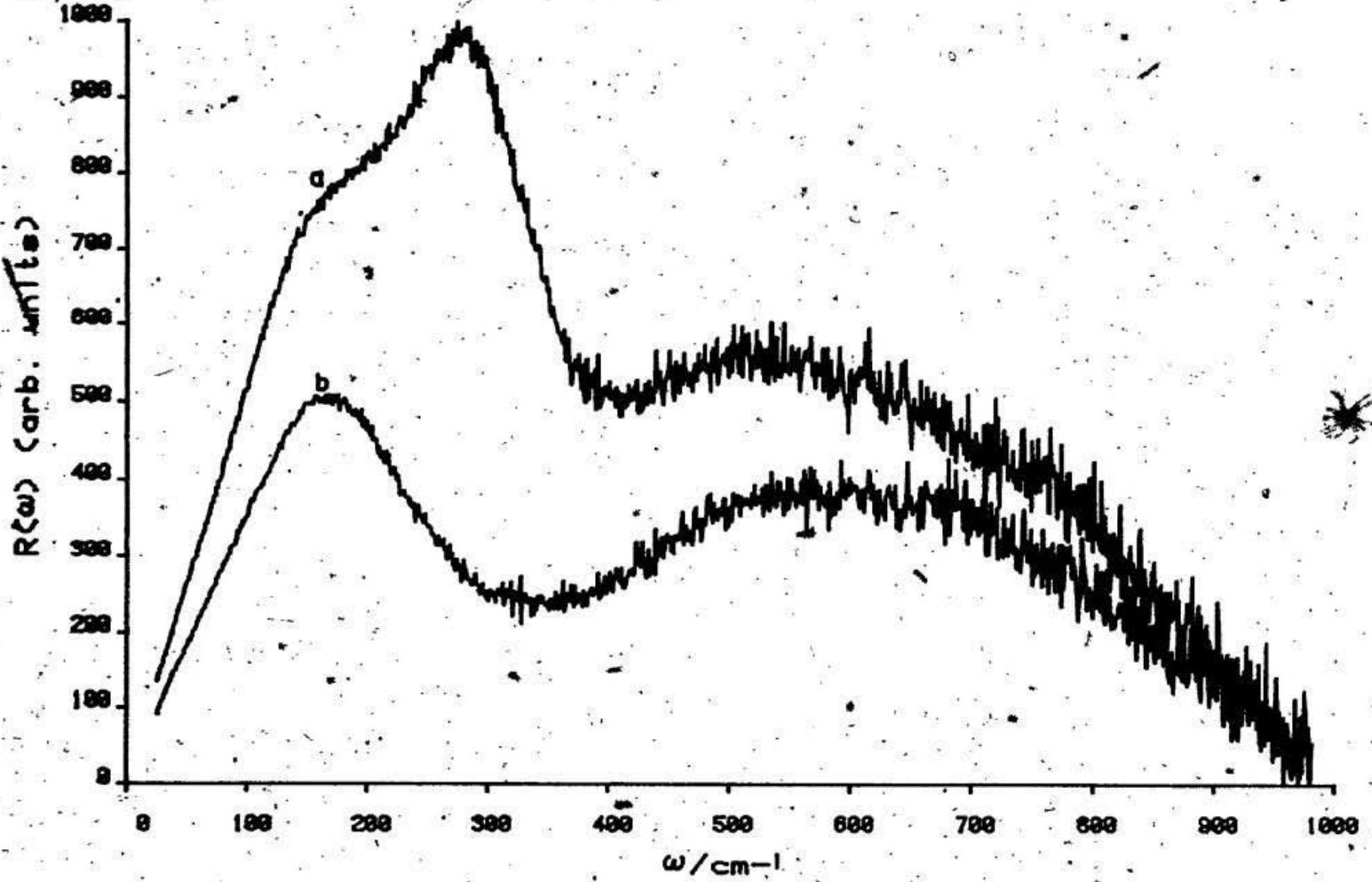
R(ω) (arb. units)
ω / cm⁻¹
a
b
0
100
200
300
400
500
600
700
800
900
1000

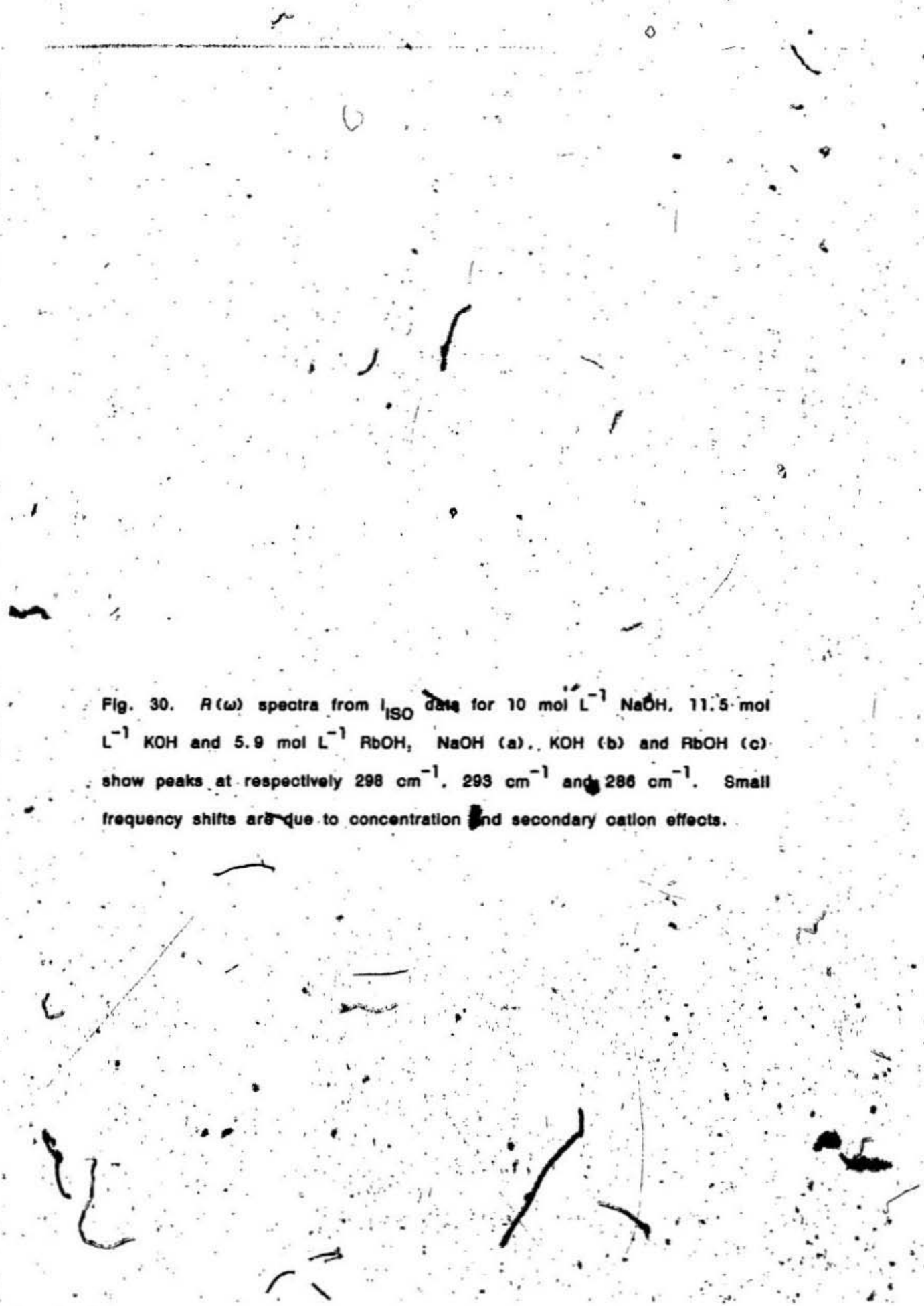

Fig. 30. $R(\omega)$ spectra from I_{ISO} data for 10 mol L^{-1} NaOH, 11.5 mol L^{-1} KOH and 5.9 mol L^{-1} RbOH, NaOH (a), KOH (b) and RbOH (c) show peaks at respectively 298 cm^{-1}, 293 cm^{-1} and 286 cm^{-1}. Small frequency shifts are due to concentration and secondary cation effects.

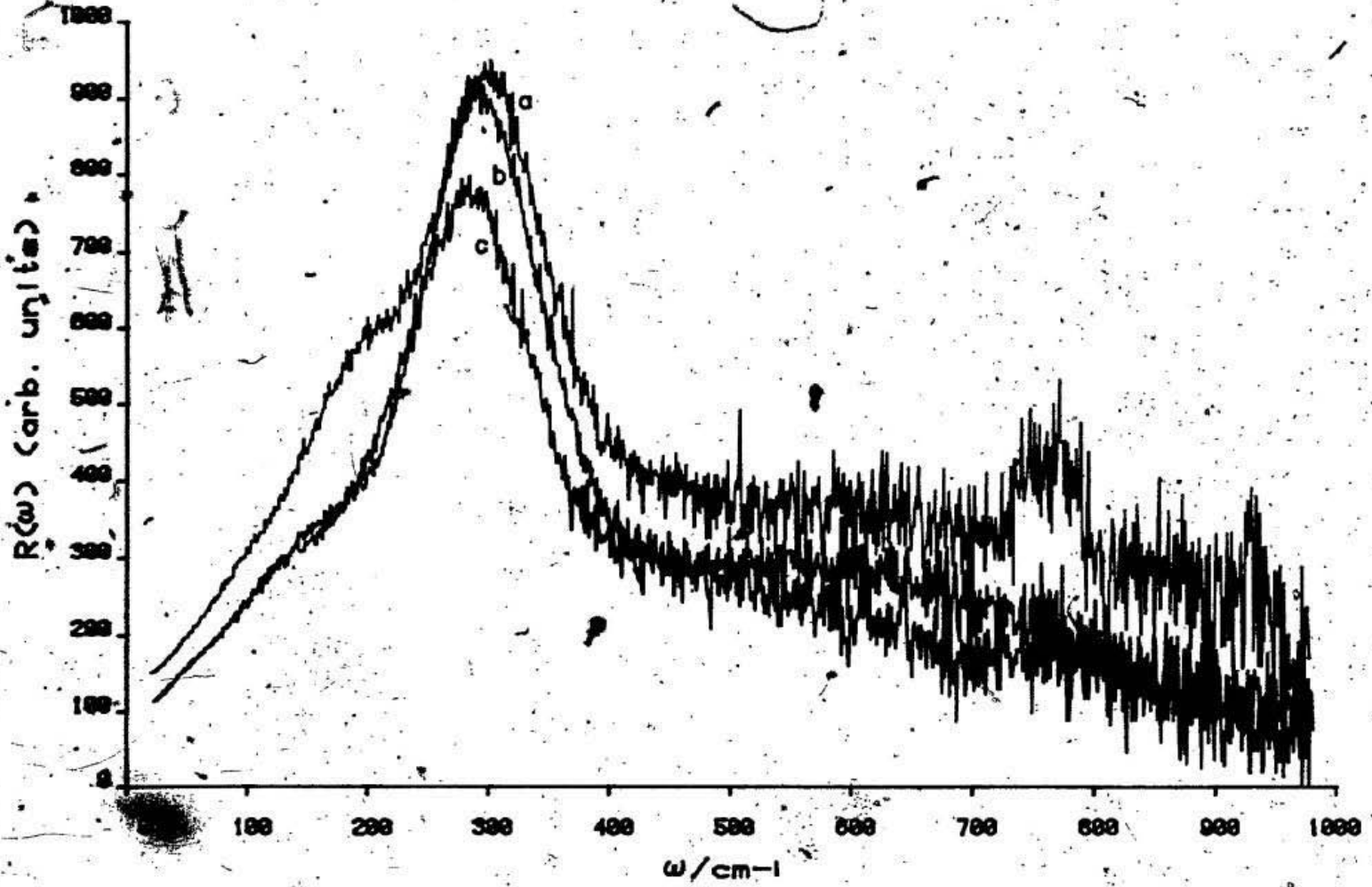
R(ω) (arb. units)
a
b
c
100
200
300
400
500
600
700
800
900
1000
ω/cm⁻¹

Fig. 31. $R(\omega)$ spectra for 8.6 mol L^{-1} CsOH (aq) : I_{VV} (a) and I_{VH} (b). The ν_{max} for H-O-H···OH^- stretching cannot be given with any certainty as the sample proved to have a high carbonate concentration. This fact along with a premature baseline subtraction at 400 cm^{-1} distorts the spectra and shifts the band positions of the active modes. The observed position of the hydroxide-water intermolecular stretch at 277 cm^{-1} is questionable for 8.6 mol L^{-1} CsOH (aq).

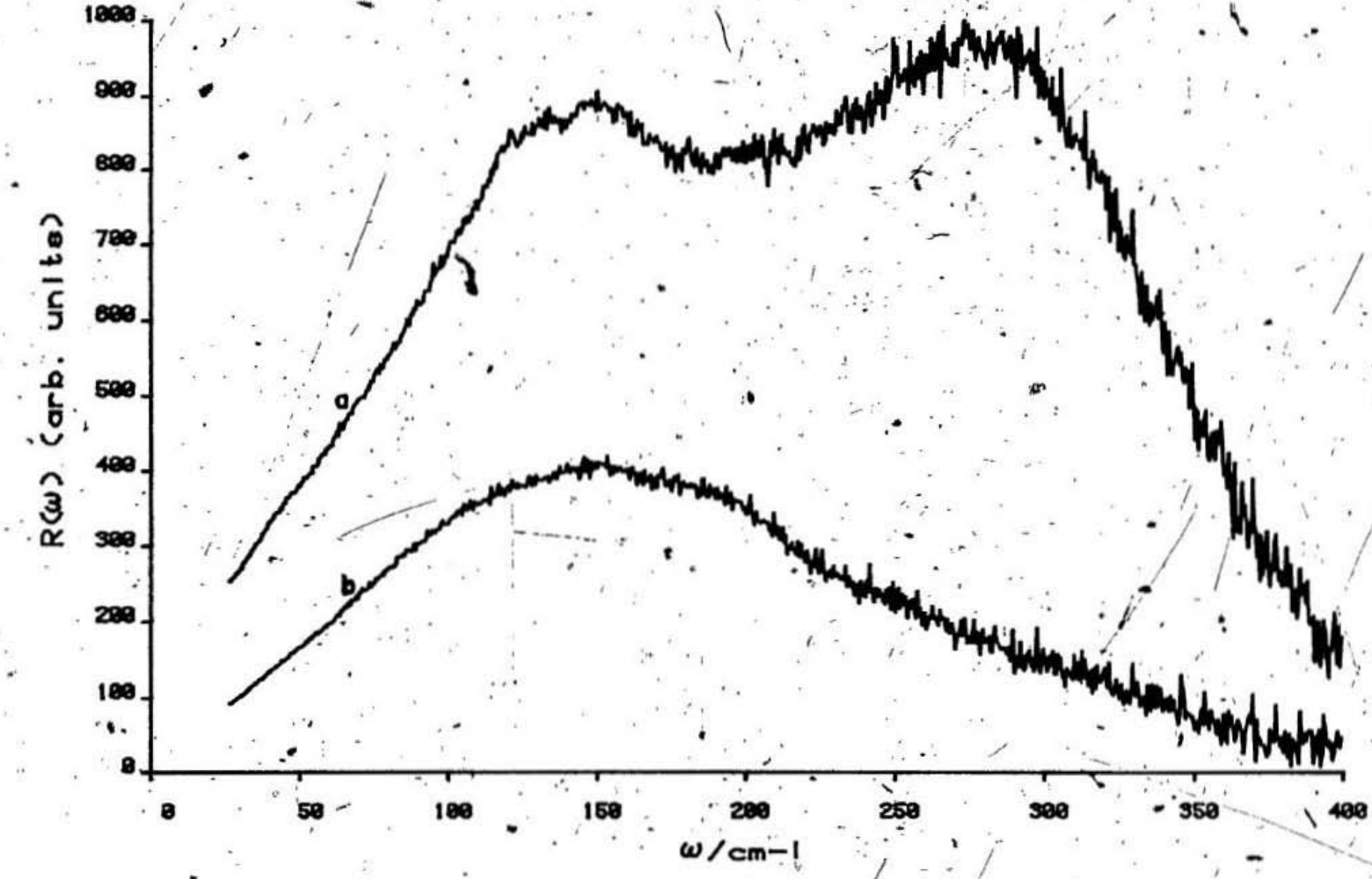
R(ω) (arb. units)
1000
900
800
700
600
500
400
300
200
100
0
a
b
0
50
100
150
200
250
300
350
400
ω/cm−1

higher energy than those of F^- with H_2O. This implies that the H_2O translation is even more restricted for hydroxide solutions than in fluoride solutions. In light of this, one might consider the following. F^- can H-bond to four hydrogens

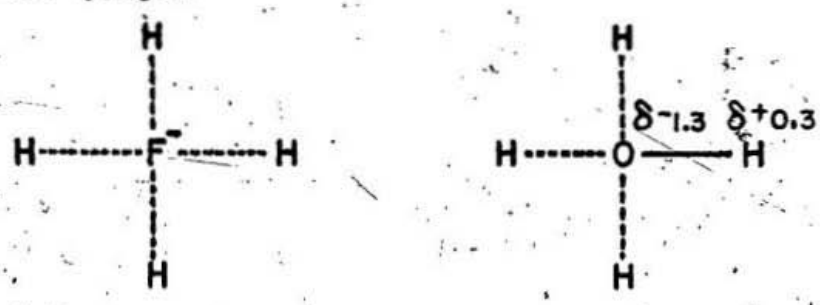

whereas OH^- can only act upon three. Interference from other possible hydrogen bonds will be less for OH^-. Additionally, the overall negative charge on the F is lower than on the O of OH^- because the O-H bond of OH^- has additional bond polarity. The charge on F^- will be -1 but the charge on O in OH^- will be about -1.3. The net effect is that the oxygen will attract the hydrogens more strongly and hence a higher frequency for hydrogen bond stretching will result.

If the $OH^- \cdots H_2O$ intermolecular separation is shorter than for $F^- \cdots H_2O$, a more negative partial molar volume would be expected for hydroxide solutions as the water would be less attracted to the fluoride. The partial molar volumes for OH^- and F^- in water are respectively -5.23 and -1.9 $cm^3\ mol^{-1}$ [40]. The negative molar volumes suggest strong hydrogen bonding for OH^- and F^- while the more negative value for OH^- implies a very strong hydrogen bond.

The data for aqueous LIOH does not fit with the data for the other alkali metal hydroxides. The spectra in Figs. 32, 33 and 34 show polarized bands at 247 cm^{-1} and 316 cm^{-1}. The weak 316 cm^{-1} band has been assigned the $H\text{-}O\text{-}H \cdots OH^-$ stretching mode. Most of the intensity

Fig. 32. $R(\omega)$ spectra for 2.5 mol L^{-1} LiOH (aq). I_{VV} (a) and $\overline{I_{VH}}$ (b).

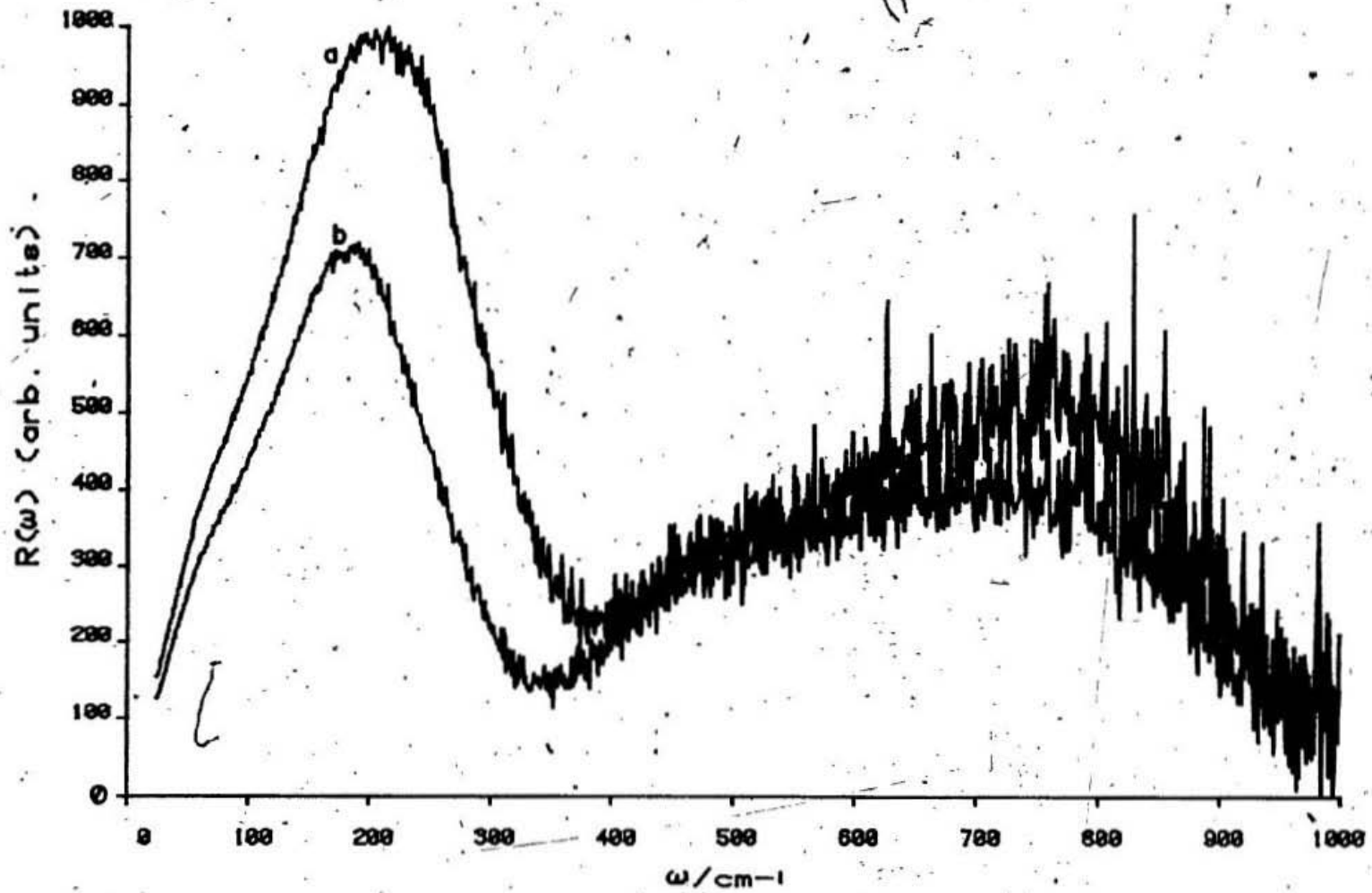
R(ω) (arb. units)
1000
900
800
700
600
500
400
300
200
100
0
a
b
0
100
200
300
400
500
600
700
800
900
1000
ω/cm⁻¹

Fig. 33. $R(\omega)$ spectra for 9.95 mol L^{-1} LiOH (aq). I_{VV} (a) and I_{VH} (b).

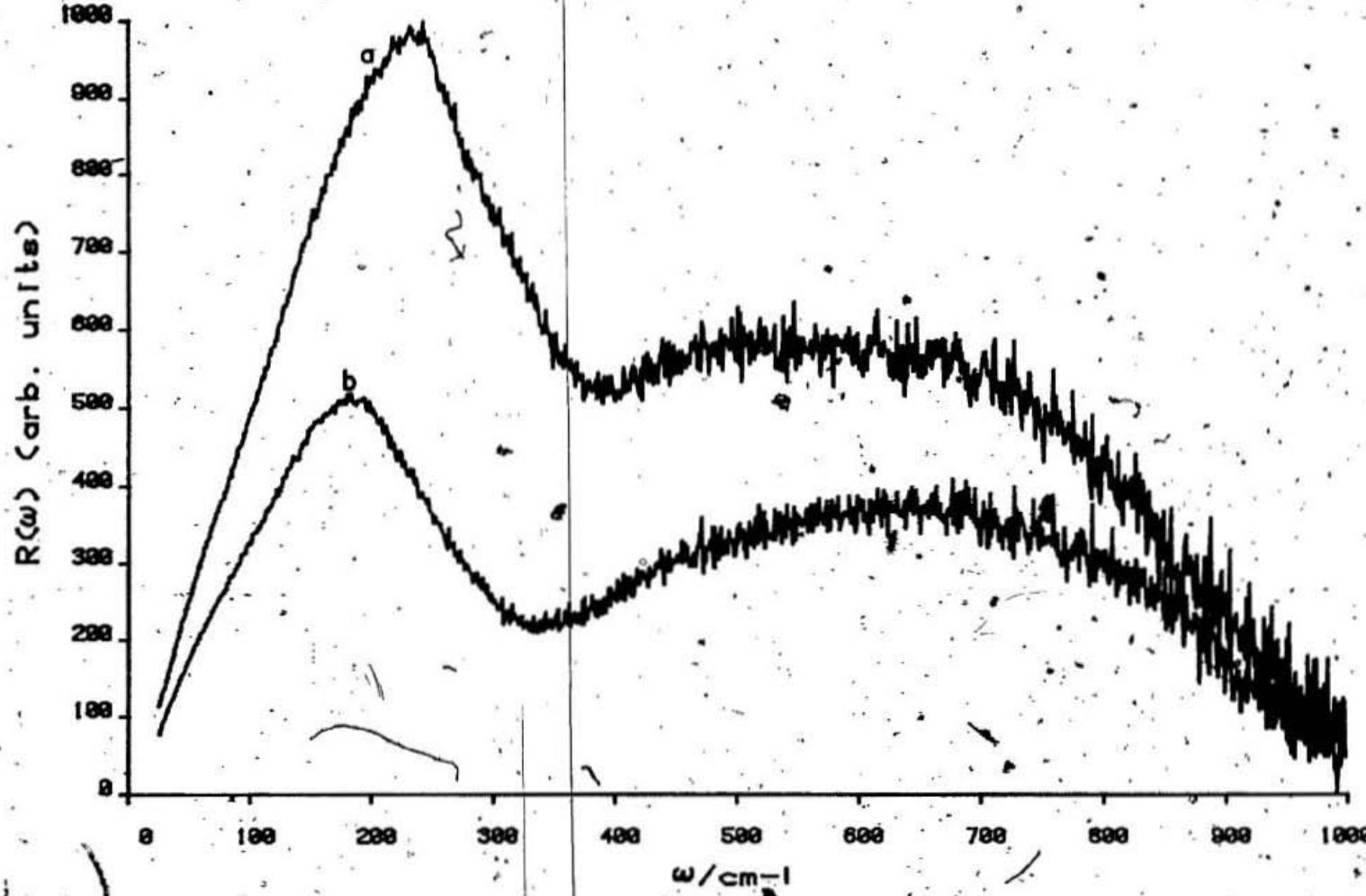
a
b
R(ω) (arb. units)
1000
900
800
700
600
500
400
300
200
100
0
0
100
200
300
400
500
600
700
800
900
1000
ω/cm⁻¹

Fig. 34. Comparison of the $R(\omega)$ isotropic components for (a) 2.5 mol L^{-1} and (b) 3.95 mol L^{-1} LiOH (aq). Growth of a weak polarized band at 316 cm^{-1} is due to an increasing prescence of H-O-H···OH^- units. The polarized band at 247 cm^{-1} is absent from the other alkali metal hydroxide solutions and possibly arises from Li^+OH^- ion pairs.

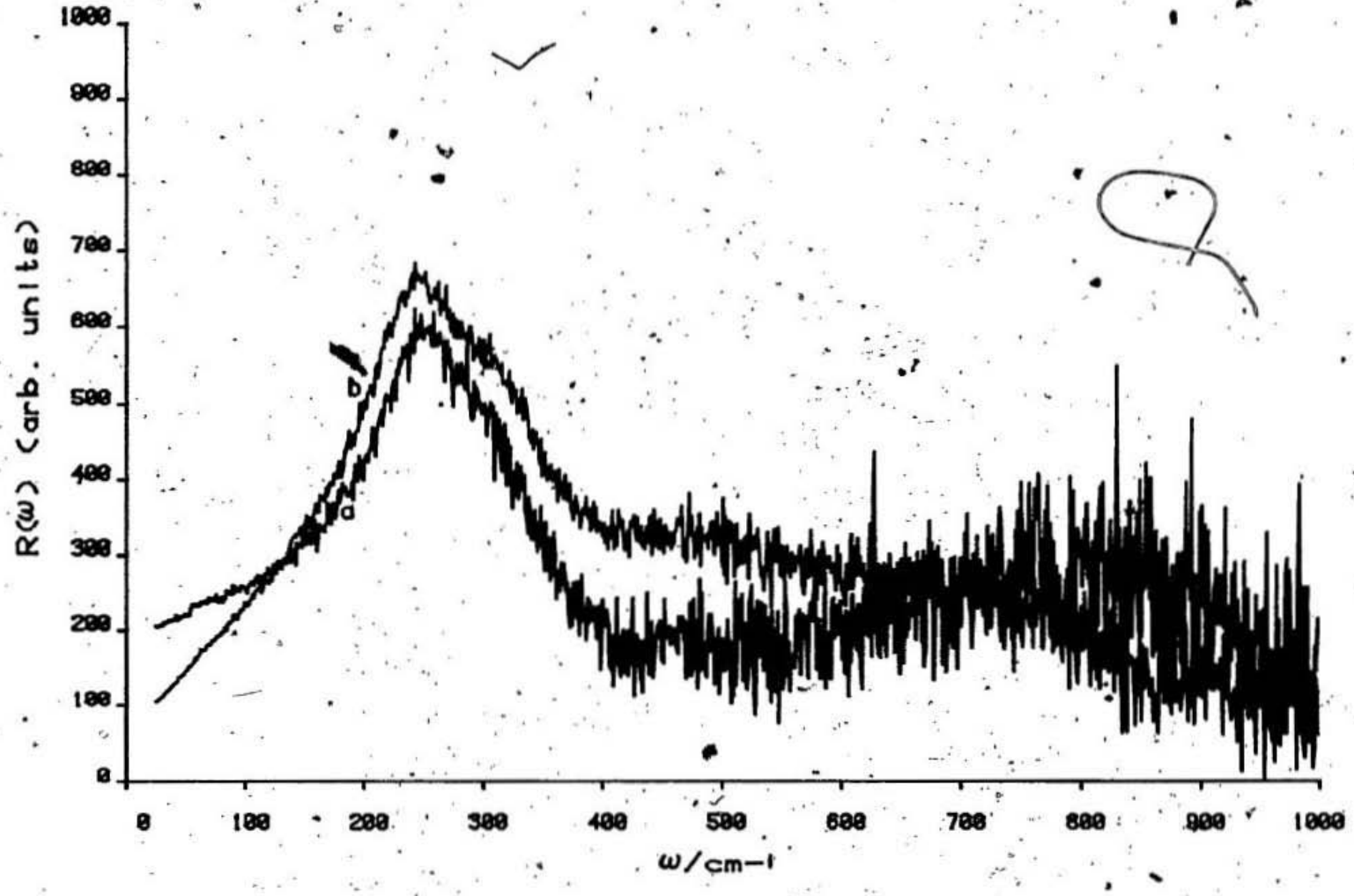
R(ω) (arb. units)
1000
900
800
700
600
500
400
300
200
100
0
0
100
200
300
400
500
600
700
800
900
1000
ω/cm⁻¹
b
a

of the polarized bands is from the 247 cm^{-1} peak and this band possibly represents the symmetric stretch of the Li^+OH^- ion pair. Moskovits and Michaelian [41] claim the presence of hydrated ion pairs in all the alkali metal hydroxide solutions but did not report the band at 247 cm^{-1} for LiOH. Sharma [42, 43] has also reported ion pairing for NaOH and KOH giving rise to polarized bands at 292 cm^{-1} and 282 cm^{-1} respectively but reports no evidence of ion pairing for LiOH. In the present work only LiOH shows ions pairing. This is consistent with the much lower solubility of LiOH in water compared to the other alkali metal salts.

The $OH^- \cdots H_2O$ hydrogen bond stretch should exhibit normal isotope effects. The 298 cm^{-1} band of NaOH shifts to 271 cm^{-1} for NaOD in D_2O (Fig. 35). The bands of the librational region also shift to lower frequencies as with D_2O. The increase in intensity from 800 cm^{-1} outward is from fluorescence of impurities and is apparent in Fig. 36.

The intensity of the $OH^- \cdots H_2O$ hydrogen bond stretch increases with increasing $[OH^-]$. The spectra for 5M and 10M NaOH to 4000 cm^{-1} is presented in Figs. 37 → 40. The symmetric stretch of the OH^- ion at 3606 cm^{-1} increases in intensity from the 5M to the 10M solution. Increased intensity is also noted in the low frequency region indicating a larger presence of $OH^- \cdots H_2O$ interactions. With the addition of $NaClO_4$ to the 5M NaOH solution (Figs. 41 and 42), bands due to the tetrahedral ClO_4^- ion appear while the low frequency $OH^- \cdots H_2O$ region seems to lose intensity and definition. In the O-H stretching region the intensity of the 3438 cm^{-1} band drops and the 3233 cm^{-1} band is more evident. This corresponds to a decrease in the number of hydrogen bonded water molecules and an increase in the number of "free" stretching water molecules. "Free" refers to the waters of hydration for ClO_4^- as

Fig. 35. $R(\omega)$ spectra for 10 mol L^{-1} NaOD in D_2O. I_{VV} (a) and I_{VH} (b). The hydroxide-water intermolecular stretch shifts to 271 cm^{-1} from that of 298 cm^{-1} for 10 mol L^{-1} NaOH (page 78). Impurities give rise to increasing intensity past 800 cm^{-1} as is evident in Fig. 36.

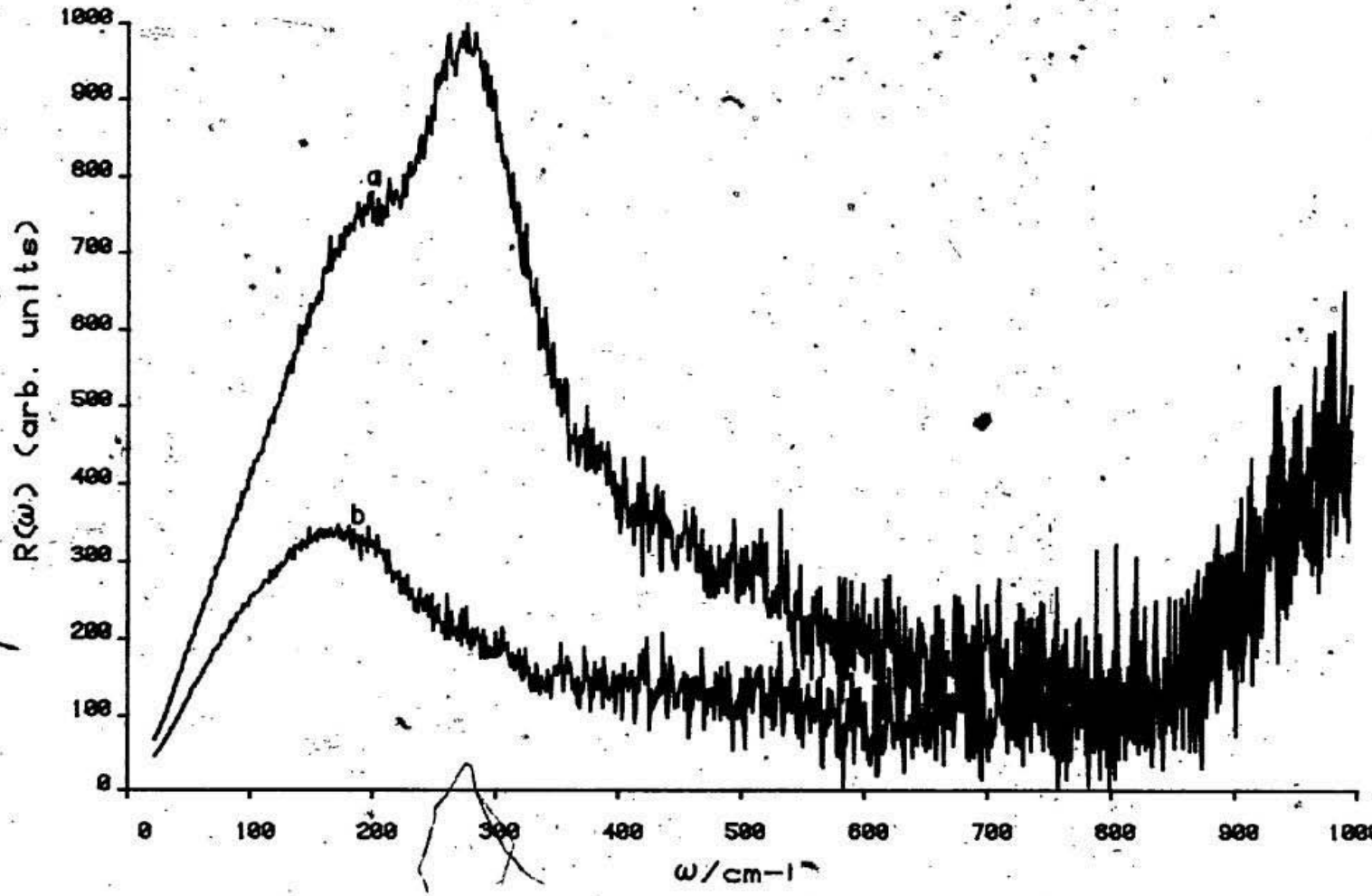
R(ω) (arb. units)
1000
900
800
700
600
500
400
300
200
100
0
a
b
0
100
200
300
400
500
600
700
800
900
1000
ω/cm⁻¹

Fig. 36. $R(\omega)$ spectra for 10 mol L^{-1} NaOD in D_2O showing increasing background intensity from fluorescing impurities.

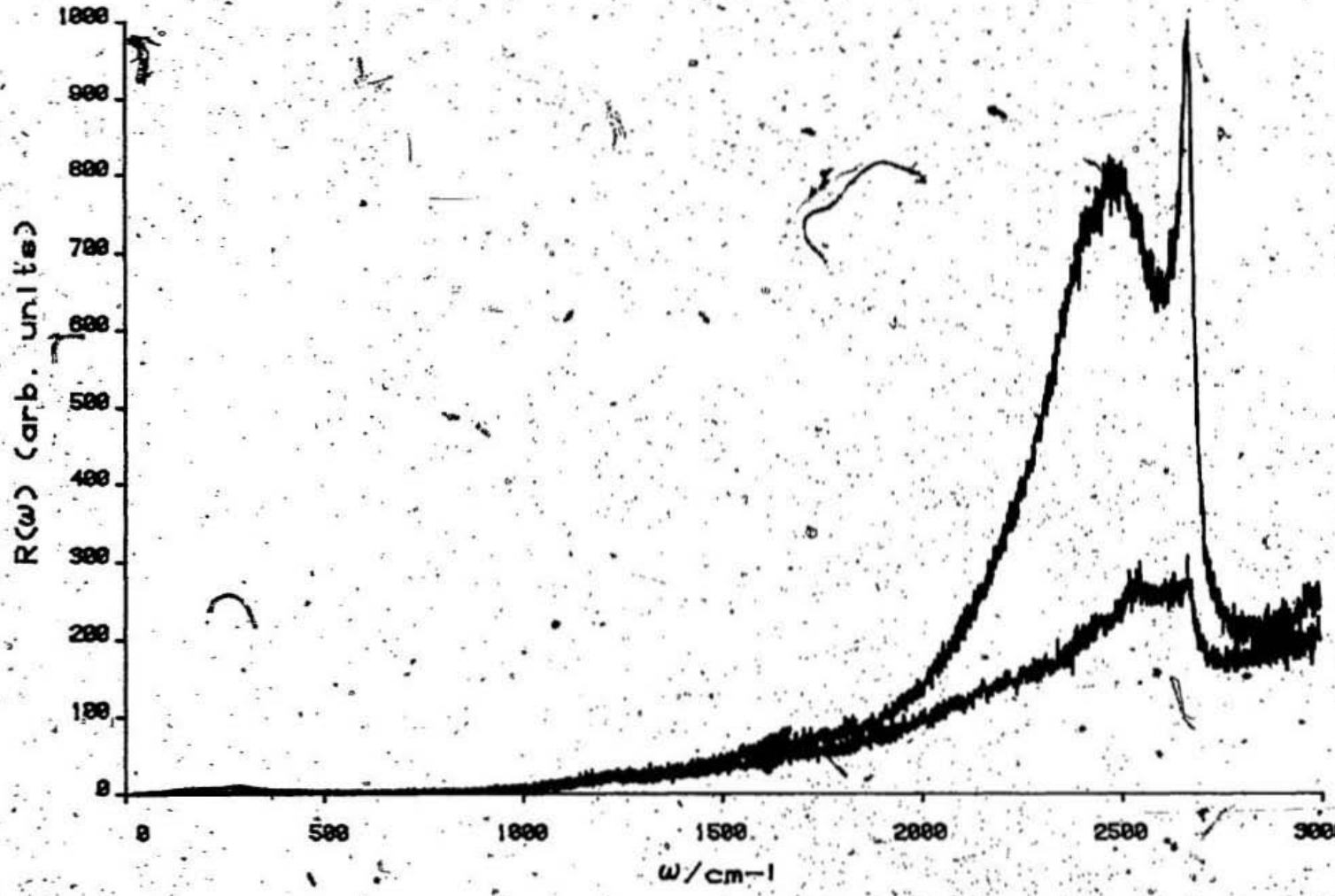
R(ω) (arb. units)
1000
900
800
700
600
500
400
300
200
100
0
0
500
1000
1500
2000
2500
3000
ω/cm-1

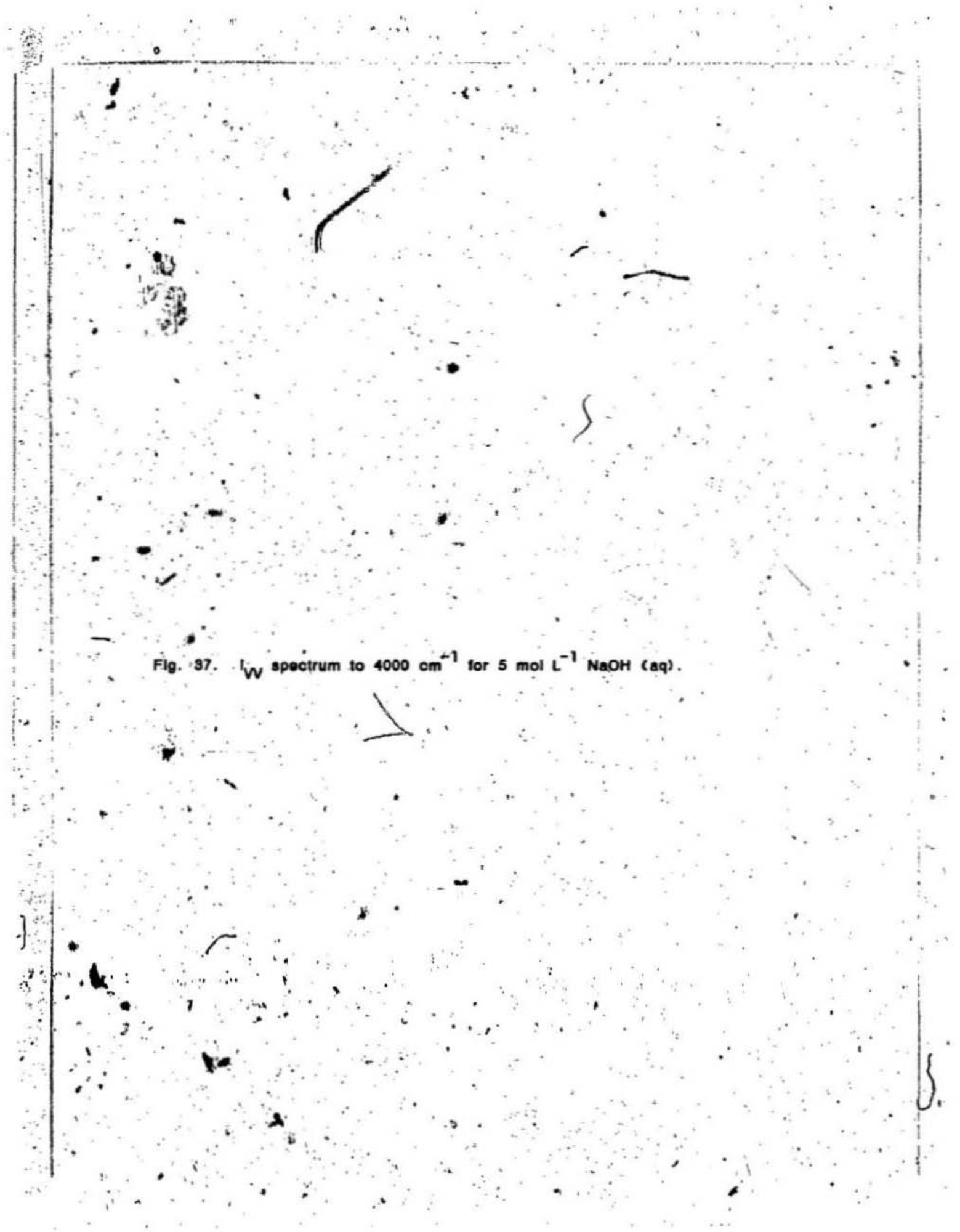

Fig. 37. I_{VV} spectrum to 4000 cm^{-1} for 5 mol L^{-1} NaOH (aq).

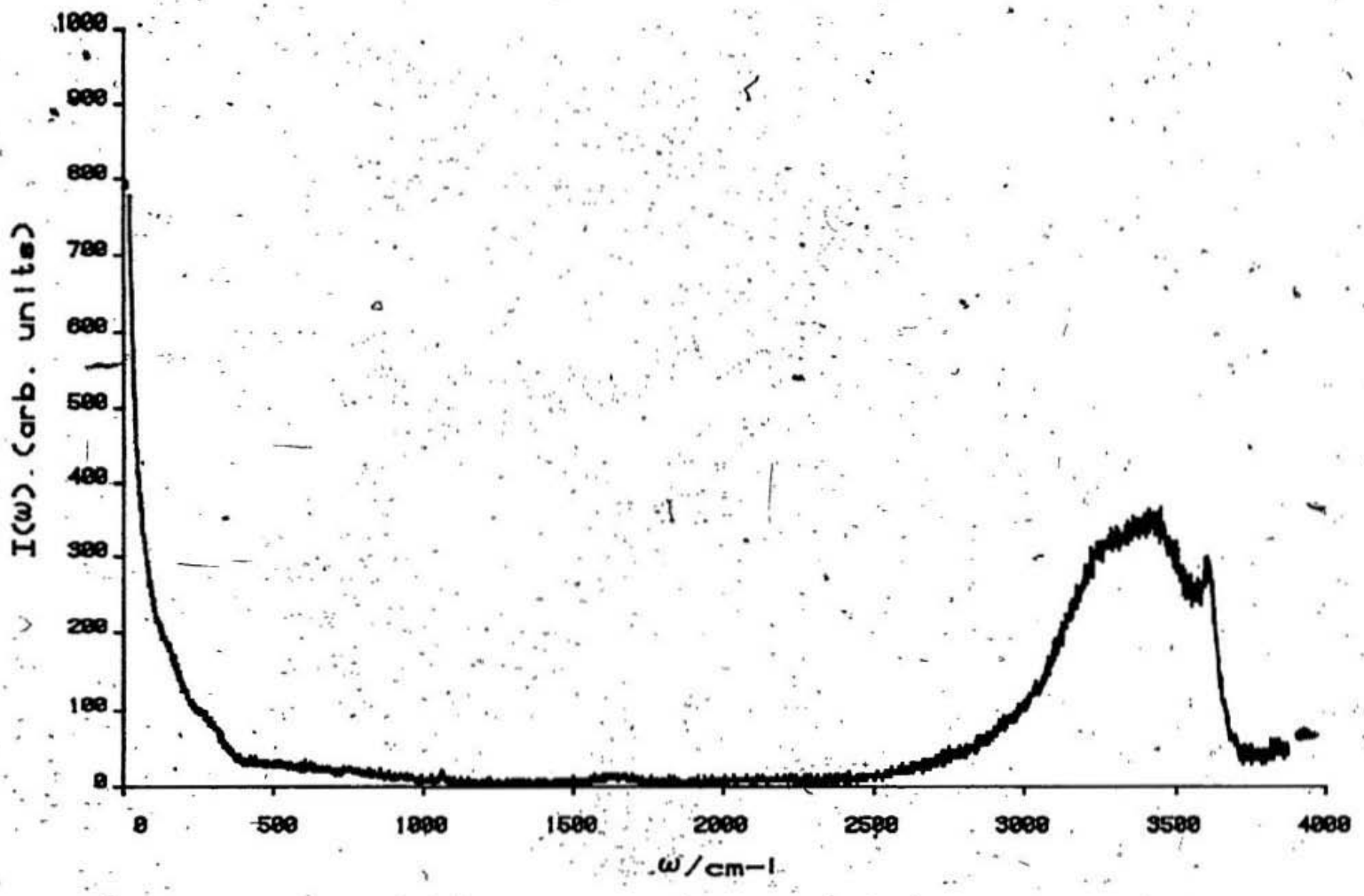
I(ω). (arb. units)
1000
900
800
700
600
500
400
300
200
100
0
0
500
1000
1500
2000
2500
3000
3500
4000
ω/cm-1

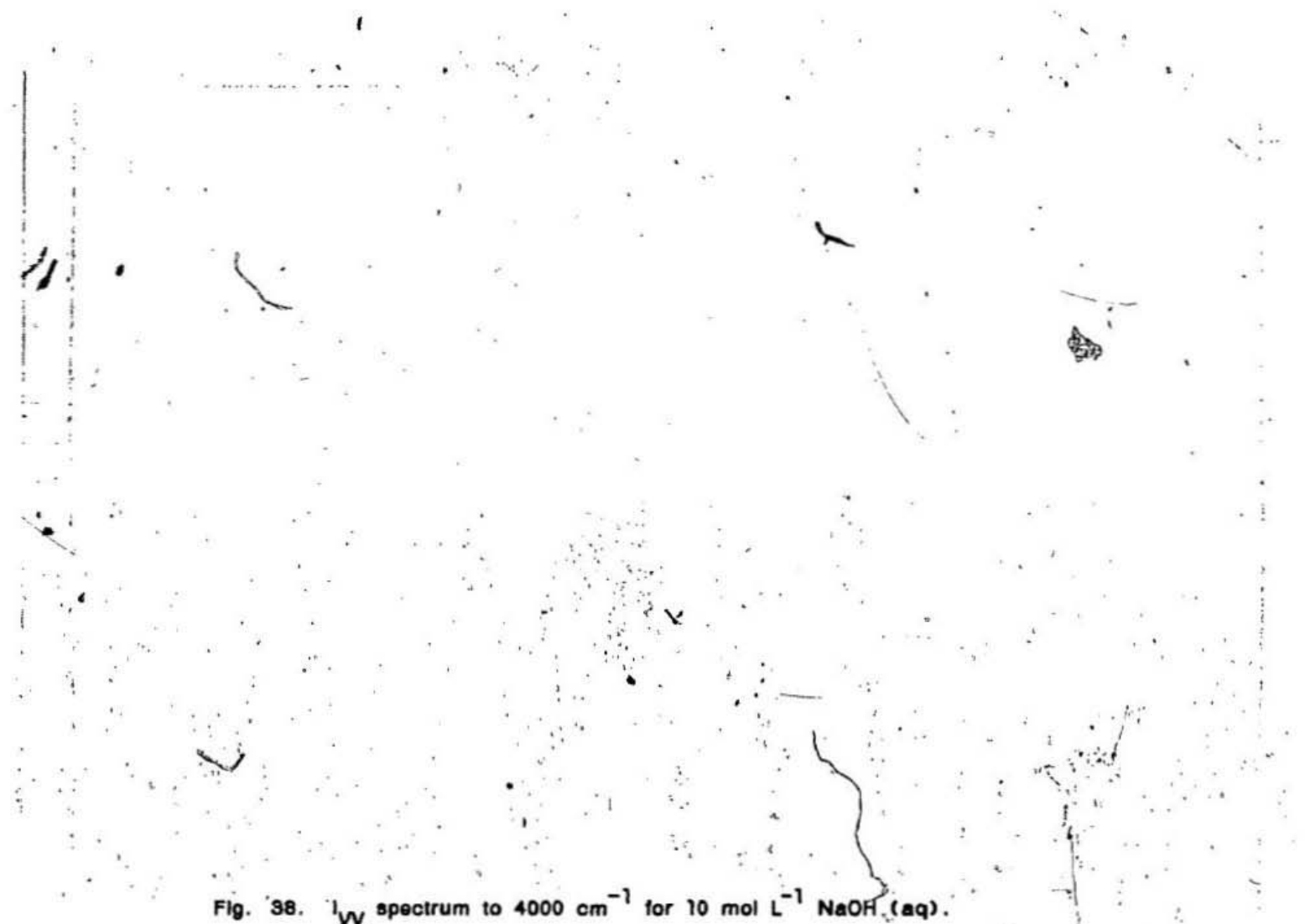

Fig. 38. I_W spectrum to 4000 cm^{-1} for 10 mol L^{-1} NaOH (aq).

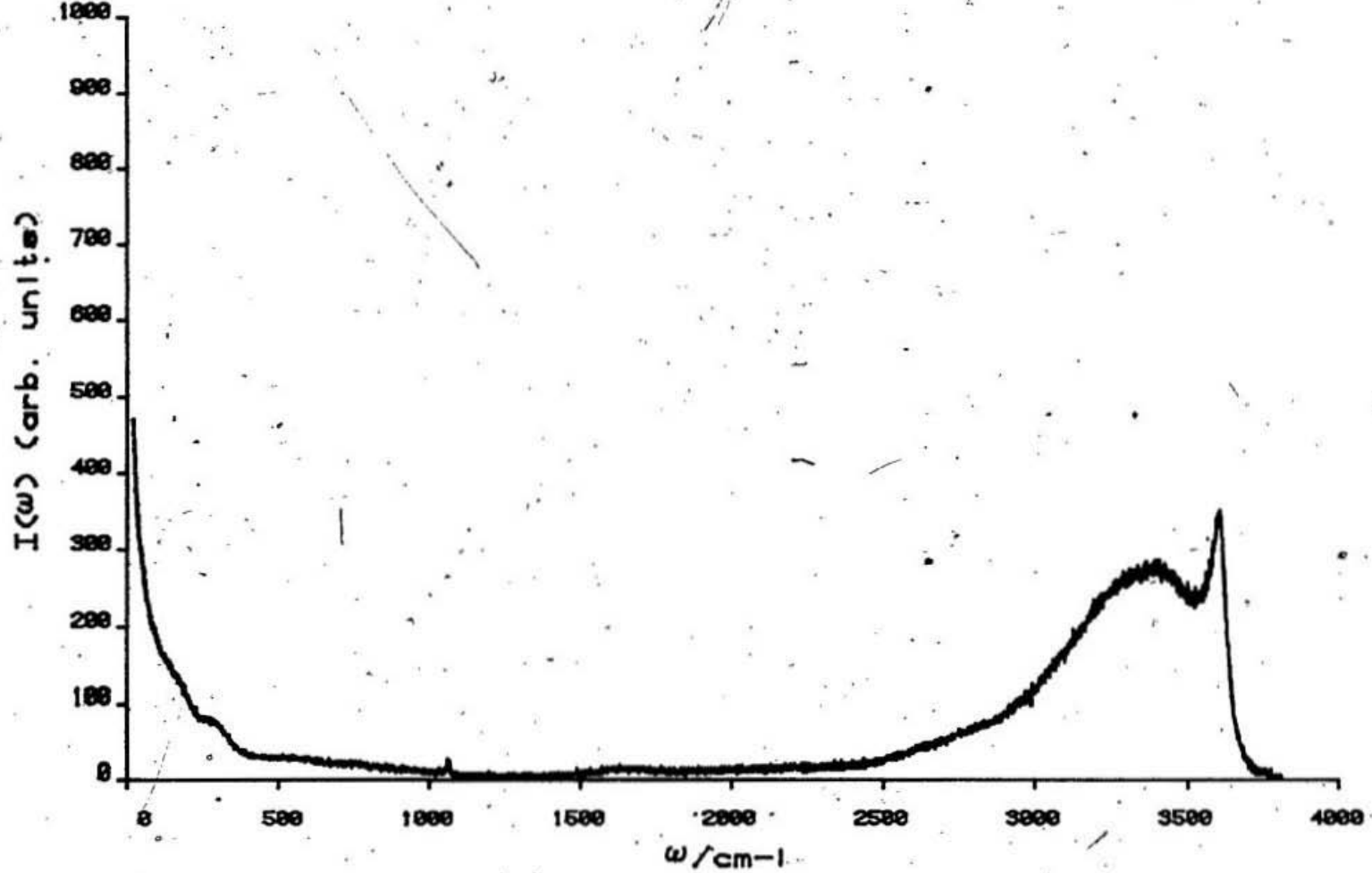
I(ω) (arb. units)
1000
900
800
700
600
500
400
300
200
100
0
0
500
1000
1500
2000
2500
3000
3500
4000
ω/cm-1

Fig. 39. $R(\omega)$ spectrum to 4000 cm^{-1} of I_{VV} data for 5 mol L^{-1} NaOH (aq).

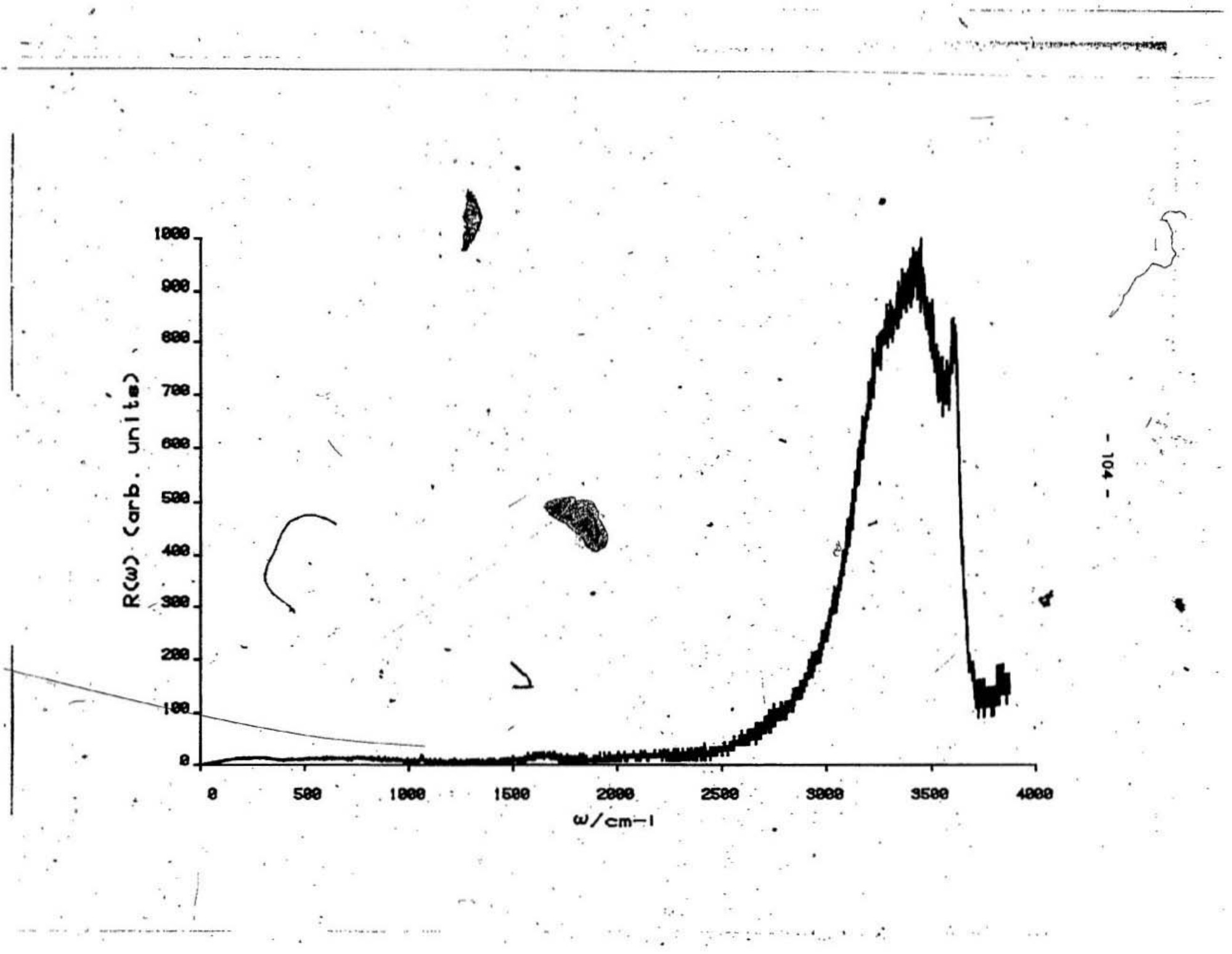
R(ω) (arb. units)
1000
900
800
700
600
500
400
300
200
100
0
0
500
1000
1500
2000
2500
3000
3500
4000
ω/cm-1

Fig. 40. $R(\omega)$ spectrum to 4000 cm^{-1} of I_{VV} data for 10 mol L^{-1} NaOH (aq). In comparison with Fig. 39 the growth of the OH^- intramolecular symmetric stretch is evident with increasing concentration. The carbonate impurity is seen to increase as the 1063 cm^{-1} ν_1 of CO_3^{2-} increases in intensity with the higher concentration of hydroxide.

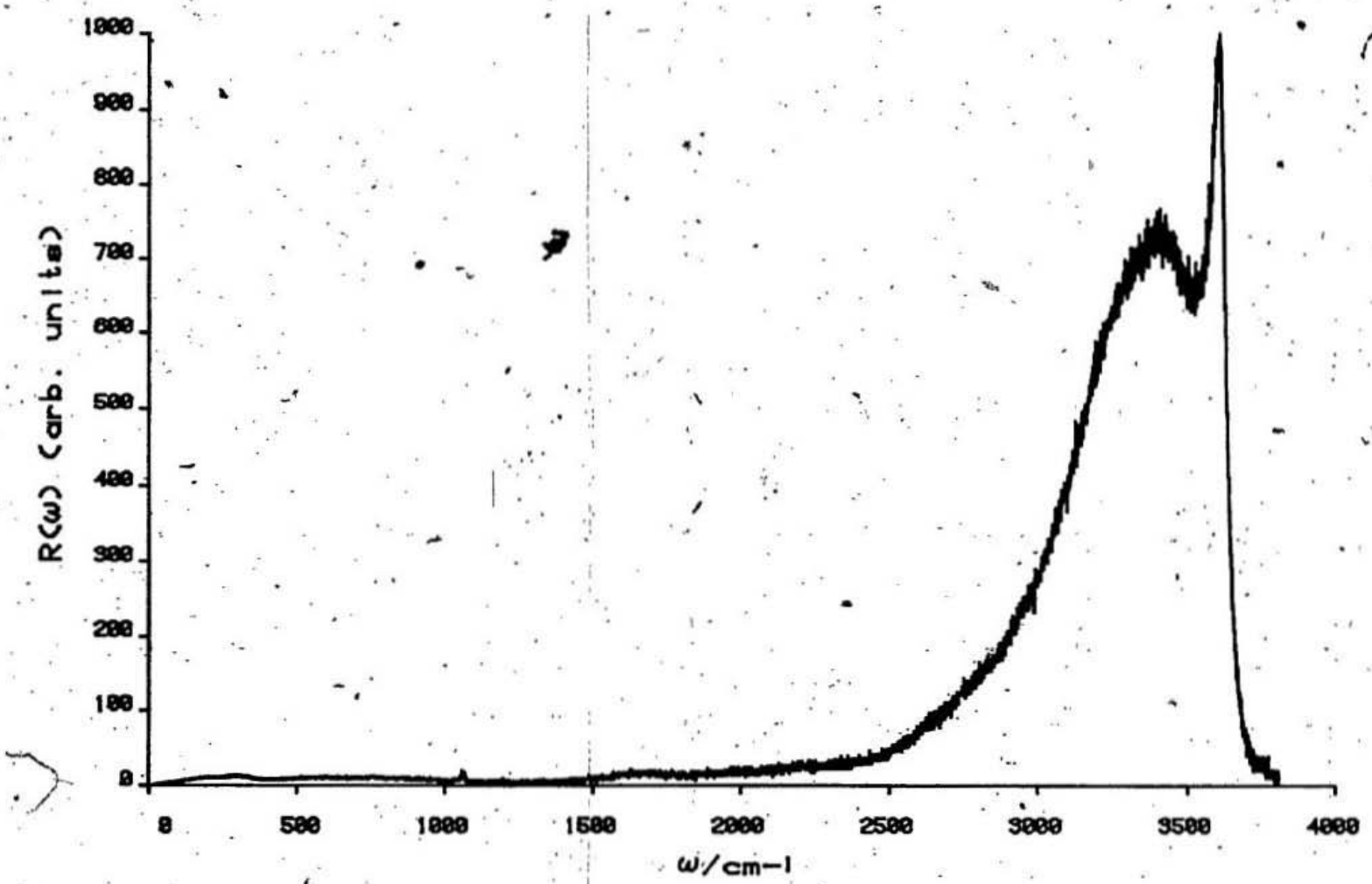
R(ω) (arb. units)
1000
900
800
700
600
500
400
300
200
100
0
0
500
1000
1500
2000
2500
3000
3500
4000
ω/cm−1

Fig. 41. - I_{VV} spectrum of $NaClO_4/NaOH$ (5 mol L^{-1} in each) to 4000 cm^{-1}. In addition to the appearance of new bands from the internal modes of the perchlorate ion there are changes in the spectrum of the OH^- solution itself in the area of intramolecular O-H stretching.

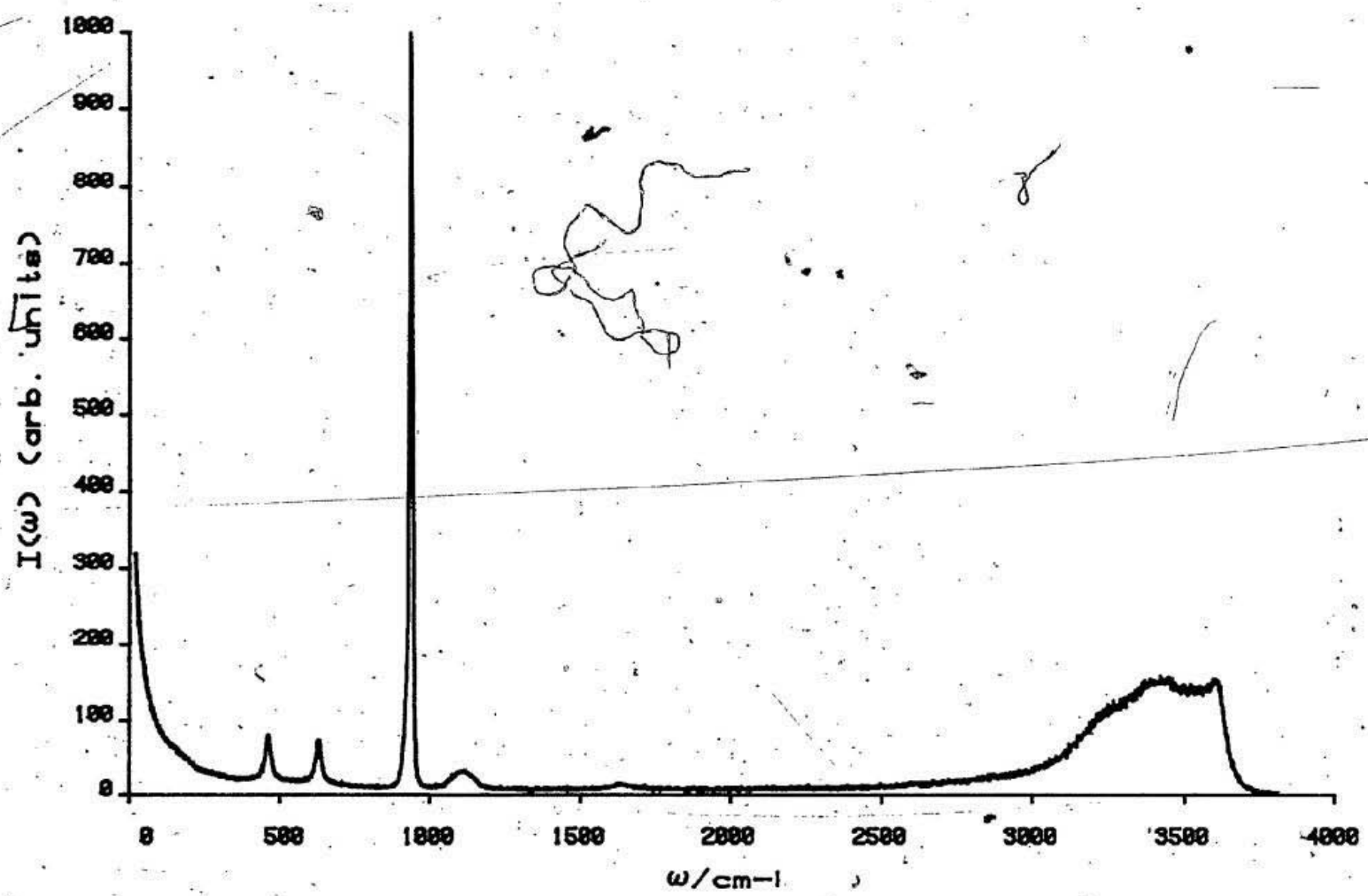
I(ω) (arb. units)
1000
900
800
700
600
500
400
300
200
100
0
0
500
1000
1500
2000
2500
3000
3500
4000
ω/cm-1

Fig. 42. $R(\omega)$ spectrum of $NaClO_4/NaOH$ (5 mol L^{-1} in each) to 4000 cm^{-1} taken from I_{VV} data. The internal modes of the perchlorate ion are visible between 300 cm^{-1} and 1200 cm^{-1}. The bands in the intramolecular stretching region change in relative intensity as the perchlorate ion breaks down the intermolecular structure. The intensity of the 3436 cm^{-1} band drops relative to the 3233 cm^{-1} band illustrating the loss of O-H stretching in water molecules hydrogen bonded to other water molecules or OH^- and an increase in the number of unassociated water molecules with O-H stretching. The loss of structure and intensity in the low frequency region also displays a loss of structure in the solution.

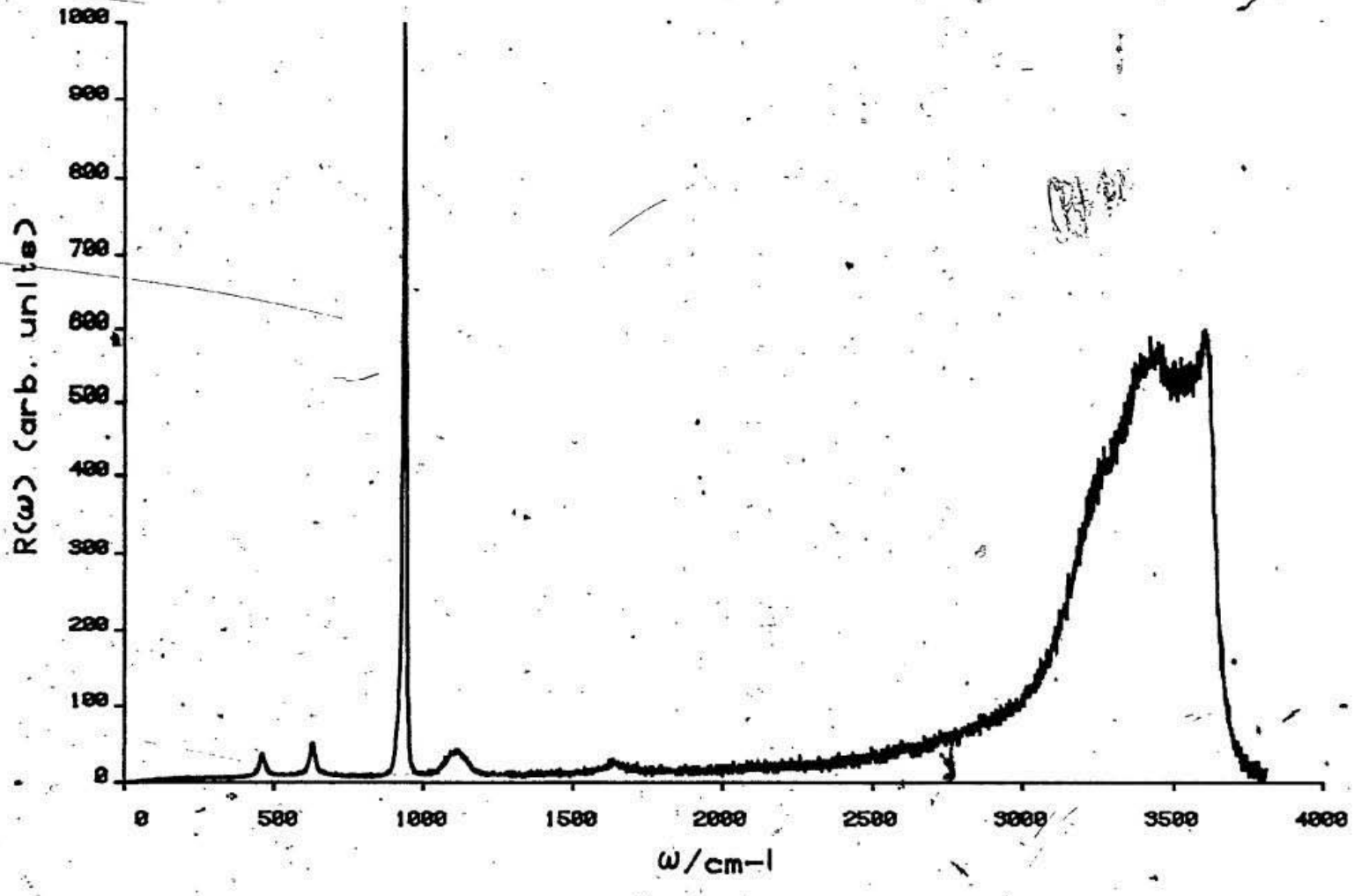
R(ω) (arb. units)
1000
900
800
700
600
500
400
300
200
100
0
0
500
1000
1500
2000
2500
3000
3500
4000
ω/cm-1

perchlorate-water interactions are weak. The spectra of the low frequency region for 10M NaOH, 5M NaOH and 5M NaOH/5M $NaClO_4$ normalized to the 3606 cm^{-1} OH^- band are shown in Fig. 43. The polarized $OH^-\cdots H_2O$ hydrogen bond stretch at 298 cm^{-1} decreases in intensity with decreasing hydroxide concentration and is absent in the presence of perchlorate. The lower frequency O···H-O stretch for water-water interactions drops in intensity showing a loss of structure in the solution when ClO_4^- is added. The absence of the 298 cm^{-1} band in the hydroxide-perchlorate mixed solution spectrum confirms that this band is not cation dependent and cannot be due to ion pairs because the addition of $NaClO_4$ increases the cation concentration. Studies of a molten mixture of NaOH and KOH at 170°C also failed to show any evidence of a polarized peak in the 250 to 300 cm^{-1} region a fact which further rules out ion pairs as the cause of the band in aqueous hydroxides [44].

CONCLUSION

In the present study use of the $R(\omega)$ function has enabled relative intensities, peak frequencies and halfwidths to be determined with greater precision than has previously been possible for spectra presented in the $I(\omega)$ format. This has greatly assisted the assignments and interpretations of spectral features. Studies of the hydrogen bond stretching mode of water showed shifts for substitutions of both $H_2{}^{18}O$ and D_2O indicating an asymmetric OHO sequence. Hydrogen bond stretching was also observed in aqueous metal fluoride and hydroxide solutions arising from an anion-water hydrogen bond stretching mode. These anion-water interactions proved to be much stronger than water-water interactions. A discrete metal-oxygen symmetric stretching band was observed in saturated solutions of LiCl and $MgCl_2$. With the possible exception of aqueous LiOH, no ion

Fig. 43. $R(\omega)$ spectra of 5 mol L^{-1} NaOH, 10 mol L^{-1} NaOH and $NaClO_4$/NaOH (5 mol L^{-1} in each) taken from I_{VV} data and normalized to the OH^- intramolecular stretch at 3606 cm^{-1}. The 10 mol L^{-1} NaOH spectrum (a) and the 5 mol L^{-1} NaOH spectrum (b) show an intensity dependence of the 298 cm^{-1} band on [NaOH]. When $NaClO_4$ is present (c) this band disappears and the intensity of the O···H–O stretch is lowered showing a drop in both water–hydroxide and water–water interactions. The assignment of the 298 cm^{-1} band to an Na^+OH^- ion pair would require an increase in the intensity of this band when $NaClO_4$ is added due to the increased sodium ion concentration.

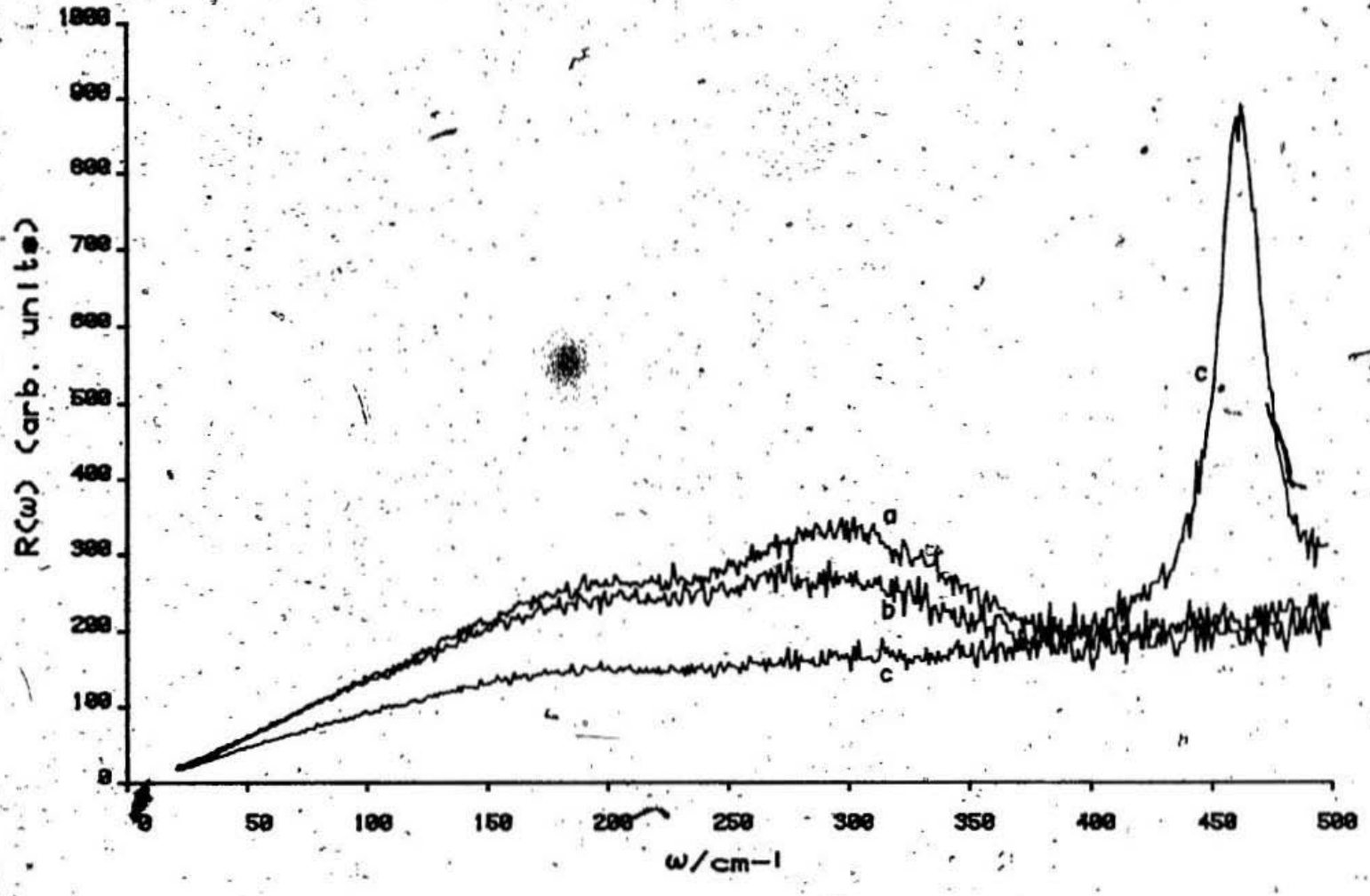
R(ω) (arb. units)
1000
900
800
700
600
500
400
300
200
100
0
0
50
100
150
200
250
300
350
400
450
500
ω/cm−1
a
b
c
c

pairing was observed for any of the alkali metal salt solutions. A band originating from reorientational motions of the CO_3^{2-} anion was superimposed on the water spectrum in concentrated aqueous carbonate solutions.

The $R(\omega)$ function has proven to be of considerable assistance in the identification of weak low frequency bands arising from scattering in liquids and glasses. The result of transforming the $I(\omega)$ spectrum into the $R(\omega)$ spectrum was a data set that is almost free of intensity from the exciting line an advantage which permits quantitative relative intensity studies for the low frequency region. Since the $R(\omega)$ function is corrected for the effect of temperature on scattering intensity the $R(\omega)$ data gives a spectrum which reflects only the $\left[\frac{\partial \alpha}{\partial Q}\right]_I^2$ terms. This feature makes the $R(\omega)$ function generally useful for studies of solids, liquids and molten salts. Although there is an apparent increase in noise with increasing $\Delta\omega$ (this is a loss of S/N in the ω=0 band and not a deterioration of the S/N of the spectrum), the effect can be minimized with good signal averaging techniques. However, digitization of the noise may still be a problem if the recording device has a small dynamic range.

REFERENCES

[1] G. E. Walrafen, *In Chap. 5 of* "Water : A Comprehensive Treatise", (F. Franks, ed.), Vol. 1, Plenum Press, New York, N. Y. (1972)

[2] D. E. Irish and M. H. Brooker, *In Chap. 6 of* "Advances in Infrared and Raman Spectroscopy", (R. J. H. Clark and R. E. Hester, eds.), Vol. 2, Heyden, N. Y. (1976)

[3] D. N. Waters, *In Chap. 2 of* "Molecular Spectroscopy", Vol. 6, The Chemical Society, London (1979)

[4] G. E. Walrafen, *J. Chem. Phys.* **36(4)**, 1035 (1962)

[5] J. Bandekar and B. Curnutte, *J. Mol. Spectrosc.* **58**, 169 (1975)

[6] M. Moskovits and K. H. Michaelian, *J. Chem. Phys.* **69(6)**, 2306 (1978)

[7] M. H. Brooker and M. Perrot, *J. Chem Phys.* **74(5)**, 2795 (1981)

[8] D. I. Page, *In Chap 9 of* "Water : A Comprehensive Treaty", (F. Franks ed.), Vol. 1, Plenum Press, New York, N.Y. (1972)

[9] N. Ohtomo and K. Arakawa, *Bull. Chem. Soc. Jap.* **51(6)**, 1649 (1978)

[10] O. F. Nielsen, *Chem. Phys. Lett.* **60(3)**, 515 (1979)

[11] M. A. Gray, T. M. Loehr and P. A. Pincus, *J. Chem. Phys.* **59(3)**, 1121 (1973)

[12] C. P. Nash, T. C. Donnelly and P. A. Rock, *J. Soln. Chem.* **6(10)**, 663 (1977)

[13] D. W. James and R. Irmer, *J. Raman Spectrosc.* **3**, 91 (1975)

[14] D. W. James and R. L. Frost, *Farad. Trans 1*, **74(3)**, 583 (1978)

[15] C. Clement et G. Fourche, *J. Chim. Phys.* **77(6)**, 545 (1980)

[16] D. W. James and R. F. Armishaw, *Inorg. Nucl. Chem. Lett.* **12**, 425 (1976)

[17] G. Brink and M. Falk, *Can. J. Chem.* **48**, 3019 (1970)

[18] G. E. Walrafen, *J. Chem. Phys.* **52**, 4176 (1970)

[19] M. Bennouna, H. Cachet, J. C. Lestrade and J. R. Birch, *Chem. Phys.* **62**, 439 (1981)

[20] K. Abu-Dari, K. N. Raymond and D. P. Freyberg, *J. Am. Chem. Soc.* **101:13** 3688 (1979)

[21] C. McM. Rohlfing, L. C. Allen, C. M. Cook and H. B. Schlegel, *J. Chem. Phys.* **78(5)**, 2498 (1983)

[22] C. J. Montrose, J. A. Bucaro, J. Marshall-Coakley and T. A. Litovitz, *J. Chem. Phys.* **60(12)**, 5025 (1974)

[23] R. H. Stolen, *Phys. Chem. Glasses* **11**, 83 (1970)

[24] M. Hass, *J. Phys. Chem. Solids* **31**, 415 (1970)

[25] R. Shuker and R. W. Gammon, *J. Chem. Phys.* **55(10)**, 4784 (1971)

[26] R. Shuker and R. W. Gammon, *Phys. Rev. Letters* **25**, 222 (1970)

[27] D. D. Klug and E. Whalley, *J. Chem. Phys.* **71(7)**, 2903 (1979)

[28] P.-A. Lund, O. F. Nielsen, and E. Praestgaard, *Chem. Phys* **28**, 167 (1978)

[29] R. G. Gordon, *J. Chem. Phys.* **43(4)**, 1307 (1965)

[30] M. Perrot, M. H. Brooker J. Lascombe, *J. Chem. Phys.* **74(5)**, 2787 (1981)

[31] J. W. Schultz and D. F. Hornig, *J. Chem. Phys.* **65**, 2131 (1961)

[32] R. E. Weston. *Spectrochim. Acta* **18**, 1257 (1962)

[33] G. E. Walrafen. *In* "Hydrogen Bonded Solvent Systems" (A. K. Covington and P. Jones, eds.). Taylor and Francis, London (1968)

[34] H. D. Downing and D. Williams. *J. Geophys. Res.* **80(12)**, 1656 (1975)

[35] R. M. Noyes. *J. Am. Chem. Soc.* **84**, 513 (1962)

[36] J. T. Bulmer, D. E. Irish and L. Odberg. *Can. J. Chem* **53**, 3806 (1975)

[37] S. P. Best, R. S. Armstrong and J. K. Beatie. *J. Chem. Soc. Dalton Trans.* 1655 (1982)

[38] K. H. Michaelian and M. Moskovits. *Nature* **273**, 135 (1978)

[39] M. H. Brooker and B. DeYoung. presented to the 58th Canadian Chemical Conference of the Chemical Institute of Canada. Toronto. May 1975

[40] E. A. Moelwyn-Hughes. "Physical Chemistry". Pergamon. New York. N. Y. (1964)

[41] M. Moskovits and K. H. Michaelian. *J. Am. Chem. Soc.* **102(7)**, 2209 (1980)

[42] S. K. Sharma and S. C. Kashyap. *J. Inorg. Nucl. Chem.* **34**, 3623 (1972)

[43] S. K. Sharma. *J. Chem. Phys.* **58(4)**, 1626 (1973)

[44] M. H. Brooker and J. G. Shapter. *private communication*